



UNIVERSITY OF THE
WITWATERSRAND,
JOHANNESBURG

**Tribology of drill bit material in deep oil drilling process: variation of
weight on bit (WOB) and bit rotating speed**

MSc (50/50) RESEARCH REPORT

Prepared by

Mats'olo Seloanyane

1439795

Submitted to

School of Chemical and Metallurgical Engineering, Faculty of Engineering and the Built
Environment, University of the Witwatersrand, Johannesburg, South Africa

Supervisor(s):

Dr. Diakanua Nkazi (University of the Witwatersrand)

Prof. Peter Olubambi (University of Johannesburg)

November, 2019

Abstract

The oil and gas industry is faced with great challenges when it comes to the drilling process due to a shift in drilling shallow onshore layers, to deep and ultra-deep offshore layers. The depletion in the onshore oil and gas reserves has resulted in the need to explore alternative reserves, to meet the constantly increasing energy demand. Due to increased drilling depth, the drilling equipment faces challenges of increased torque and drag, which lead to friction and wear, as a result of complicated drilling environments. These challenges eventually lead to serious equipment failure, resulting in increased production costs. It is therefore of paramount importance to find different combinations of drilling parameters that will give the highest production rates at minimum costs while also paying attention to strict environmental and safety regulations. In this research, different drilling parameters such as weight-on-bit (WOB) and drill bit rotating speed, including different drilling environments such as dry and wet environments were studied, to determine how their different combinations affect the coefficient of friction (COF), when used in three different rock types; Fine-grained Arkose sandstone, Coarse-grained Arkose sandstone and Quartzite. In dry environments, varying the WOB and drill bit rotating speed greatly affects the COF. Higher speeds and low loads resulted in reduced COF while low speeds and high load portrayed increased COF. For wet environments, different nanoparticles were used in water-based and oil-based fluids. The oil used was environmentally friendly and biodegradable vegetable oil named castor oil. The nanoparticles (NPs) of bentonite, attapulgite, sepiolite and cellulose nanocrystals (CNC), were used as additives in drilling muds, to reduce the COF. These NPs were successful in the reduction of COF, but they performed better in the oil-based fluids than in the water-based fluids.

Declaration

I declare that this report is my own, unaided work. I have read the University Policy on Plagiarism, and hereby confirm that no Plagiarism exists in this report. I also confirm that there is no copying nor any copyright infringement. I willingly submit to any investigation in this regard by the School of Chemical and Metallurgical Engineering and I undertake to abide by the decision of any such investigation.

Signature

04/11/2019

Date

Dedication

To Deliwe,

My little sister,

My light during the darkest of times,

May this be motivation to shoot for the stars,

And follow your passions no matter how complicated they may be.

Love you eternally.

Acknowledgement

I would like to take this opportunity to thank my amazing supervisor, Dr. Diakanua Nkazi, for his never-ending encouragement and motivation throughout my research work. There were times when I lost hope and didn't have the strength to push on, but he was always there, believing in me and cheering me on till the very end. For sharing his knowledge and wisdom, I will forever be grateful.

To my co-supervisor, Prof. Peter Olubambi, words can never explain how grateful I am to him for opening up his doors for me. For sharing his expertise and allowing me to use his research facilities to conduct my experiments, I am forever indebted to him.

A great thank you to Dr. Hembe Mukaya for his assistance in everything I needed during this research period. For always being available to listen to and solve my never-ending challenges, I will forever be thankful. You gave your time so willingly and thank you so much for never being too busy or too tired to assist.

To my friends and family who were my pillars of strength, my guides, my motivation, my counsellors, I have no words to express how grateful I am, because this journey would not have been possible without you.

Table of Contents

Abstract	- 1 -
Declaration	- 2 -
Dedication	- 3 -
Acknowledgement	- 4 -
LIST OF TABLES	- 10 -
CHAPTER ONE	- 11 -
INTRODUCTION	- 11 -
1.1 BACKGROUND	- 11 -
1.2 PROBLEM STATEMENT	- 13 -
1.3 AIM	- 14 -
1.4 RESEARCH OBJECTIVES	- 14 -
CHAPTER TWO	- 15 -
LITERATURE REVIEW	- 15 -
2.1 DEEP DRILLING PROCESS AND TRIBOLOGY	- 15 -
2.3 Wear	- 17 -
2.3.1 Characteristics of Wear	- 18 -
2.3.2 Wear of PDC bits	- 19 -
2.4 BIT TOOL MATERIALS	- 19 -
2.5 ROP AND SELECTION OF DRILLING PARAMETERS	- 20 -
2.5.1 Geological Drilling Process	- 21 -
2.6 TRIBOLOGICAL SURFACE MODIFICATION	- 24 -
2.7 RHEOLOGY AND VISCOSITY OF FLUIDS	- 25 -
2.8 LUBRICATION	- 25 -
2.8.1 Lubricants in Drilling Fluids	- 27 -
2.8.1.1 Biodegradable Lubricants	- 27 -
2.8.2 Fluid Behavior	- 30 -
2.8.2.1 Newtonian fluid behaviour	- 30 -
2.8.2.2 Non-Newtonian Lubrication	- 31 -
2.8.3 Lubricants Classification	- 32 -
2.8.3.1 Oil-Based Mud	- 32 -
2.8.3.1.1 Vegetable oils as base stocks for bio-lubricants	- 35 -
2.8.3.1.2 Castor Oil as an oil base	- 36 -
2.8.3.2 Water-based mud (WBM)	- 38 -

2.9 USE OF NANOPARTICLES IN DRILLING FLUIDS	38 -
CHAPTER THREE	46 -
3.0 METHODOLOGY	46 -
3.1 MATERIALS	46 -
3.2 EQUIPMENT DESCRIPTION	47 -
3.3 HARDNESS TESTING	49 -
3.4 XRF ANALYSIS	49 -
3.5 XRD ANALYSIS.....	50 -
3.6 SCANNING ELECTRON MICROSCOPY/ ENERGY DISPERSIVE SPECTROSCOPY (SEM/EDS) ANALYSIS.....	50 -
3.7 SYNTHESIS OF DRILLING MUDS	51 -
3.8 FRICTION AND WEAR TESTS	51 -
3.8.1 Test Conditions.....	51 -
CHAPTER FOUR.....	53 -
4.0 RESULTS AND DISCUSSIONS.....	53 -
4.3 XRD ANALYSIS.....	66 -
4.5 DRY TESTING	70 -
4.5.1 Stainless Steel ball/Rock disc contact under dry conditions	70 -
4.6 USE OF NANOPARTICLES IN DIFFERENT CLAYS USING FRESH WATER AND SEA WATER.....	84 -
4.6.1 Freshwater as the Base Fluid	84 -
4.6.2 Seawater as the Base Fluid.....	86 -
CHAPTER FIVE	89 -
5.0 CONCLUSIONS AND RECOMMENDATIONS.....	89 -
REFERENCES.....	92 -

LIST OF FIGURES

CHAPTER 2

Figure 1: Components of the Drill String (MacDonald et al., 2001).....	16 -
Figure 2: Improvement in the rate of penetration (ROP) (Abdo and Haneef, 2011).....	41 -
Figure 3: {A}: Rock samples (i) Quartzite, (ii) Fine-grained Arkose Sandstone (iii) Coarse-grained Arkose Sandstone. {B}: 6 mm diameter stainless steel balls from Anton Paar.	46 -
Figure 4: The Ball-on-disc CETR-UMT-2 Tribometer from Anton Paar used in dry testing (University of Johannesburg, 2019).....	47 -
Figure 5: Sample holder from the ball-on-disc tribometer used in wet testing (University of Johannesburg, 2019)	48 -
Figure 6: The Ball-on-disc CETR-UMT-2 Tribometer from Anton Paar used in wet testing (University of Johannesburg, 2019).....	49 -
Figure 10: Section of the Quartzite showing different phases available	54 -
Figure 11: SEM image showing the clean surface of the Quartzite rock sample	55 -
Figure 12: EDS elemental analysis of the clean surface of the Quartzite rock sample	55 -
Figure 13: SEM image showing the contaminated surface of the Quartzite rock sample	56 -
Figure 14: EDS elemental analysis of the contaminated surface of the Quartzite rock sample	57 -
-	
Figure 15: Section of the fine-grained sandstone showing different phases available	58 -
Figure 16: SEM image showing the clean surface of the fine-grained sandstone rock sample	59 -
-	
Figure 17: EDS elemental analysis of the clean surface of fine-grained sandstone rock sample.....	59 -
Figure 18: SEM image showing the contaminated surface of the fine-grained sandstone	60 -
Figure 19: EDS elemental analysis of the contaminated surface of the fine-grained sandstone rock sample	61 -
Figure 20: A section of the Coarse-grained Sandstone showing different phases of the rock sample	62 -
Figure 21: SEM image showing the clean surface of the coarse-grained Sandstone	63 -
Figure 22: EDS elemental analysis of the clean surface of the coarse-grained sandstone	63 -

Figure 23: SEM image showing the contaminated surface of the coarse-grained sandstone rock sample - 64 -

Figure 24: EDS elemental analysis of the contaminated surface of the coarse-grained sandstone rock sample - 65 -

Figure 7: X-ray Diffractogram of Quartzite - 67 -

Figure 8: X-ray Diffractogram of Coarse-grained Sandstone - 68 -

Figure 9: X-ray Diffractogram of Fine-grained Sandstone - 68 -

Figure 25: Coefficient of friction for different rock materials at 100 rpm under dry conditions ... - 70 -

Figure 26: Coefficient of friction on different rock materials at 200rpm under dry conditions - 72 -

Figure 27: Coefficient of friction on different rock materials at 300 rpm under dry conditions - 73 -

Figure 28: The coefficients of friction at 1 N using speeds of 100 rpm, 200 rpm, and 300 rpm ... - 74 -

Figure 29: The coefficients of friction at 3N using speeds of 100 rpm, 200 rpm, and 300 rpm- 75 -

Figure 30: The coefficients of friction at 5 N using speeds of 100 rpm, 200 rpm, and 300 rpm ... - 75 -

Figure 31: The coefficients of friction at 7 N using speeds of 100 rpm, 200 rpm, and 300 rpm ... - 76 -

Figure 32: The coefficients of friction at 9 N using speeds of 100 rpm, 200 rpm, and 300 rpm ... - 77 -

Figure 33: Coefficient of friction on different rock materials at 300 rpm using 25 wt% of additives in the water - 78 -

Figure 34: Coefficient of friction on different rock materials at 300 rpm using 50 wt% additives in the water..... - 79 -

Figure 35: Coefficient of friction on different rock materials at 300 rpm using 25 wt% additives in castor oil..... - 80 -

Figure 36: Coefficient of friction on different rock materials at 300 rpm using 50 wt% additives in castor oil..... - 81 -

Figure 37: Coefficients of friction for fine-grained sandstone under different lubrication concentrations - 82 -

Figure 38: Coefficients of friction for coarse-grained sandstone under different lubrication concentrations - 82 -

Figure 39: Coefficients of friction for quartzite under different lubrication concentrations ... - 83 -

Figure 40: Coefficients of friction for different rock types when using CNC-Bentonite-Freshwater solution at 300 rpm..... - 85 -

Figure 41: Coefficients of friction for different rock types when using CNC-Attapulgite-Freshwater solution at 300 rpm..... - 85 -

Figure 42: Coefficients of friction for different rock types when using CNC-Sepiolite-Freshwater solution at 300 rpm..... - 86 -

Figure 43: Coefficients of friction for different rock types when using CNC-Bentonite-Seawater solution at 300 rpm - 87 -

Figure 44: Coefficients of friction for different rock types when using CNC-Attapulgite-Seawater solution at 300 rpm..... - 87 -

Figure 45: Coefficients of friction for different rock types when using CNC-Sepiolite-Seawater solution at 300 rpm - 88 -

LIST OF TABLES

CHAPTER 2

Table 1: ASTM specification for Quality Castor Oil (Pradhan et al., 2012)	37 -
Table 2: Parts of the CETR-UMT-2 Tribometer equipment.....	48 -
Table 4: Major compounds found in the three rock samples Quartzite, Coarse-Grained Sandstone and Fine-Grained Sandstone.....	53 -
Table 5: Chemical composition of the clean surface of the Quartzite rock sample.....	56 -
Table 6: Chemical composition of the contaminated surface of the Quartzite rock sample ...	57 -
Table 7: Chemical composition of the clean surface of the fine-grained sandstone rock sample ..	60 -
Table 8: Chemical composition of the contaminated surface of the fine-grained sandstone rock sample	61 -
Table 9: Chemical composition of the clean surface of the fine-grained sandstone rock sample ..	64 -
Table 10: Chemical composition of the contaminated surface of the coarse-grained sandstone rock sample	65 -
Table 3: Load at failure for rock samples during Uniaxial Compressive Strength testing	69 -

CHAPTER ONE

INTRODUCTION

1.1 BACKGROUND

To add to the ever-increasing demand for oil and gas, large discoveries have been made in deep-sea areas. This has been a game changer for the Petroleum industry, though deep-sea drilling has been found to face multiple technical challenges (Shaughnessy *et al.*, 2007; Wang *et al.*, 2018; Zhao *et al.*, 2017). These challenges may include unstable wellbore (Gradishar *et al.*, 2014; Zamora *et al.*, 2000), increased drilling depths which result into increased daily drilling costs as compared to onshore drilling processes (Gao *et al.*, 2019) and increased operating temperatures and pressures which also add significantly to the cost of drilling (Wang *et al.*, 2018).

During rotary drilling processes, which is the most common type of drilling, the drill bit is connected at the far end of the drill string operated from the surface using a rotary table. The drill bit breaks into the formation due to the weight that is applied by the drill string. The energy to drill is passed through the drill string to the drill bit and its magnitude is determined by the highest torque that the drill string can handle. During this drilling process, the drill string and drill bit are constantly in contact with the casing and the rock formation resulting in friction due to the drag on the drill string and drill bit. To combat this friction, more power is needed in rotating the drill string. The friction between the drill string and casing or formation may be greater than the torque on the drill string. In this case, the best solution would be to improve the lubricity of the drill fluids (Foroulis and Tsao, 1987).

The rate of drilling a hole is primarily dependent on the rotating speed of the drill string and the weight at the bottom or the force used by the drill bit to break into the rock. The force is governed by adding drill collars on the drill string as they have a greater diameter and greater mass than the drill string. This makes it possible to minimize friction while increasing the horsepower of the drill bit. In some offshore drilling operations, the vital rig expenses are \$50 000.00 or higher per day. It is therefore of great importance to drilling at high rates of penetration (ROP) using minimal equipment and power (Dodd, 1978).

Drilling muds also help in the increase of the rotating torque and pipe drag. To improve the lubricating effect of bentonite, additives that include saturated and unsaturated fatty acids, natural triglycerides, vegetable oils, sulfated fatty acids, and alcohols are used (Dodd, 1978).

To improve the lubricity of the drilling fluids, bentonite is usually added as it reduces the friction between the drill string and the formation. Other drilling fluids used to reduce friction are diesel and other mineral oils as they are known as lubricants, but there are environmental concerns when it comes to deposition of the drilling fluids when it comes to these types of lubricants (Foroulis and Tsao, 1987).

There are different types of drill bits used in the oil and gas industry, and they include the roller cone bit which is the most popular one due to its aggressive cutting mechanism and high penetration rates (Dougherty *et al.*, 2014; Koltermann and Dick, 2009). The bit is usually rotated from the surface using the drill string or by the use of a bottom-hole motor. The drill bit is secured with cutters or cones that engage with the formation as the drill string rotates. The cutters are equipped with teeth that penetrate the bottom-hole due to the exerted weight from the drill string (Koltermann and Dick, 2009).

The drill bits are equipped with lubrication systems that increase the life span of the bit through friction reduction. Apart from the bearing and lubrication improvements, technology advancements are still needed to increase the performance of the bearing system hence improve the life of the bit. The polycrystalline diamond (PDC) bit has been anticipated to have the potential to increase the wear resistance of bearing tools in the deep hole (Koltermann and Dick, 2009).

Tribology is a science that has been employed to solve challenges of deep oil and gas drilling. It includes the effects of friction, wear, and lubrication at the interface of the contacting surfaces (Boneh and Reches, 2018). The contacting surfaces may be the drill string and the drill bit against the formation or the well casing. Tribology makes this study easier as it allows a simultaneous study of friction and wear, and how they are affected by different lubrication systems (Dougherty *et al.*, 2015).

The lubrication of drilling fluids is a very important factor in rock bits in ensuring the prolonged life span of the drill bits. The drilling mud and rock debris create an abrasive environment which is common for a drilling process, therefore, it is imperative to formulate a drilling fluid that will serve as a lubricant in high temperature and pressure environments of diamond bearing structures (Koltermann and Dick, 2009).

In this research, stainless steel balls were used to investigate the stainless steels' friction and wear behavior when used against sedimentary rock formations of sandstone and quartzite. This knowledge was used to solve the friction, wear problems of drill bits, and suggest the best-operating conditions suitable for different formations.

1.2 PROBLEM STATEMENT

The world energy demand is continuously increasing and this together with the decreasing production from major production sites in the world, has led to the exploration of different areas such as deep offshore operations. This move faces challenges that could arise due to changes in drilling depth, the complex drilling processes and mostly harsh environmental restrictions from numerous governing structures (Shah *et al.*, 2010). For a successful drilling operation, it is of paramount importance to know and understand these challenges to provide appropriate mitigation strategies.

Drilling of deep formations results in increased operational costs because of the hard rock encountered, longer drilling depths and equipment that is not equipped for such drilling operations (Wang *et al.*, 2017). Dougherty *et al.*, (2015) concluded that the drilling costs increase with depth, as it gets harder and harder as the depth increases and equipment usually breaks down resulting in lost time and replacement of worn out bits (Beste and Jacobson, 2008; Lyons *et al.*, 2008).

To solve these challenges, improved technology was introduced into the drilling process such as introduction of diamond and tungsten carbide manufactured drill bits which possess good frictional and wear resistant properties that operate effectively under complicated bottom-hole conditions (Beste, 2002). The exceptional blend of hardness and toughness is the driving factor that makes these tools applicable for wear resistant parts for rock drilling equipment. The friction

and wear data of a particular rock drill bit within a certain rock type is a characteristic of that specific situation and would not necessarily be applicable to other rock drill bits in other rock types (Beste, 2004).

A successful drilling operation means achieving very little friction between the drill string and the formation and casing (Green *et al.*, 2007). Reduced friction means maximized production and reduced COF and reduced non-productive time (NPT) (Wang *et al.*, 2018). For a drilling process, the solution to high friction and drag experienced is the use of drilling which lubricates the contacting interface (Ling *et al.*, 2013).

A clear comprehension of the influence of drilling fluid rheology on the drilling process is needed to particularly design drilling muds that could sustain a variety of challenges experienced when drilling. The major concern, which has attracted considerable attention, is the modification of the available drilling tools to operate under the extreme conditions of high pressures and temperatures, and high friction and wear conditions.

This therefore means that research work should be conducted to clearly measure the friction between the drill bit in different rock surfaces and determine how the use of different drilling fluids reduce the friction. This is going to be the focus of this research.

1.3 AIM

This research aims to provide guidance to increase the effectiveness of a drilling process by successfully reducing the coefficient of friction (COF). The drilling parameters such as weight on bit (WOB), drilling rotation speed and lubrication were studied extensively to determine their influence on the COF when used in different rock formations.

1.4 RESEARCH OBJECTIVES

- To determine how mineral composition of different rock types affect their drillability;
- To investigate the effect of drill bit rotation speed (DBRS) and the weight on bit on the COF using different rock types;
- To analyse the drill bit frictional behaviour against different rock types in dry and wet drilling conditions;

CHAPTER TWO

LITERATURE REVIEW

2.1 DEEP DRILLING PROCESS AND TRIBOLOGY

Conventionally, a drilling process involves drilling a well using either a drill string where a drill bit is connected at the bottom and a hollow unit being a jointed pipe or coiled tube that is connected to the drilling assemblage and extends to the top. When drilling has been completed on one part of the well, the drill string is pulled back to the surface and a casing is placed to maintain the well stability. After casing, further drilling and casing continue alternatively until the desired length is reached (Hahn and Makohl, 2002).

A drilling process cannot be made possible without the use of a drill rig. The bottom section of the rig is made up of three parts, the bottom-hole-assembly (BHA), the transition pipe and the drill pipe (Macdonald and Bjune, 2007). The BHA is composed of the drill collar that breaks the rocks and the drill bit, the heaviest component of the bottom-hole-assembly that is designed with a tube which enables passage of the drilling fluid to be pumped through then send back to the annulus as shown by Figure 1 (4A). The next section is the heavy weight-drill-pipe (HWDP) that allows and simplifies transition from the drilling collar to the drill pipe. It aids to reduce fatigue failures occurring just above the BHA and adds more weight on the drill bit, demonstrated by Figure 1 (4B) (Albdiry and Almensory, 2016; MacDonald *et al.*, 2001). Lastly, the drill pipe which is known as the major constituent of the drill string that leads back to the surface (Albdiry and Almensory, 2016). This is illustrated in Figure 1 (4C) (MacDonald *et al.*, 2001).

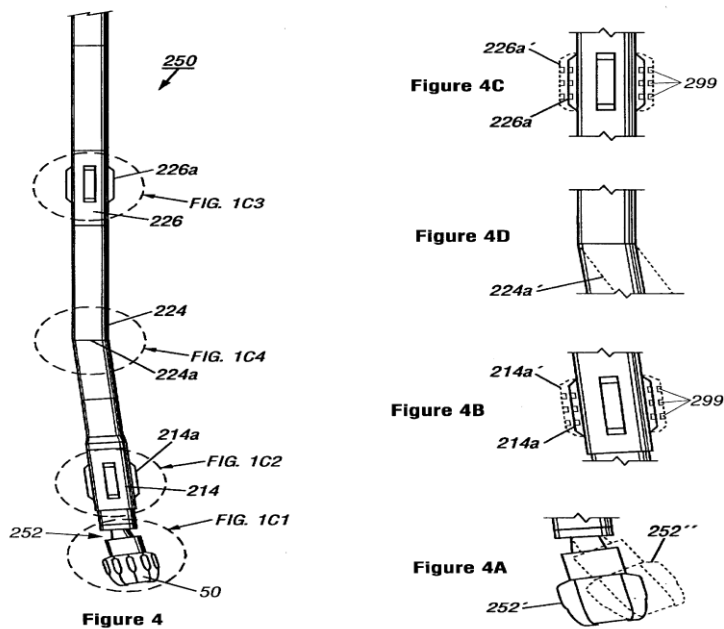


Figure 1: Components of the Drill String (MacDonald et al., 2001)

The BHA is equipped with sensory equipment that determines the well-being of the BHA, the state of the hole, the characteristics of the formation and monitors the chemical and physical characteristics of the drilling mud. The sensory equipment also evaluates the bedrock border environment, around and before the bit, the seismic maps and required drilling parameters which include WOB, drilling bit speed and the flowing rate of the drilling mud. The down-hole processor regulates the operations of the multiple devices in the hole to ensure effective changes on the drilling parameters and drilling course to enhance the drilling efficiency (MacDonald *et al.*, 2001).

2.2 Friction

In all processes that involve motion, there is always some resistance to motion, and this occurs in the form of friction. The results of this friction are due to physical contact between two bodies in relative motion. Classification of friction can be in two parts; based on the type of motion involved which could be sliding or rolling friction or based on the material involved which could be dry friction, air friction or friction under lubrication system (Allen and Ball, 1996a).

For a dry static condition, when the load applied tangentially to the contacting surfaces goes beyond a certain value, gross sliding then occurs. In this case, the following rules apply experimentally;

In the presence of tangential motion between two bodies in contact, the friction force always opposes the relative velocity of the contacting surfaces.

The friction force becomes proportional to the normal force.

$$F_F = f F_N \quad \text{eq 1}$$

This relationship makes the definition of the coefficient of friction easy,

$$f = F_F / F_N \quad \text{eq 2}$$

Where: F_F = Friction Force, lbf

F_N = Normal Force, lbf

f = Friction coefficient

The friction force is independent of the nominal geometric contacting area. When two surfaces are contacting each other through an apparent geometric area, only their asperities are in contact and this is called micro-contacts. The added micro-contacts give the actual area of contact carrying the normal load (Allen and Ball, 1996b).

The cleanliness of a surface is the greatest determining factor for friction, but deformation properties also play a significant role. Minimal traces of oxygen or contaminants can greatly reduce adhesion and friction, due to this observation, lubrication concept was introduced within all tribological processes which may include contact, friction, and wear processes physically interacting surfaces in relative motion (Allen and Ball, 1996a).

2.3 Wear

The wear of equipment and machinery used for many industrial purposes results in challenges such as unexpected breakdowns leading to serious financial losses. Small material losses on the

equipment cause a reduction in the performance of the equipment resulting in lost time. Wear can also cause material failure by brittle fracturing, fatigue or stress corrosion cracking (Allen and Ball, 1996a).

2.3.1 Characteristics of Wear

Wear can be characterized into three main classes, and these are; abrasive, adhesive and erosive.

2.3.1.1 Abrasive wear

Abrasive wear includes mechanisms such as scoring, gouging, cutting, ploughing and micromachining and is typical for rock or sand particles moving relative to a metallic surface. Abrasive wear can occur at the continuous load of the rock particles and this is known as two-body or low-stress abrasion or it can also occur where a third body causes the displacement of the particles and this is referred to as three-body or high-stress abrasion. The stresses, strains and strain rates are very high and confined in this type of wear (Allen and Ball, 1996a).

2.3.1.2 Adhesive wear

Adhesive wear includes galling, fretting, scuffing and surface fatigue. The damage results when two surfaces in contact are moving relative to each other at normal load. The surface asperities on the contacting surfaces connect resulting in high stress, strain and strain rates at local regions. The continuous interaction at the interface normally results in increased interface temperatures. Thermal fatigue, recrystallization, and phase transformations are also common under adhesive wear (Allen and Ball, 1996a).

2.3.1.3 Erosive wear

This describes the damage caused as a result of particles that move in a fluid stream of either a gas or liquid. Erosive damage happens at individual microscopic strikes and continuous strikes are needed to result in eventual material loss. The factors influencing the severity of erosive wear include size, mass, shape, and velocity of the erosive particles together with their angle of impact. The area of impact is exposed to very high stresses, strains, and strain rates where heat may be generated due to the impact energy. In such conditions, oxidation can easily occur, and corrosion can lead to total material losses in aqueous surroundings (Allen and Ball, 1996a).

2.3.2 Wear of PDC bits

The major tools used in the drilling of oil and gas are the roller cone bits and the drag bits. The roller cone bits operate by an impact excavation method and mainly function in very hard formation due to their high wear resistance. The drag bits operate by shearing mode mostly used in soft to medium-hard rock formations. However, they are affected by thermal abrasion wear while drilling inter-bedded rock formations. Their operation creates frictional forces that generate heat. Drilling costs are reduced when using drag bits with PDC cutters than when using roller cone bits. Wise *et al.*, (2002) found that PDC bits drill faster and longer than the roller cone bits in hard formations.

Drag bits are usually destroyed through abrasive wear (Ersoy and Waller, 1995) and their quality can be defined by the material wear rate and excavation activity. The PDC bit is very adaptable hence they can be used in a variety of rock formations such as soft to medium hard rock (Brett *et al.*, 1989; Bruton *et al.*, 2014; Pessier and Damschen, 2011). Despite this advantage, wear of PDC bits during drilling sometimes results in drill bit failure. The PDC is composed of individual cutters mounted all over the surface of the bit and the wear of this cutters is the main reason for the PDC bit failure (Appl *et al.*, 1993). This wear results in increased destruction of the PDC bits leading to reduced drilling efficiency.

Appl *et al.*, (1993) observed that the heat generated by the cutters highly reduces the bit operating life. Even though the PDC drag bit is very effective, the shearing ability of this bit results in large friction forces at the cutter/rock interface. The vigorous flow of the drilling fluid around the cutters affects the cutter temperature through the following ways;

- Provision of the overall heat removal from the contacting surfaces
- Lubricating the interface of the cutters and the rock
- Removal of rock debris and other obstructions affecting the cutting effectiveness.

2.4 BIT TOOL MATERIALS

In the oil and gas industry, of the three types of drilling, which are rotary/percussive drilling, rotary/crushing drilling and cutting; rotary/percussive drilling is the popular one. Modern rotary bits have been manufactured since the 1800s and have since undergone some improvements. There were also fishtail bits produced from black diamond steel having 0.3% carbon content.

The fishtail bits drilled faster than the three and flour-blade bits, but they did not last as long. Different water and oil quenching methods were used to prolong the life of the fishtail bits in the year 1909. In 1922, hard facing was incorporated on the fishtail bits and this greatly improved their wear (Allen and Ball, 1996a).

Drilling bits were developed further by welding steel on the surface of the bit. Drag bits were developed by the replacement of the steel alloy treated blades with tungsten carbide, which exhibits greater hardness and resistance to corrosion and wear. In 1973, a technique was developed to bind synthetic diamonds on tungsten carbide substrate by General Electric Company. After this development, the Polycrystalline Diamond Compact (PDC) bits were manufactured (Allen and Ball, 1996a).

The PDC bits are the advanced or high technology drag bits. This type of bit consists of a solid head with cutters welded onto the surface. The PDC bits differ in shape, size, number, and position of the cutters and the design of the hydraulic system. These are the determining factors for the performance of the drill bits. They have been found to have long life in bottom-hole drilling due to the absence of moving parts and the use of synthetic diamond, making them highly wear resistant. The PDC bits were announced as the replacement to the roller cone bits as they proved more efficient and cost-effective (Allen and Ball, 1996a).

At high temperatures over 350°C, the synthetic diamond was found to deteriorate quickly losing its strength and abrasive resistance. Therefore, these drill bits faced great challenges when drilling hard abrasive rock formations like granite and quartz, as these formations create high friction at the rock/bit interface such that the drilling fluid is ineffective in cooling the drill bit. The presence of this friction at the interface means that there is heat produced due to shearing of the PDC cutters against the rock surface (Allen and Ball, 1996a).

2.5 ROP AND SELECTION OF DRILLING PARAMETERS

The rate of penetration (ROP) is very important as it is the main factor that determines the effectiveness of a drilling operation in very complicated geological locations (Gan *et al.*, 2019). The improvement of the ROP has proven to be very essential as a result of increasingly depleting shallow resources leading to the discovery of mineral resources in deep geological locations

(Fetting, 2016). The optimization (Gan *et al.*, 2018a, 2018b) and control (Haber *et al.*, 2009; Pavković *et al.*, 2011) of the ROP for a successful drilling operation is still challenging due to complexity of drilling conditions which include high pressure, high temperature, and interchange between soft and hard formations.

The ROP can be defined as the footage of the drill bit per unit time and it is highly influenced by these major factors: formation drillability (FD) (Ataei *et al.*, 2015; Ma, 2011; Zhang *et al.*, 2011), mud logging parameters and operating drilling parameters (Deng *et al.*, 2016; Guan and Chen, 2006). The formation drillability is a comprehensive guide that quantifies the difficulty of the rocks to be broken down by the drill bit. It is influenced by the following aspects: seismic parameters, well-logging parameters, mud logging parameters and operating drilling parameters (Ma, 2011). The calculation of the FD is highly needed in the proper prediction of the ROP.

2.5.1 Geological Drilling Process

The characteristics of the drilling process in relation to the ROP model are summarized as follows (Gan *et al.*, 2018):

- a. The complexity in the geological drilling locations: The complexity here is the result of drilling through a variety of formations to get to the target zone, where the formations vary greatly, as well as the hardness and plasticity of the rocks as the drilling depths increase (Gan *et al.*, 2018).
- b. Security challenges: The alternating soft and hard rock formations and the natural deflecting rule of the formation create serious safety challenges such as collapsing, shrinkage, mud loss, and loss of drilling equipment in the drilled well (Gan *et al.*, 2018).
- c. Different kinds of drilling parameters: The drilling parameters can be classified into five groups (Gan *et al.*, 2018):
 - I. Seismic parameters:

These define the formation attributes and they are collected before the drilling process is initiated. The parameters involved here include seismic velocity, seismic wave time, and seismic wave impedance (Gan *et al.*, 2018).

- II. Operational drilling parameters:

These include weight-on-bit (WOB), rotations per minute (RPM), flow rate (Q), and the kind of drill bit used. These are the parameters which are in the elementary control loops of the process. The first three parameters are determined using sensory equipment in the drilling rig, then the type of drill bit is chosen depending on the specific drilling requirements (Gan *et al.*, 2018).

III. Mud logging parameters:

The mud logging parameters are mud weight (MW), mud viscosity, temperature, and drilling depth. They are also included in the basic control loops of the process. They can indirectly show the condition of the bottom-hole formation and drill bit through the mud (Gan *et al.*, 2018).

IV. Well logging parameters:

These logging parameters are gamma ray, porosity, and resistivity, and they indicate the formation characteristics. They clearly show the state of bottom-hole formation by use of sensory equipment located in the bottom-hole assembly. Another set of well logging parameters include inclination angle and azimuth angle, which define the drilling course (Gan *et al.*, 2018).

V. Formation characteristic parameters:

The formation characteristic parameters are formation drillability (FD), uniaxial compressive stress (UCS) the pore pressure. They are important parameters in the process, as they clearly indicate the type of the drilling field (Gan *et al.*, 2018).

d. Strong non-linearities:

The drilling process is non-linear. There exists a strong fluid-solid-heat interactive reaction amongst the drill string, drill bit, mud, and rock formation. Because of this, the relationship between the five main parameters becomes complex and non-linear (Gan *et al.*, 2018).

e. Couplings: These parameters can couple in any of the following ways (Gan *et al.*, 2018);

i. Couplings between seismic and well logging parameters: These parameters indicate the formation characteristics and they work one besides the other.

ii. Couplings between mud logging and operational drilling parameters: The mud logging and operational drilling parameters are the mechanical drilling parameters, which also work hand in hand.

- iii. Couplings between seismic, operational drilling, mud logging, well logging, and formation characteristic parameters: These are the parameters, which directly influence the ROP.
- f. Incomplete Data: The data during drilling always seems to be incomplete because of the time sequence of several drilling data, which is inconsistent (Gan *et al.*, 2018).

The five main drilling parameters have proven to have varied influences on the drilling ROP. The operating drilling parameters mostly interrelate with the WOB and rotational speed. There are four main ideas used in the evaluation of the drilling effectiveness and these are drilling costs, ROP, drill bit life and drill bit's specific energy (Gan *et al.*, 2018).

The life of the drill bit is also important in the determination of drilling efficiency and is dependent on the wear rate of the bit tooth and bit (Schorode *et al.*, 2016; Zha *et al.*, 2017). The specific energy of the drill bit is the mechanical work performed to drill a certain volume of rock and could give an evaluation of the drilling efficiency (Chen *et al.*, 2016; Li *et al.*, 2015).

The rate of penetration can be expressed in the following equation (Gan *et al.* 2018):

$$ROP = K_R C_P C_H (W - M) N^\lambda \frac{1}{1 + c_2 h} \quad \text{eq 3}$$

Where K_R is the coefficient of formation drillability,

C_P is the coefficient of pressure difference,

C_H is the coefficient of drill hole cleaning,

W is the weight on bit (KN)

M is the threshold of weight on bit (KN),

N is the rotational speed (r/min),

λ is the coefficient of the rotational speed,

h is the wear of the drill bit, and

C_2 is the coefficient of the wear of the drill bit (Gan *et al.* 2018).

The life of the drill bit T_f is dependent on the wear speed of the drill bit tooth and bearings, and is calculated by the following equation (Chen *et al.*, 2016) (Gan *et al.* 2018):

$$T_f = \left[\left(\frac{C_1}{2} + 1 \right) - \left(\frac{C_1}{2} h^2 + h \right) \right] \frac{D_2 - D_1 W}{A_f (a_1 N + a_2 N^3)} \quad \text{eq 4}$$

Where C_1 is the reduction coefficient of drill bit's wear,
 D_1 and D_2 and are the influence coefficient of weight on bit,
 A_f is the coefficient of the formation grindability,
 A_1 and a_2 are the influence coefficient of rotational speed, and
 h , W , and N are as mentioned in Eq. 1 (Gan *et al.* 2018).

2.6 TRIBOLOGICAL SURFACE MODIFICATION

In any type of operation, the tribological surfaces are usually modified due to the composition, structure, hardness and other characteristics induced by tribological action. The new type of surface exhibited friction and wear properties that are different from the original bulk material (Jacobson and Hogmark, 2009; Vingsbo and Hogmark, 1981). This is because the properties at the interface are constantly changing over prolonged use.

The surface modifications usually include topography changes, which are smoothening or roughing of the original surface, forming micro-cracks, phase transformations, deformation hardening, the formation of oxides, and solid films and the transfer of material from one surface to the other. The thickness of these layers varies depending on the type of actions taking place at the interface (Jacobson and Hogmark, 2009).

During the drilling process, the wear behavior of cemented carbide drill buttons is affected by the composition and microstructure of the carbide material and the drilling conditions such as drilling parameters, drill button geometry and the nature of the rock material. All these differences mean that the cemented carbide is exposed to different mechanical and thermal stresses (Olsson *et al.*, 2017).

For conditions of high mechanical and thermal stresses, which are common for rocks with high abrasivity such as granite, the wear on the cemented carbides is usually a smooth layer with roughness restricted to the individual WC grains. When the conditions have changed to moderate mechanical and thermal stresses typical of rocks with softer abrasivity such as magnetite, the damage on the buttons become macroscopic surface patterns known as reptile skin. If the reptile skin is not repeatedly ground off, the patterns will eventually lead to cracks resulting in

catastrophic fracturing of the button. Though the wear rate is small, the life of the drill buttons becomes affected by the cracks (Lagerquist, 1975; Larsen-Basse, 1973; Montgomery, 1968).

In percussive rock drilling, coarse-grained WC/Co CC was said to be the best material suitable for high abrasive contact against the rock formation (Beste and Jacobson, 2008). Beste (2004), however, found that the surface of the CC drill bits transforms to a different material before its removal from the bit (Beste, 2004; Beste and Jacobson, 2008; Beste *et al.*, 2006).

The small buttons on the CC are the elements that are responsible for crushing and fragmentation action of the rock drill bits. It is believed that the drilling temperature is very low to melt the rock material. Jacobson and Hogmark (2009), found that there was a layer of re-solidified rock on the CC surface. The TEM analysis showed that below the outer surface, Co-matrix of the CC was slowly intermixing with rock material before removal. The result was a completely new and different composite of a WC hard-phase composite that was held intact by a Co-enriched binder phase of quartz.

2.7 RHEOLOGY AND VISCOSITY OF FLUIDS

Rheology is defined as the study of how fluids flow and how solids are deformed when exposed to mechanical forces. Some material can be classified as ideal solids because they obey Hooke's law or ideal fluids because they obey the Newtonian law, most of them are classified under non-Newtonian fluids because they portray viscoelastic behavior which means that their response to subjected force is expressed in terms of viscous and elastic constituents. The non-Newtonian fluids have shown time-dependent properties, by having rheological properties that depend on the previously applied forces. Their response to the force is also dependent on the temperature and concentration of the individual constituents. They also show yield stress when they behave like solids under a given stress (Ibarz *et al.*, 2015).

2.8 LUBRICATION

A friction force arises when bodies slide against each other and restricts their movement at the interface. The friction force normally results in the removal of material from the surface of one or more of the contacting surfaces in a process called wear. The known and trusted mechanism to reduce the wear and friction at the interface is called lubrication (Jones, 1971).

The whole idea of lubrication is the separation of surfaces in relative motion using a film of a material that can be sheared easily because of low resistance and result in no damage to the moving surfaces. Lubrication modes can be divided into three depending on the thickness of the film, the interfacial thickness distribution of the film and the extent of geometric conformity (Allen and Ball, 1996b);

- Hydrodynamic lubrication: In this type of lubrication, the lubricating film separating the two surfaces is thicker than the combined surface portion of the interacting surfaces. The resistance of friction is the result of the internal friction of the lubricant. The tribology of the system is determined by the rheological properties of the lubricant. There is no wear in this mode of lubrication because there is no physical contact between the surfaces.
- Mixed lubrication: This occurs when the lubricant viscosity or its velocity drops or the load is decreased in hydraulic lubrication, resulting in a thinner lubricating film between the surfaces. Here, the load is divided between the fluid film and the asperities on the contacting surfaces. This means that the friction resistance is from the shearing of the lubricant and the interacting asperities. The boundary lubrication is when the interactions of the asperities are increased, decreasing the film thickness. The following characteristics are possible for this mode of lubrication (Allen and Ball, 1996b):
 - The interacting surfaces are so close together that there is great contact between asperities.
 - The hydrodynamic effects and influence on the total rheological characteristics of the lubricant are irrelevant.
 - The surface interactions of the contacting surfaces determine the tribological behaviour.
- Boundary lubrication: The processes that take place at the lubrication boundary are a factor of the physical and chemical properties of the solid/lubricant/solid interface. The solid/lubricant interaction which gives rise to the protective boundary film can be classified into the following processes (Allen and Ball, 1996b);
 - Physical adsorption
 - Chemical adsorption
 - Chemical reaction

2.8.1 Lubricants in Drilling Fluids

Lubricants are the materials added to the drilling muds to enhance their lubricity and reduce friction (Espagne *et al.*, 2014). A drilling fluid that has high lubricating effect has the potential to increase the rate of penetration, thus leading to reduced cost of drilling (Li *et al.*, 2015a). Poor lubricity of drilling fluid can bring adverse consequences such as bit bearing and casing wear, torque and drag problems and differential sticking issues (Brandon *et al.*, 1993; Brazzel, 2009; Foxenberg *et al.*, 2008).

For a lubricant to qualify as a good lubricant, it should have very high viscosity, high lubricating film strength, low corrosivity, low pour point, low flammability, high solubility, high thermal and oxidative stability, and low toxicity. The lubricants are mainly used in water-based muds (WBM) because of its inadequate lubricity and WBM are commonly used due to their desired properties of non-toxicity, affordability and biodegradable nature (Fink, 2015).

A very little amount of lubricants is needed to achieve efficient lubricity of the drilling mud. Teng *et al.*, 2013, proved that as little as 1% of the lubricant added to the drilling fluid can reduce torque by at least 20%. The commonly used lubricants are oils, graphite, powder, surfactants, and soaps (Li *et al.*, 2015a; Skalle, 2011).

2.8.1.1 Biodegradable Lubricants

Strict environmental rules on offshore and natural gas drilling has put great interest in the use of biodegradable lubricants manufactured from organic materials. It has been concluded that waste petroleum-based lubricants have high toxicity to human health and the environment and have low biodegradability (Getliff and James, 1996; Neff *et al.*, 2000). Because of this, the vegetable oil was found to be the best alternatives as they are biodegradable, easily available and non-toxic (Addy *et al.*, 1984; Atabani *et al.*, 2013; Campanella *et al.*, 2010; Darley and Gray, 1988; Mueller *et al.*, 2004). Bio-lubricants are the type of lubricants that are biodegradable and renewable (Bart *et al.*, 2012).

Performance of Drilling Fluids

The performance of bio-lubricants in the drilling fluids is determined by the study of the lubricating effect, rheological properties, filtration properties and differential sticking tendencies

of the drilling fluids. These results will determine whether the added bio-lubricants have any impact on the performance of the drilling fluids in extreme drilling environments (Kania *et al.*, 2015).

Mud lubricity

To determine the capability of drilling fluids in the reduction of friction, lubricity tests are performed. Lubricity tests reproduce the drill pipe rotation speed and the pressure which the drill pipe endures from the rock formation. The lubricity test gives the mud lubricity as the coefficient of friction and helps to determine the kind and amount of lubricant needed for each type of drilling fluid (Kania *et al.*, 2015).

The addition of lubricants has been found to reduce the coefficient of friction by 15-20% (Livescu and Craig, 2015). The coefficient of friction is also affected by the quality of the drilling fluid, filter cake, lubricant type, and concentration, interface roughness and temperature (Livescu and Craig, 2015; Maidla and Wojtanowicz, 1990). When drilling temperature increase above 50°C, the coefficient of friction is also increased.

Filtration properties

These are determined by measurement of the fluid loss and the characterization of the filter cake properties. A low fluid loss is one of the desired characteristics of drilling mud. Differential sticking of the drill pipe occurs when the drill string becomes fixed in the filter cake. This means that when the filter cake is thinner, differential sticking is reduced and vice versa (DeGeare, 2014).

Rheological properties

A viscometer is used to measure the rheology of the drilling fluids as to how the lubricants affect the flow behavior of the drilling fluids. These rheological properties include viscosity and gel strength of the mud. Argillier *et al.*, (1996) discovered that low concentrations of lubricants added to the drilling fluids does not give significant changes to the rheology of the fluids.

Studies have shown that the effects of friction are the major determining factors for elongating the bit life and these effects are much stronger than that of the convective cooling from the constantly circulating drilling mud. Enhancement of the drilling mud chemistry to reduce the coefficient of friction has been found to significantly improve the lifespan of the PDC cutters (Allen and Ball, 1996a).

The increased cost of drilling fluid may be due to increased depths of drilling, complicated rock formations and very hard to reach areas of production. To ensure a successful drilling operation that also reduces costs, drilling fluid properties must be well maintained throughout the process. The drilling fluid must also carry out functions such as cooling of the bit, lubricating the drill pipe, and efficient cleaning of the borehole. Failure to achieve these functional requirements would result in challenges such as lost circulation, rock formation destroyed, pipe sticking, borehole erosion, low bore-hole cleaning and increased torque and drag problems that largely reduce the drilling effectiveness (Abdo and Haneef, 2011; Bourgoyne *et al.*, 1986; Caenn *et al.*, 2011).

Generally, the selection and application of drilling muds is of paramount importance in ensuring the success of a drilling operation. This is because drilling muds perform multiple functions that make oil and gas production efficient and these include data collected from debris in mud during mud circulation, fluid return quantities, pressures and temperatures, are very important for efficient drilling (Darley and Gray, 1988).

To avoid these challenges, drilling fluids should be uniquely designed to operate optimally while maintaining their functionality through a range of operating conditions such as temperature, pressure, formations, and drilling environments (Torbacke *et al.*, 2014). The type of reservoir and the drilling techniques used to drill a reservoir are unique for each case, this means that the drilling mud has to be custom designed to fit each drilling process and reservoir conditions (Shah *et al.*, 2010). The rheology of a drilling fluid is of paramount importance; therefore, monitoring it throughout the drilling process is necessary, as it determines the successful operation of the drilling fluid, and helps to predict undesirable situations during drilling (Abdo and Haneef, 2011).

2.8.2 Fluid Behavior

Primarily, fluids are classified as Newtonian or non-Newtonian depending on whether or not they obey Newton's law of viscosity. Non-Newtonian fluids are further broken down into time-dependent and time-independent fluids. The time-dependent fluids have rheological properties that are only dependent on the shear stress at constant temperature, while the time-independent fluids have viscosity that is dependent on the shear stress and the amount of time that the stress has been applied on the fluid. These are the type of fluids that show viscous and elastic characteristics and they are named viscoelastic fluids (Ibarz *et al.*, 2015).

2.8.2.1 Newtonian fluid behaviour

The Newtonian fluids are fluids that show a constant viscosity at all shear rates. The relationship between the shear stress (τ) and the shear rate ($\dot{\gamma}$) is a straight line that passes through the origin (Chhabra and Richardson, 2011; Karol, 2003; Krizek and Pepper, 2004). The viscosity or Newtonian viscosity is independent of the shear strain rate and time (Ibarz *et al.*, 2015);

$$\eta(\dot{\gamma}) = \eta = \text{constant} \quad \text{eq 5}$$

For a thin layer of fluid placed between two parallel surfaces having a distance dy between them, when a force, F , is applied, this force was balanced out by the opposing internal friction forces within the fluid. For a fluid that is Newtonian and with a laminar flow, the relationship between the shear stress is the same as that of the product of viscosity and shear rate. The shear stress is then equivalent to the exerted force on the fluid per unit area and the shear rate becomes the difference in velocity with respect to y measured as the normal to the plane (Chhabra and Richardson, 2011);

$$\frac{F}{A} = \tau_{yx} = \mu \left(-\frac{dV_x}{dy} \right) = \mu \dot{\gamma}_{yx} \quad \text{eq 6}$$

Where F is the force applied

A is the surface area of contact

μ is the coefficient of dynamic viscosity

τ is the shear stress

γ is the shear rate

and the subscript yx in τ and γ show that the direction of the motion is normal to shear force, while the second subscript shows the direction of fluid flow.

The coefficient of dynamic friction is also known as the Newtonian viscosity and it depends on the type of material, temperature, and pressure. The plot of the shear stress against the shear rate is called a rheogram and its slope is the μ which known as the Newtonian viscosity and it is used to fully define the fluid flow behavior (Haldenwang, 2003).

Taylor (1997) established that fluids that have a simplified and stable molecular organization seem to obey the Newtonian law, and these may include water and some very thin motor oils. Gases, simple organic liquids, solutions made from low molecular weight organic salts, as well as molten metals and salts are Newtonian fluids (Chhabra and Richardson, 2011). Basically, Newtonian fluids are those fluids whose viscosity remains the same no matter the viscometer type used and at any given temperature (Brookfield Engineering Labs Inc., 2010).

2.8.2.2 Non-Newtonian Lubrication

A non-Newtonian fluid is a fluid that has a flow curve that is non-linear or that is not passing through the origin. This means that the apparent viscosity, which is the ratio between the shear stress and the shear rate, is not a constant at any given temperature and pressure but depends on the flow conditions such as flow geometry and shear rate (Chhabra and Richardson, 2011).

For non-Newtonian fluids, the viscosity is dependent on the shear strain rate and the apparent viscosity (Ibarz *et al.*, 2015);

$$\eta_a = \frac{\sigma_{12}}{\gamma} = \eta(\gamma) \quad \text{eq 7}$$

Non-Newtonian fluids are known to have a mixture of constituents that consist of a variety of shapes and sizes. As these particles move past each other during flow, the forces that are needed to initiate their motion are highly determined by the size, shape, and cohesiveness of the particles (Brookfield Engineering Labs Inc., 2010).

Caenn *et al.*, (2011) mentioned that for suspensions such as drilling fluids which usually contain huge particles than those of water molecules, do not obey the Newton law, therefore these are classified as the Non-Newtonian fluids. The shear rate and shear stress ratio of these drilling fluids depends on the composition of the fluid.

2.8.3 Lubricants Classification

A drilling fluid is an intricate fluid composed of multiple additives. There are Newtonian and non-Newtonian fluids used in the drilling of oil. Drilling muds can easily be classified as water-based mud (WBM), oil-based mud (OBM) and synthetic based mud (SBM), emulsions, air and foam (Caenn *et al.*, 2011).

The drilling fluids are normally classified according to the type of base fluid used (Caenn *et al.*, 2011);

- Water-Based Fluids (WBFs) – The water becomes the continuous phase and solids are suspended in it or in brine, or sometimes oil may be emulsified in water.
- Oil-Based Fluids (OBFs) – The oil becomes the continuous phase and the solids are suspended. The water or brine may be emulsified in the oil.
- Gas – A flow of air or natural gas can be used to carry cuttings to the surface.

2.8.3.1 Oil-Based Mud

These are types of drilling fluids that use oil as the base fluid. This type of fluid preparation has a higher complexity compared to WBM. They have many advantages that may include great fluid loss control, low shale swelling, sufficient drill bit lubrication and excellent debris carrying capability. The disadvantages may include poor bonding of cement and rock formation due to rock oil wetting, low filter cake cleaning up, and possible pollution of environment and aquifers. The ongoing developments of the OBM incorporate the use of crude or palm oil instead of diesel. These would be ideal for many additives due to decreased aromatics and less toxicity to the sea and freshwater organisms (Shah *et al.*, 2010).

Mohamed *et al.*, (2012) concluded that oil-based drilling fluids have great stability, lubricity and stability at elevated temperatures. Nonetheless, extravagant use of oil-based muds may cause harm in the environment. Therefore, it is of paramount importance to create drilling fluids that are environmentally friendly. This is where the water-based drilling fluids come into play.

Additives such as bentonite are added to the water-based muds to improve its hole cleaning properties and create thin filter cakes with low permeability. Bentonite also improves the viscosity of the water-based fluids and the fluid loss properties. All these improvements using additives on the water-based drilling fluids are done to give it the same rheological properties as those of the oil-base drilling fluids. These reduce the cost of drilling while saving the environment from toxic substances.

During the drilling process, reducing friction becomes a priority in drilling long deviated wells. The WBFs have been found to have a coefficient of friction that is larger than 0.1, while the OBFs have one that is less than 0.1. For ideal operation, the drilling muds should have the lowest possible coefficient of friction for the reduction of wear on the drill string (Rafati *et al.*, 2018).

In the case of high-pressure high temperature (HPHT) operations, both oil-based and water-based lubricants have been greatly used. However, oil-based muds are more preferred as they are able to operate when bottom-hole temperatures are extremely high and there are contaminants available. Water-based muds have been found to break down and lose their viscosity at elevated temperatures. Oil-based muds also provide extraordinary corrosion protection. It can be used repeatedly and stored for a longer time as compared to water-base drilling fluids (Amani *et al.*, 2012).

The use of oil-based muds has not always been feasible as the initial cost of using them is very high. There are also greater environmental and health concerns when dealing with oil-based muds with relation to the discharging of the cuttings, losing of the entire mud during the drilling process, and the eventual disposal of the mud. Extreme care also has to be taken to avoid skin contact, which may lead to allergic reactions, and inhalation of the fumes produced from the fluids may be irritating. Oil-based muds have also created potential fire hazards as a result of the low flash point of the oils used. Extra equipment and modifications have to be added on the drilling rig to minimize the loss of the oil-based mud and this means additional costs to the drilling operation (Amani *et al.*, 2012).

For oil-based muds to be used successfully, emulsifiers are added to the fluids to change the wettability of the rocks to oil-wet condition. Because of the high compressibility of the oil-based muds as compared to water-based muds, their density may change in bottom-hole from that measured at the surface. The circulating fluid also acts as a heat exchanger, and the rate of heat exchange in the mud, casing and formation is dependent on the temperature, thermal conductivity and specific heat capacity of the materials and the velocity of the drilling mud. When circulation is stopped, weighting material of the drilling mud may be forced to settle down and this may lead to density segregation or sagging (Amani *et al.*, 2012).

Amani *et al.*, (2012) conducted experiments to determine the properties of oil-based and water-based muds in HPHT drilling processes and decide on the one most suitable for HPHT drilling. The experiments were conducted in the temperature ranges of 100 to 600 °F and pressure ranges of 5000 to 25000 psi. They concluded that the oil-based drilling fluid has a higher viscosity than the water-based fluid, and the oil-based fluid showed failure at 400 °F while the water-based fluid was at 250 °F. This is an indication that the oil-based fluid has more tolerance to high temperatures than the water-based muds.

Amani *et al.*, (2012) further discovered that, when considering the yield points, the oil-based mud and the water-based mud failed at 400 °F and 250 °F, respectively. The yield point of the oil-based mud was much higher, and this means that the cuttings carrying capacity of the oil-based mud is higher than that of the water-based mud, making it a more favorable choice. They also looked at the gel strength and observed that the gel strength of the oil-based muds was very high at both low and high temperatures and that of the water-based muds reached the minimal figures at 250 °F. Oil-based muds became more tolerant to high temperatures until 400 °F where the gel strength drastically dropped.

When determining the failure temperature for both fluids, it was found that the oil-based mud's rheological properties decreased as the sample was being thermally degraded until the temperature of 420 °F where it failed, while the water-based mud failed at 250 °F. The oil-based drilling fluid proved operate at temperatures up to 420 °F while the water-based fluid can only go up to 250 °F (Amani *et al.*, 2012).

Environmental concerns are of great importance when dealing with drilling fluids. Oil-base muds have been found to have the potential to pollute the earth and aquifers so much that their use has been banned in countries such as the USA, UK, Holland, Norway, Nigeria, European countries, Saudi Arabia and Qatar. In some areas where the use of oil-based fluids is allowed, there are requirements that the muds and cuttings should be taken to approved dumping sites and this may be costly for the operating firm. Water-based mud has been found to be less harmful on the environment hence they are more preferred for HPHT operations in these countries (Amani *et al.*, 2012).

2.8.3.1.1 Vegetable oils as base stocks for bio-lubricants

Castor, jojoba, palm, coconut, soybean, olive, sunflower and rapeseed oils are the major vegetable oils used as base stocks for bio-lubricants. These oils have sparked a great interest in use in drilling fluids due to their biodegradable and renewable nature (Addy *et al.*, 1984; Patel *et al.*, 2013; Zhou *et al.*, 2013).

The triglycerides are the major components of the vegetable oils and they produce a lubricant film with strong interactions with the metallic surfaces with this results in a reduction of friction and wear in the oil and gas drilling processes (Amorim *et al.*, 2011). Despite their advantages, Fink (2015) discovered that untreated vegetable oils cannot be used directly in drilling fluids as they are prone to hydrolysis and hence increased viscosity. Borugadda and Goud (2016) further observed that, the use of vegetable oils in the drilling fluids is limited due to their poor cold flow behavior, low thermal and oxidative stability. The viscosity range of the vegetable oils is in the range of 27.2-53.5 mm²/s and it is not flexible hence not ideal for use in the drilling fluids (Demirbis, 2008).

Vegetable oils are said to be unstable for use in drilling fluids. This means that the knowledge of fatty acid composition in the vegetable oils will help in the manufacturing of bio-lubricants. Vegetable oils that contain oleic, linoleic or linolenic acids are hydrogenated to create saturated material that may have properties of grease (Rudnick, 2005).

2.8.3.1.2 Castor Oil as an oil base

The castor plant seeds are known to produce natural oil called castor oil, which is a *triglyceride*, also known as an ester of fatty acids. Its major constituent is *ricinoleic acid*, which constitutes 80–90 % of the castor oil, an 18-carbon acid containing a double bond between the 9th and 10th carbon, and a hydroxyl group attached to the 12th carbon (Akpan *et al.*, 2006; Cyr, 2008).

The industry recognizes vegetable oil and fatty acid esters as lubricants. However, mineral oils are the commonly used lubricant base oils. They highly contain hydrocarbons, some amounts of sulphur and nitrogen compounds and some trace metals. Because of their natural toxicity and non-biodegradable behavior, they become a danger to the environment and underground water reserves (Adhvaryu *et al.*, 2005). These ecological concerns and high lubricity capability, place vegetable oils as possible replacements for conventional mineral oil-based products (Asadauskas *et al.*, 1996; Randles, 1992). Knothe (2005) added that the lubricity of fatty acid methyl esters is greater than that of conventional diesel fuel.

The vegetable oils have characteristics essential for lubricants, which include increased index viscosity, decreased volatility and great lubricity and can act as solvents in fluid additives. Castor oil is, however, the best choice as it has increased lubricity when compared to ordinary vegetable oils making it a major choice as a diesel fuel additive (Goodrum and Geller, 2005; Hincapié *et al.*, 2011; Peña *et al.*, 2009).

Table 1: ASTM specification for Quality Castor Oil (Pradhan *et al.*, 2012)

Parameter	Specification	Selected
	Clear, Pale Yellow, Viscous	
Appearance	Liquid	Complies
Major Acid	<i>Ricinoleic acid</i> : 80-90 %	89 %
Identification A	Optical Value	Complies
Identification B	Hydroxyl Value	Complies
Identification C	Iodine Value: 82-90	85.2
Optical Rotation	+ 3.5 to + 6.0	+ 4.6
Hydroxyl Value	150 Max.	160
Peroxide Value	5 Max.	3.30
Acid Value	2 Max	0.30
Water	0.3 % Max	0.3%

Table 1 shows some characteristics of the castor oil that make it the best choice in multiple applications. The great viscosity associated with Castor Oil Methyl Ester (COME) is due to the presence of the free hydroxyl groups. The presence of the high amounts of *ricinoleic acid* is the contributing factor to the great lubricity of the castor oil. Drown *et al.* (2001) in their investigations concluded that the castor oil-based esters offer greater lubricating properties, whereas the ethyl esters act better as additives. Drown *et al.*, (2001), Goodrum and Geller, (2005) and Cvengroš *et al.* (2006), were successful in proving that fuel blends which contain small amounts of fatty acid esters (1 %) exhibit outstanding lubricating characteristics.

Pradhan *et al.*, (2012) calculated the price of COME; they established that it was lesser compared to current petroleum diesel fuel as well as the refined soybean biodiesel, which go for \$5.0/gal and \$4.5/gal, respectively. Therefore, it is of paramount importance to consider the cost of the feedstock when deciding the value of the product and in deciding whether the process is economically viable.

The observations have shown that COME has displayed improved low-temperature fluidity and efficient anti-friction and anti-wear properties concerning lubrication. Therefore, because of its

high viscosity, it has the potential to be a bio-lubricant. The price of COME acquired in their research was estimated to be \$3.71/gal and this is low as compared to the conventional petroleum diesel and soybean oil biodiesel (Pradhan et al., 2012).

2.8.3.2 Water-based mud (WBM)

These are the types of fluids that have water or brine as the base fluid. They are found to be environmentally friendly, making the disposition of the drill cuttings easy. A current WBM utilizes a polymer as a viscosifying agent. The types of polymers are either linear, cross linked, synthetic, or biopolymers. A viscoelastic surfactant (VES) drilling mud is one, which utilizes a surfactant that has viscous and elastic properties and has the potential to adjust itself and regain its rheological characteristics. The VES based drilling fluids are more expensive in comparison to the current WBM; the VES based drilling fluids do not need recurrent conditioning and thus saves a significant amount of production time. Ogugbue *et al.*, (2010) suggested that further research that combines great properties of both VES and biopolymers must be conducted, to attain a blend that outweighs both their individual disadvantages.

Dougherty *et al.*, (2014) concluded that WBM had two effects on the drilling process. The first effect is being a lubricant at the interface reducing the friction force and increasing the ROP on the Mancos Shale, Carthage Marble and Nugget Sandstone used. Then it deteriorated the quality of the rocks allowing for increased ROP. The above scenarios are very important for the drilling process as the former helps protect the cutters while the latter maximizes the ROP.

In dry and wet conditions, Dougherty *et al.*, (2014) observed that different rock samples utilized at the same load gave different behaviors. This is an important observation as it is an indication of the resistance in different rock types in PDC drilling.

2.9 USE OF NANOPARTICLES IN DRILLING FLUIDS

The rheological properties of the drilling fluids should display shear thinning properties that are resistant at high shear rates. At low shear rates, the viscosity of drilling fluid should be enough to hold the cuttings and prevent them from falling back into the drilled hole. The behaviour of the drilling fluids is defined by the following parameters; the apparent viscosity (AV), which is the relationship between the shear stress and shear rate of the drilling fluid, the plastic viscosity

(PV), which is the resistance of the fluid to flow. The yield point (YP), is the minimum shear stress needed to initiate motion of the drilling fluid and the gel strength, which is the measure of the fluid's capability to act like a gel and be able to suspend cuttings in cases where fluid circulation is stopped (Rafati *et al.*, 2018).

There are a few rheological models used in the evaluation of shear stress-shear rate ratio of non-Newtonian fluids and these are the Bingham plastic model, the power law and the Herschel-Bulkley model. The Herschel-Bulkley model was concluded to be the best model to characterize the non-Newtonian behaviour of muds in a non-linear way (Barry *et al.*, 2015). The three parameters observed in this model are the yield point (τ_o), the consistency coefficient (K), and the flow behaviour index (n) (Rafati *et al.*, 2018; Song *et al.*, 2016a);

$$\tau = \tau_o + K\gamma^n \quad \text{eq 8}$$

Where τ is the shear stress (lb/100ft²),

τ_o is the yield point (lb/100ft²),

K is the consistency index,

γ is the shear rate (s⁻¹), and

n is the flow behaviour index (dimensionless) that needs to be less than 1 for shear thinning fluids.

Macro and micro materials are added to the drilling fluids, and limitations were observed in the reduction of torque and drag challenges in deep drilling. Through extensive research, it was concluded that the addition of NPs to the drilling fluids greatly reduce the friction between the drill string and the formation because of a fine film produced that generates a constant lubricating system at the interface (Amanullah and Al-Tahini, 2009).

The use of macro and micro particles causes fractures to develop during over-balanced drilling as a result of heavy solid content. In the drilling fluid the incorporation of nanoparticles has greatly reduced the solid content hence, the low density of the fluid is seen to increase the ROP. The dispersion and sagging of solid content in the fluid is removed. These smart fluids created from

the use of nanoparticles help in the reduction of torque and drag problems. This is because nanoparticles create a constant thin film around the drill-pipe that provides lubrication and thus reduces the torque and drag problems (Shah *et al.*, 2010).

The nanoparticles have been found to have economic and technical advantages in the drilling process (Abdo and Haneef, 2011);

Cost

- Reduction in drilling fluid cost that result in overall reduced drilling costs due to the replacement of very expensive additives with the NPs.
- Improvement in the oil recovery through easy access of deep underlying reservoirs.
- Reduction in NPT through drilling problem elimination hence saving on costs.

Technical

- Best options to use in new technical developments like horizontal or directional well drilling.
- Controlled and under-balanced drilling processes.

Nanoparticles have been added to the drilling fluids to achieve a certain functionality, stability, and adaptability in a variety of operating conditions without much alteration to the composition and size of the nanoparticles (Evdokimov *et al.*, 2006). The increased surface area to volume ratio of the nanoparticles is responsible for their high reactivity. This means that small amounts of the NPs are needed for any application resulting in reduced costs (Shah *et al.*, 2010).

Within the large variety of available clay minerals, there are three clays that are mainly used as additives in the drilling muds. They are attapulgite, sepiolite, and bentonite. These clays are the principal contributor of active solids in the drilling mud and are the determining factor for the rheological and chemical properties of the muds. Attapulgite and sepiolite are needle-shaped, non-swelling clay minerals. Attapulgite is the standard clay amongst fuller's earth class and its performance can be improved through certain heat activation and size control techniques (Singer and Galan, 2000; Sudo and Shimoda, 1978). The highly fragmented attapulgite particles greatly

absorb water due to the increased surface area, thus improving the suspension of the debris in the drilling mud during the drilling process (Abdo and Haneef, 2011).

Abdo and Haneef (2011) created attapulgite nanoparticles through a process of mechanical attrition, then formed drilling mud samples which contained different concentrations, size range and material of the NPs. They measured the rheological properties of the samples and concluded that NPs will ensure that the drilling process runs smoothly and effectively. They also concluded that using NPs to solve drilling challenges will result in improved rates of penetration that results in reduced costs. To determine the effectiveness of a drilling operation, the depth reached should be compared against the time taken to reach that depth. Use of NPs aid in reaching the target at a shorter time, as shown in Figure 2.

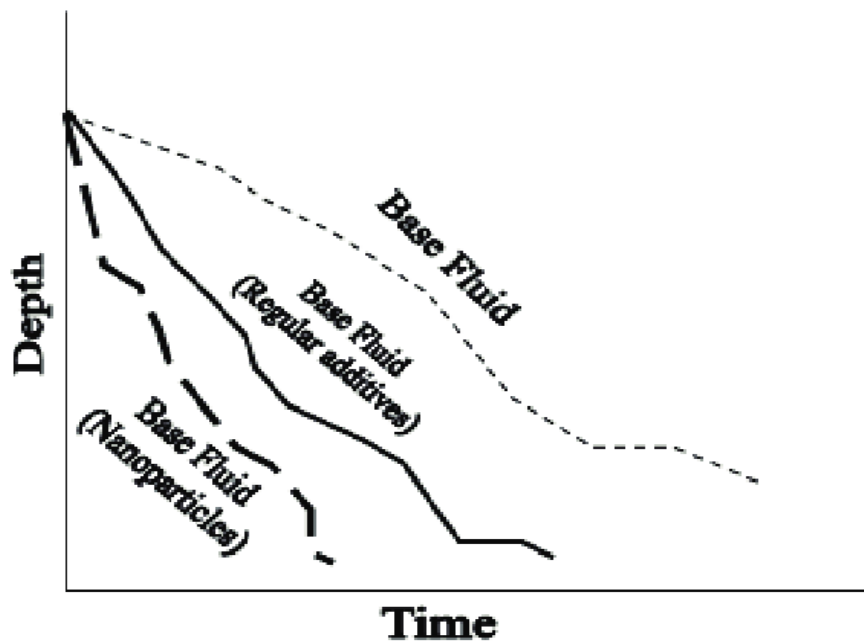


Figure 2: Improvement in the rate of penetration (ROP) (Abdo and Haneef, 2011)

Needaa *et al.*, (2016) conducted experiments using sepiolite NPs that contained silica. The experiments showed an increase in the PV and YP in comparison to the base fluid sample. It was therefore concluded that the addition of NPs to the drilling muds improves the rheological properties of the drilling muds especially the WBFs.

Bentonite (BT) is known to be a montmorillonite clay that is usually utilized in drilling fluids as a result of its great rheological characteristics (Bourgoyne *et al.*, 1986; Temraz and Hassanien, 2016). The bentonite suspensions demonstrated properly controlled shear thinning properties that allow the fluid to be easily pumped and carry cuttings easily to the surface (Bourgoyne *et al.*, 1986a). In the traditional drilling fluids, usually great amounts of bentonite are used to accomplish the expected rheological and filtration properties of the drilling fluids. Nevertheless, it has been found that large bentonite concentrations can reduce the drilling effectiveness and result in operational challenges such as differential sticking, insufficient well-bore cleaning, increased torque and drag and formation damage (Song *et al.*, 2016).

Bentonite particles of sizes 4 and 9 nm were used as additives to the WBFs and their rheological properties were compared with those of American Petroleum Institute (API) standard bentonite and local bentonite of micro size particles. The rheological properties such as AV, PV, and YP were seen to decrease due to the addition of bentonite NPs and the solid content of the drilling fluids was also seen to decrease (Abdo and Haneef, 2013).

In salt-water when the use of bentonite becomes inefficient, attapulgite is used as a viscosifier. The crystalline needle-shaped structure of attapulgite behaves differently from the platelets in seawater. It has great shear-thinning properties but cannot control fluid loss due to its structure (Darley and Gray, 1988). Filtration, also known as fluid loss, is the loss of fluid through the walls of the formation and it is controlled by using a drilling mud that forms a thin hard filter cake on the walls to prevent loss of the filtrate (Abdo and Haneef, 2011).

The viscosity of the drilling fluid is the determining factor of the muds' ability to carry cuttings to the surface. It has been observed that bentonite performs very well in freshwater even though it swells a few times its size. Bentonite does not do well in seawater as it gives a low yield of the clay. Attapulgite, however, has a higher yield of clay when used in both freshwater and seawater and swells very little. Bentonite also does not create viscosity in seawater, instead, it absorbs water without changing the viscosity like attapulgite does (Abdo and Haneef, 2011).

An accurately designed low-solid drilling system is estimated to increase penetration rate, form thinner mud cakes, increase well-bore cleaning efficiency, improve fluid maintenance and improve hydraulics. The low solid drilling muds can be prepared by the use of one or multiple polymers to replace bentonite and give the same rheological and fluid loss properties similar to those of fluids containing high concentrations of bentonite. Materials such as xanthan gum, starch, sodium carboxymethyl cellulose and polyanionic cellulose (PAC) can be mixed into the drilling fluid to achieve the anticipated rheological and filtration characteristics (Ahmadi et al., 2015; Baba Hamed and Belhadri, 2009; Fereydouni *et al.*, 2012; Hossain and Wajheuddin, 2016).

The rheological and filtration properties of drilling muds are modified through the change in the kind, composition, size distribution and surface characteristics of the NPs to meet the standard specifications of any specific drilling and production operation. Amanullah *et al.*, (2011) found that, for some situations, concentrations as low as 1% and below are needed of NPs to produce the desired nano-enhanced drilling fluids.

In the oil and gas drilling processes, the development of drilling muds that contain a low solid load are the desired fluids because they are easier to control, have easy fluid maintenance, quicker penetration rates, and better hydraulics in exploration of bentonite added to traditional drilling fluids. The cellulose nanoparticles (CNPs) which may include cellulose nanocrystals (CNC) and cellulose nanofibers (CNFs) are also added with the aim of improving cost efficiency, environmental friendliness and fluid safety (Song *et al.*, 2016).

Cellulose is a highly abundant renewable and biodegradable biopolymer found naturally in a variety of sources which may include wood, cotton, hemp, linen, chitin, and bacteria (Moon *et al.*, 2011; Song *et al.*, 2014; Wei and McDonald, 2016). These cellulose nanoparticles can easily be extracted from the cellulosic materials through purification pretreatment accompanied by chemical or mechanical degradation processes such as acid hydrolysis, enzyme hydrolysis, 2,2,6,6-Tetramethyl-1-piperidinyloxy (TEMPO) mediated oxidation, ultrasonic grinding and high-pressure homogenizing processes (Guo *et al.*, 2016; J. Moon *et al.*, 2011; Zhang *et al.*, 2015a).

Cellulose nano-particles are equipped with very high definite surface area, large aspect ratio, and also increased thermal stability (Wei and McDonald, 2016; Zhang *et al.*, 2015b). These NPs are not ideal in creating low solid drilling muds, but they aid in building the viscosity of drilling fluids using the small mass of solid content through the increase of wetted surface area, which is the same as when using attapulgite clays in typical drilling fluids. The NPs aid in improving the low-solids mud filtration properties by controlling the filter cake properties of the drilling fluids instead of the filtrate properties as done in normal low-solid drilling fluids (Song *et al.*, 2016).

Cellulose is a naturally biodegradable material that was first introduced as an additive to drilling fluids by Li *et al.* (2015b). They concluded that changing concentrations of CNC from 0 to 6.0 wt% improved significantly the viscosity and shear rate of the drilling fluids. Song *et al.*, (2016a, 2016b) investigated that the addition of cellulose nanoparticles (CNPs) in the form of cellulose nanocrystals (CNCs) and cellulose nanofibers (CNFs) are used as eco-friendly additives in WBFs. In their study, they used concentrations from 0.05 wt% to 0.4 wt% for CNC and CNF while they reduced bentonite concentrations to 0.0 wt% when CNP concentration was 0.4 wt%. When the concentration of the CNPs was 0.05 wt%, the rheological properties of the drilling fluid portrayed a minor increase as compared to the base fluid, but as the concentration of the CNPs was increased and that of bentonite decreased, the rheological properties decreased. At bentonite concentration of 0.0 wt%, the values of AV, PV, and YP decreased by 85 %, 82 %, and 92 %, respectfully in the case of CNC.

The blending of CNPs and bentonite in suspensions show a difference in the rheological properties between CNC and CNF drilling fluids and this could be due to the different interactions these NPs have with bentonite. It has been recorded that the bentonite nano-platelet layers have surfaces with a negative charge (Bourgoyne *et al.*, 1986a; Luckham and Rossi, 1999). These negative charges repel the negative charges found on the surface of the CNCs. The negative forces encourage the formation of aggregations of CNCs and bentonite resulting in their phase separation (Song *et al.*, 2016).

2.9.1 Tribo-film Formation

The oils that have serpentine powder display increased friction reduction and anti-wear characteristics. These characteristics are due to the multi-fractured oxide tribo-film formed on the surface that has good mechanical properties. Attapulgite has been proven to have similar characteristics as those of serpentine, but attapulgite is more preferred because of its lower costs. It has also been found that attapulgite greatly decreases the friction coefficient and wear loss in carbon-steel friction pair (Wang *et al.*, 2017; Zhang *et al.*, 2016).

Yu *et al.*, (2008) in their study found that the optimum quantity of attapulgite used is 0.5wt%. This observation may be in line with the balance between the generation of the tribo-film and the abrasion of the tribo-film. In the case where the added amount of attapulgite is low, the tribo-film is abraded faster than it is formed. Increasing the amount of attapulgite will ensure that sufficient tribo-film is created as well as the improvement in the tribological properties. Excess amounts of attapulgite will reduce the liquidity of the lubricating oil, reducing the strength of the tribo-film formed. The tribological properties will also be reduced.

The tribo-film formed in the friction process was found to tolerate very high loads. The best anti-wear performance was found to be at the load of 50 N. This may be because when the load is small, the production of energy due to sliding friction becomes low to generate a tribo-chemical process between the metal and the oxygen atoms. Increasing the load means that greater heat was generated, making it easier for the atoms to react and quickly form the tribo-film. Increasing the load further will weaken the anti-wear performance due to the high abrasion of the tribo-film (Talke, 1997).

The surface-modified attapulgite powders added to oil base fluid have shown great tribological improvements. The 0.5 wt% amount of attapulgite has significantly reduced friction and wear. Attapulgite powders help in the generation of tribo-films with a high complexity on the worn surfaces and this tribo-film has been found to tolerate increased loads (Nan *et al.*, 2014).

CHAPTER THREE

3.0 METHODOLOGY

This section provides a detailed description of the experimental work that was carried out. The materials used were clearly stated and the equipment thoroughly defined. All sample preparations were described as well as the analytical techniques used for this investigation.

3.1 MATERIALS

Three different rock samples were cut into discs shape to investigate the Tribological behavior of various drill bits on the rock samples using the ball-on-disc Tribometer as shown in Figure 3. The rock types were quartzite obtained from the University of the Witwatersrand, the fine-grained sandstone obtained from Maseru, Lesotho, and the coarse-grained sandstone was obtained from Mozambique. The type of balls used was 6mm diameter stainless steel balls that were obtained from Anton Paar. Bentonite, sepiolite, attapulgite, and cellulose nanocrystals, as well as freshwater, seawater and castor oil and sodium chloride, were used in different concentrations as drilling fluids in this investigation.

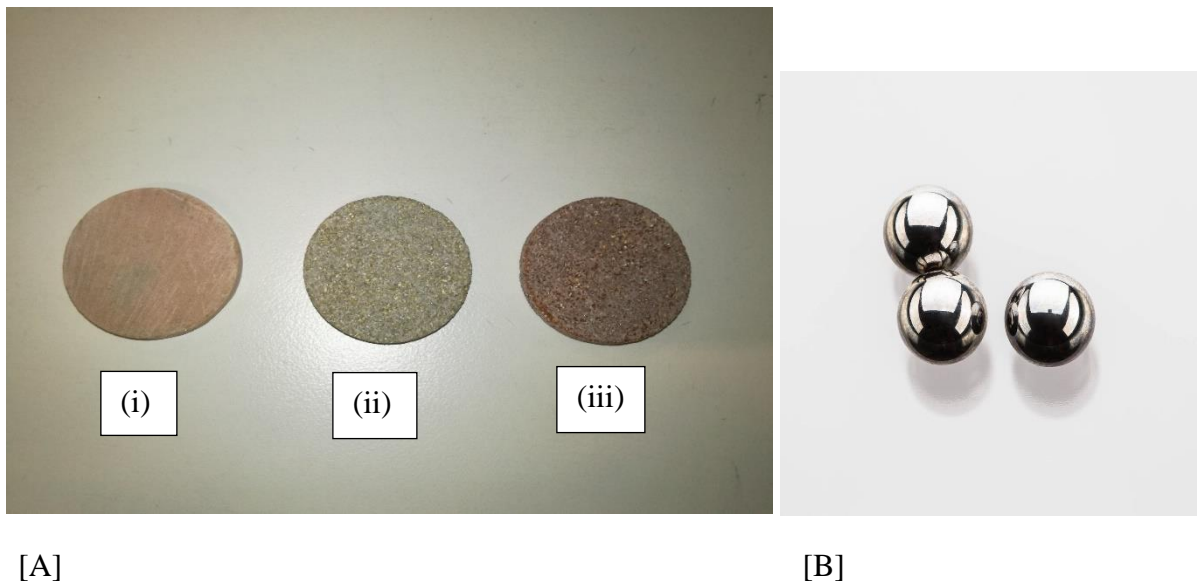


Figure 3: {A}: Rock samples (i) Quartzite, (ii) Fine-grained Arkose Sandstone (iii) Coarse-grained Arkose Sandstone. {B}: 6 mm diameter stainless steel balls from Anton Paar.

3.2 EQUIPMENT DESCRIPTION

Figure 4 shows a Pin-on-disc CETR-UMT-2 Tribometer found at the University of Johannesburg manufactured by Anton Paar. This equipment was used to study the friction and wear between two different materials in different operating environments. The equipment consists of a load arm [2], that allows different loads of up to 60 N to be added. At the end of the load arm, a ball holder is connected [4] and the maximum diameter of the balls that can be used on this equipment is 6 mm. There is also a spindle [7] that allows connection of the shaft or rotating module [6] which acts as a sample holder in dry testing conditions and the fluid cup [8] used in wet testing conditions. The shaft can hold samples of up to 60 mm as seen in Figure 4 and the fluid cup has a sample clamping ring [9] that holds the sample in place as seen in Figure 5. The amount of lubricant should just be enough to cover the sample and this amount also depends on the viscosity and speed of the rotation, just enough not to spill over as observed in Figure 6. The counterweight [1] helps to balance out the load arm by canceling off the normal load so that the load acting on the sample is from the loads added only.

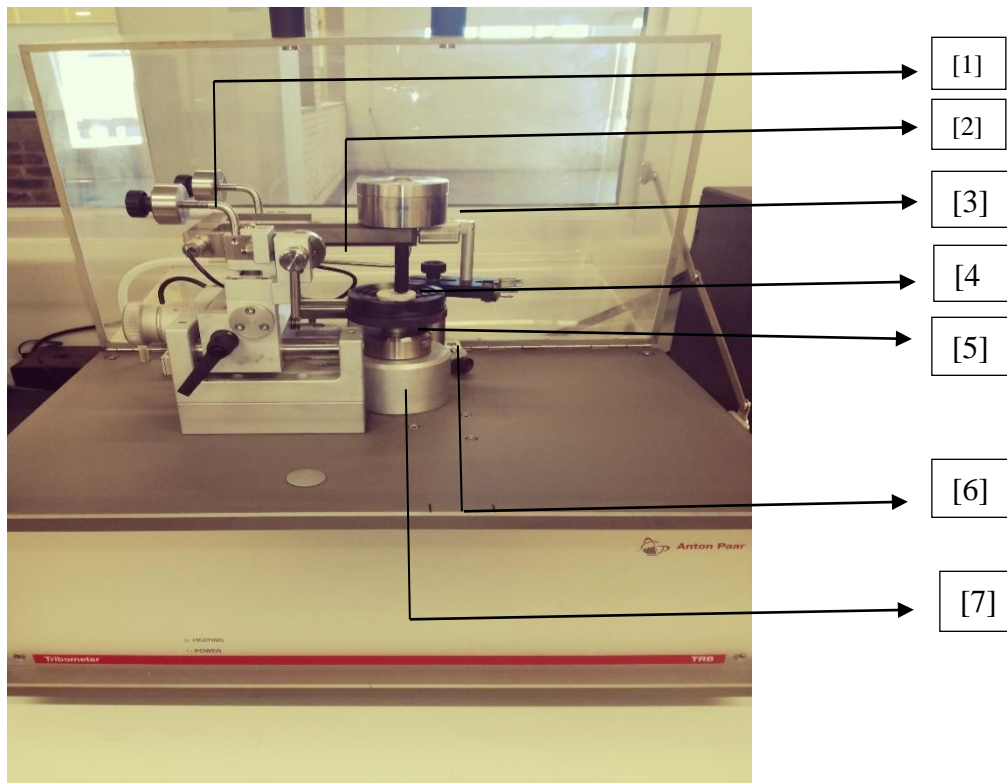


Figure 4: The Ball-on-disc CETR-UMT-2 Tribometer from Anton Paar used in dry testing (University of Johannesburg, 2019)

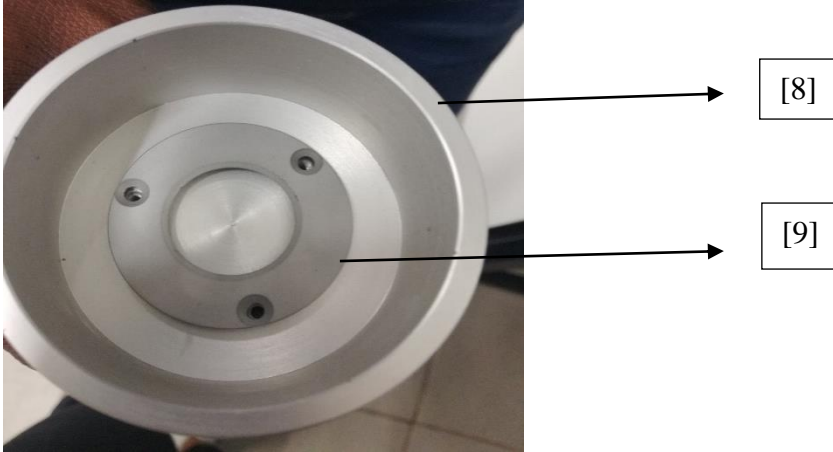


Figure 5: Sample holder from the ball-on-disc tribometer used in wet testing (University of Johannesburg, 2019)

Table 2: Parts of the CETR-UMT-2 Tribometer equipment

Equipment parts	
1	Counterweight
2	Load arm
3	Load
4	Ball holder
5	Sample
6	Shaft/ Rotating module
7	Spindle
8	Liquid cup
9	Sample clamping ring

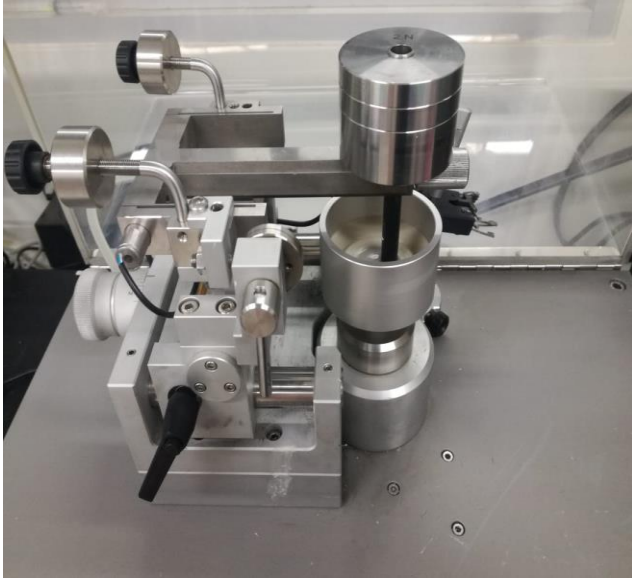


Figure 6: The Ball-on-disc CETR-UMT-2 Tribometer from Anton Paar used in wet testing (University of Johannesburg, 2019)

3.3 HARDNESS TESTING

To determine the hardness of the rock samples, uniaxial compression stress (UCS) tests were conducted at the School of Mining, University of the Witwatersrand. The aim of these tests was to classify rock samples in terms of their hardness. Cylindrical rock samples were prepared with the length to diameter ratio of 2:3. The samples were then polished using black silicon carbide powder to remove any irregularities on the surface. The biaxial string gauges were mounted onto the rock samples with glue to hold them in place. An MTS Rock Mechanics Testing System was used to apply and measure the load on the specimen. The strain gauge was connected to a DAQ system that allows specifying testing conditions. A constant load was then applied continuously on the specimens at a constant stress rate. The rock was expected to fail within 5-10 minutes and this failure occurred at a maximum load at which the rock would handle.

3.4 XRF ANALYSIS

The rock samples investigated were of three different types; Fine-grained Arkose Sandstone, Coarse-grained Arkose Sandstone, and Quartzite. The rocks were ground/ pulverized to reach the particle size less than 100 μ m as required by the XRF equipment. The XRF analysis was carried out in the Geology Laboratories, Faculty of Sciences, University of the Witwatersrand. Major elements were determined using the Norrish Fusion technique using in-house correction

procedures and using a Panalytical PW2404 X-ray fluorescence spectrometer. Major elements were fused using Johnson Matthey Spectroflux 105 at 1100°C and raw data corrected using in-house software. Standard calibrations were made using synthetic oxide mixtures and international standard rocks as well as in-house controls. The sample weight and flux weight that were used were 0.35 mg and 2.5 mg, respectively. Calibration standards were primary International Reference Materials USGS series (USA) and NIM series (South Africa). Precision was taken as 1% for elements in abundance of greater than 5 % by weight, and 5 % for elements in abundance less than 5 %.

3.5 XRD ANALYSIS

Pulverized rock samples of Coarse-grained Arkose sandstone, Fine-grained Arkose sandstone and Quartzite analyzed at the Microscopy and Microanalysis Unit (MMU), at the School of Biology, University of the Witwatersrand, Johannesburg, for X-ray diffraction. This technique is a useful tool in the determination of components of different rock samples. This data was used to determine the purity of rock samples by determining other minerals present in the rock samples. The samples were analyzed using a Bruker D2 Phaser diffractometer that uses a Copper (Cu) anode with a diffraction wavelength (λ) of 1.54184 Å. The X-ray generator operates at 30 kV, and 10 mA, in the 2θ range of 10-90°, at 0.0260° with a counting time of 31.4000 s per step. This diffractometer uses a Theta/2Theta system. After the XRD patterns have been obtained, the Panalytical X'Pert Highscore analytical software compares the diffraction data against the ICDD database, that is able to identify all the phases available.

3.6 SCANNING ELECTRON MICROSCOPY/ ENERGY DISPERSIVE SPECTROSCOPY (SEM/EDS) ANALYSIS

In order to conduct SEM analyses, the rock samples were mounted on slides and polished at the school of Geography, University of the Witwatersrand, Johannesburg. The mounted slides were coated using one layer of the SEM carbon coating at the Microscopy and Microanalysis Unit (MMU), at the School of Biology, University of the Witwatersrand, Johannesburg. The samples were then analyzed using the Carl Zeiss Field Scanning Electron Microscope (FESEM) equipped with an Oxford X-act Energy Dispersive X-ray (EDX) detector. The SEM uses a focused beam of electrons to produce high-resolution images of the surface topography of different materials. The different grey scales produced were analyzed to determine the chemical composition of the

available phases. The combination of SEM and EDS gives a more comprehensive structural and elemental composition of different materials.

3.7 SYNTHESIS OF DRILLING MUDS

A variety of drilling muds were synthesized to determine how different concentrations of the additives in the base fluid affect the performance of the drilling equipment. For the first set of drilling fluids, sodium chloride (NaCl), nano-bentonite and freshwater, were used in the ratio of 1:4:15, respectively, to create a 25 wt% solution of freshwater and additives and then a ratio 1:4:5, respectively to create a 50 wt% solution. The same ratios were used when castor oil was used as the base fluid. For the second set of drilling fluids, 6wt% solutions of attapulgite, bentonite, and sepiolite were made and then cellulose nanocrystals (CNC) were added to create a final 1.2 wt% solution of the clay solution and the added CNC crystals. Wet tests were then conducted to determine the influence of drilling fluids on the effectiveness of a drilling operation.

3.8 FRICTION AND WEAR TESTS

A ball-on-disk wear-testing tribometer (CETR-UMT-2), as shown in Figure 4, was used to evaluate the friction and wear behavior of the drill bits on the rock samples. The 6 mm diameter stainless steel was used as the counter surface that represented the drill bit material. Test surfaces of the rock samples was ground using the 1200 Silicon Carbide (SiC) paper to create the needed surface finish (Obadele *et al.*, 2016). To determine the effect of drill bit rotation speed on the friction and wear behavior between the rocks and the drill bit material, the same equipment was used which allows varying of the weight on bit and rotational speeds (Green *et al.*, 2007). For the dry and wet tests, rock samples were mounted on the fluid cup holder as shown by Figure 5, and the tests were conducted to determine the effect of lubrication on the friction and wear of the rocks and the drill bit (Dougherty *et al.*, 2014).

3.8.1 Test Conditions

In the determination of friction and wear behavior of the drill bit on the rock samples, the tests were conducted at room temperature. The loads were varied in the range of 1 – 9 N for 1200 s while the coefficient of friction was continuously monitored. Each test was conducted once and the coefficient of friction was determined according to Obadele *et al.*, 2015. The determination of the effect of rotational speed on the friction and wear behavior was conducted, and the weight

on the bit was varied in the range of 1 – 9 N while the rotational speeds used were 100rpm, 200rpm and 300rpm (Greene *et al.*, 2006). During the dry and wet testing, different solutions were created as mentioned in Section 3.7, which were used as drilling muds. The tests were carried out at room temperature and pressure (Dougherty *et al.*, 2014). Coefficients of friction were generated and were used as an indication of the influence of drilling fluids in a drilling operation.

CHAPTER FOUR

4.0 RESULTS AND DISCUSSIONS

This section outlines the results obtained from the investigation of friction and wear behaviour of the drill bit on the selected rock samples in the absence and presence of a variety of drilling fluids, including the mineralogical and chemical composition analysis of the three rock samples using XRF, XRD, and SEM/EDS.

4.1 XRF Analysis

The data shown in Table 4 indicates that the rock samples mostly contain SiO₂ with traces of compounds such as Al₂O₃, Fe₂O₃ (Hematite) and K₂O. The loss-on-ignition (LOI) is an indication of the amount of the water, carbon, organic matter and volatile compounds that are found in each rock sample. The presence of this mineral matter reduces the purity of the rock samples.

Table 3: Major compounds found in the three rock samples Quartzite, Coarse-Grained Sandstone and Fine-Grained Sandstone

	SiO ₂	Al ₂ O ₃	Fe ₂ O ₃	MnO	MgO	CaO	Na ₂ O
Quartzite	97.2	0.55	0.44	0.01	0.08	0.08	-0.03
Coarse-Grained Sandstone	94.21	1.93	0.69	0.01	0.08	0.08	0.02
Fine-Grained Sandstone	89.35	4.66	1.25	0.02	0.21	0.21	0.79

	K ₂ O	TiO ₂	P ₂ O ₅	Cr ₂ O ₃	NiO	LOI	Total
Quartzite	0.16	0.02	0.1	0.03	0	0.34	98.99
Coarse-Grained Sandstone	1.15	0.04	0.03	0.06	0	0.38	98.68
Fine-Grained Sandstone	1.01	0.23	0.03	0.02	0	1.42	99.19

Quartzite was found to have the highest content of silica as compared to fine-grained and coarse-grained sandstone. Silica (SiO₂) constitutes most of the rock mineral content, as it is the second most abundant element found in the Earth's crust after Oxygen (O₂), this shows that these rock

samples are silica based. Quartzite is found to have 8.79 % and 3.17 % more silica than fine-grained and coarse-grained sandstone, respectively.

4.2 SEM/EDS ANALYSIS

The SEM gave information on the surface topography of the phases present in the different rock types. The chemistry data as well as the EDS spectra of the different phases, further proved the accuracy of the XRF and XRD data above. The rock samples are found to contain the SiO_2 as the dominant phase, then traces of other minerals in different forms and ratios.

These SEM/EDS results show that the rock samples were not pure, and the minerals not evenly distributed and different phases captured by these images portray different phases.

4.2.1 Analysis of Quartzite

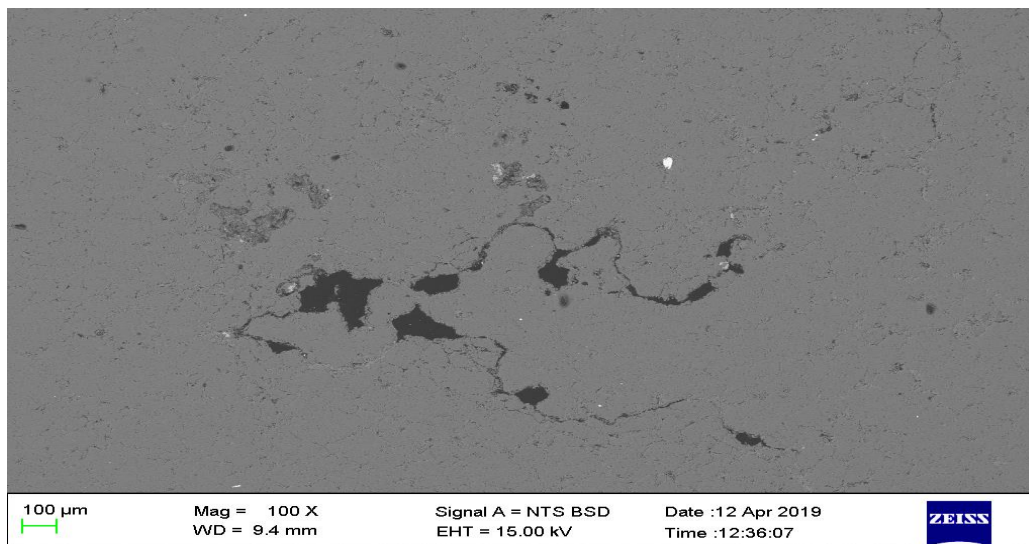


Figure 7: Section of the Quartzite showing different phases available

Rocks are usually composed of a combination of minerals depending on where and how they are formed (Penuel et al., 2017). Because of how rocks are formed, there is always an uneven distribution of rock minerals as seen in figure 10, which shows a section on the quartzite rock with different phases representing different minerals. The gray phase shows the dominant phase in the rock and the darker phase represents the cracks or fractures within the rock. The lighter phases are the heavier minerals.

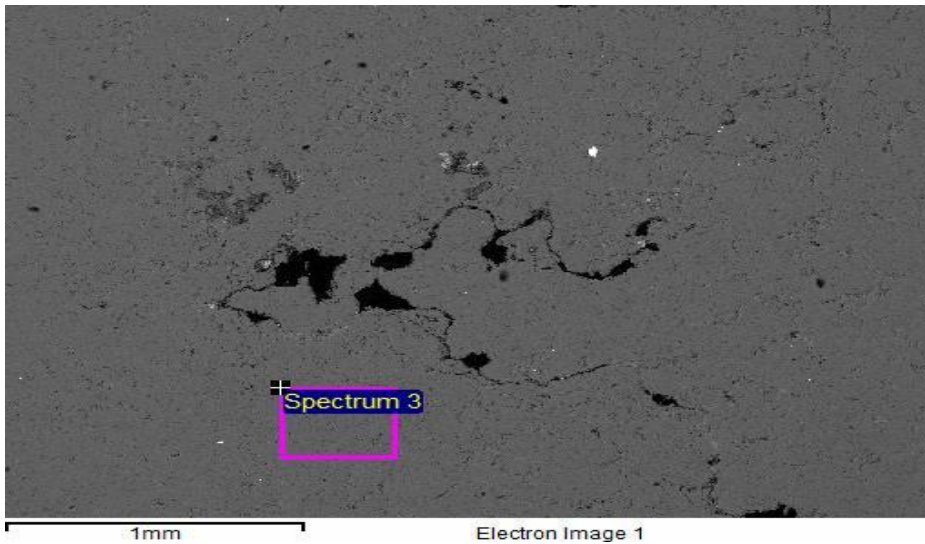


Figure 8: SEM image showing the clean surface of the Quartzite rock sample

Spectrum 3 on Figure 11 represents the dominant phase of the quartzite rock which is mainly SiO_2 . This data also correlates with that from the XRF analysis, which shows SiO_2 as the major constituent of the quartzite rock. Despite SiO_2 being the major component of the quartzite rock, it is not evenly distributed throughout the rock because of the presence of other minerals and formation of fractures.

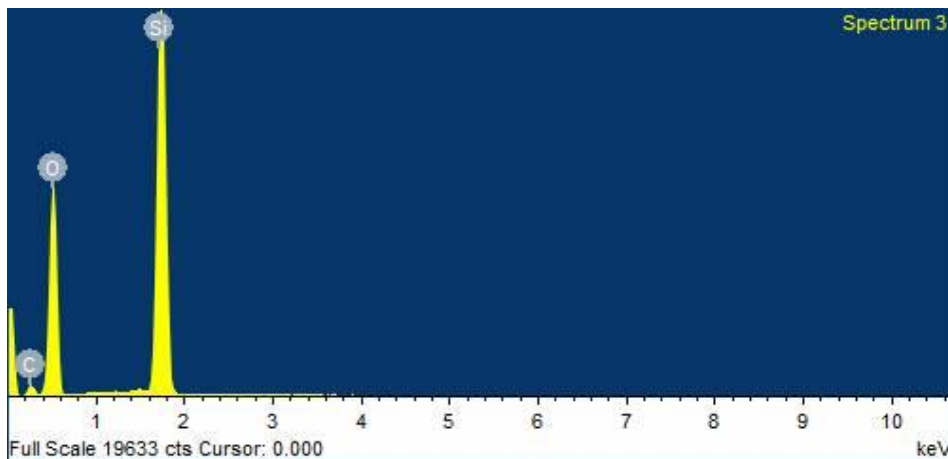


Figure 9: EDS elemental analysis of the clean surface of the Quartzite rock sample

The EDS image in Figure 12 is mainly a confirmation of the chemical composition of the clean and dominant phase of the quartzite rock. It shows the presence of Si and O which exist as SiO_2

in the rock sample. The presence of the Carbon (C) is from the coating used for the SEM analysis.

Table 4: Chemical composition of the clean surface of the Quartzite rock sample

Element	Weight%	Atomic%
C K	10.67	16.07
O K	54.23	61.32
Si K	35.10	22.61
Totals	100.00	

Table 5 is also a confirmation of the presence of the SiO_2 in the rock. The molecular weight percentage shows the quantities in which these minerals are available in the rock. These quantities do not correlate to the molecular formula of SiO_2 which show a silica to oxygen ratio of 1:2. In the table, the ratio is roughly 1:3 and this was not investigated in this research work.

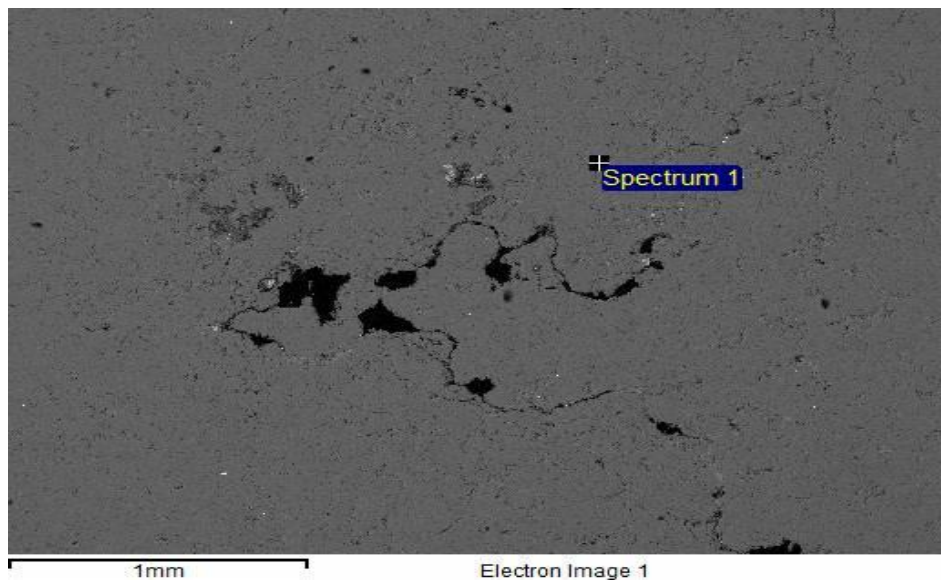


Figure 10: SEM image showing the contaminated surface of the Quartzite rock sample

Figure 13 shows spectrum 1 on the quartzite rock which represents a contaminated phase. This lighter phase is representing a heavy mineral. A few more phases are seen spread out across the quartzite rock, though they are available in very small quantities.

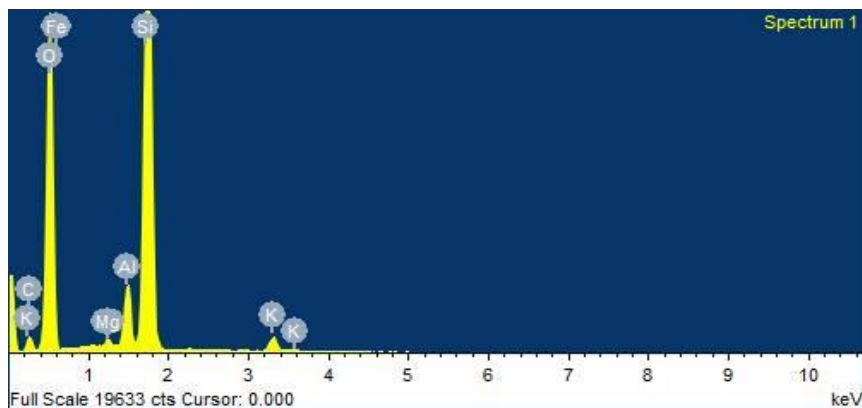


Figure 11: EDS elemental analysis of the contaminated surface of the Quartzite rock sample

The EDS data on Figure 14 shows the chemical composition of the heavy mineral on the quartzite surface. It shows the presence of Si, O, Fe, Al, K, and Mg. Si, O, Al and Fe are the major components, while K and Mg are available as the trace minerals. This data is also in correlation with the elemental composition data from the XRF analysis.

Table 5: Chemical composition of the contaminated surface of the Quartzite rock sample

Element	Weight%	Atomic%
C K	7.65	11.69
O K	57.27	65.71
Mg K	0.36	0.27
Al K	3.40	2.31
Si K	29.23	19.10
K K	1.65	0.78
Fe K	0.43	0.14
Totals	100.00	

Table 6 shows all the chemical elements that are available in the contaminated phase of the quartzite rock sample. The elemental weight percentage shows that O, Al, Si, and K are the major elements present, while Fe and Mg are the trace elements.

4.2.2 Analysis of Fine-Grained Sandstone

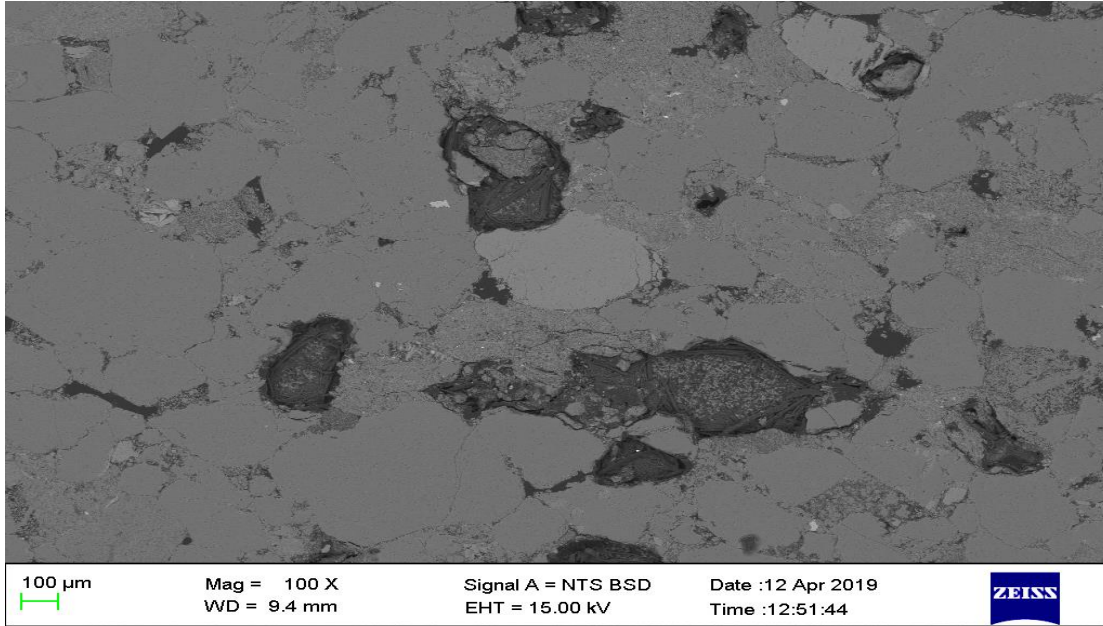


Figure 12: Section of the fine-grained sandstone showing different phases available

Figure 15 is a section of the fine-grained sandstone that shows the diversity of mineral phases that are available in the rock sample. This further shows that formation of the rocks results in a non-uniform distribution of the minerals present.

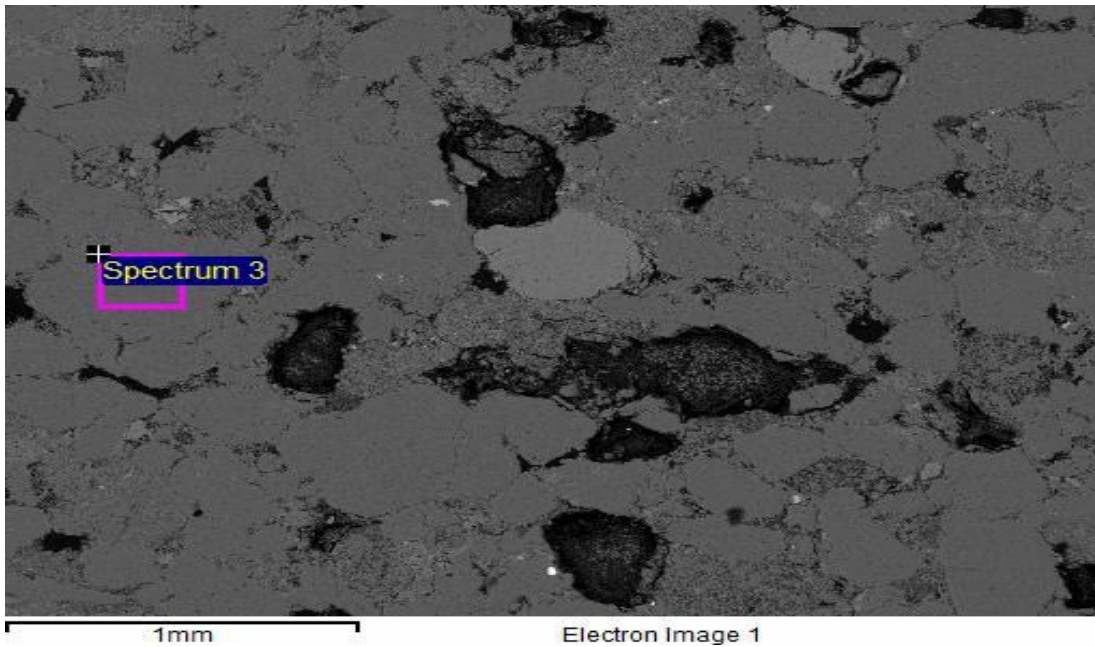


Figure 13: SEM image showing the clean surface of the fine-grained sandstone rock sample

Figure 16 shows Spectrum 3 which represents the dominant phase of the fine-grained sandstone. This is the clean phase that consists of SiO_2 without contamination from other minerals.

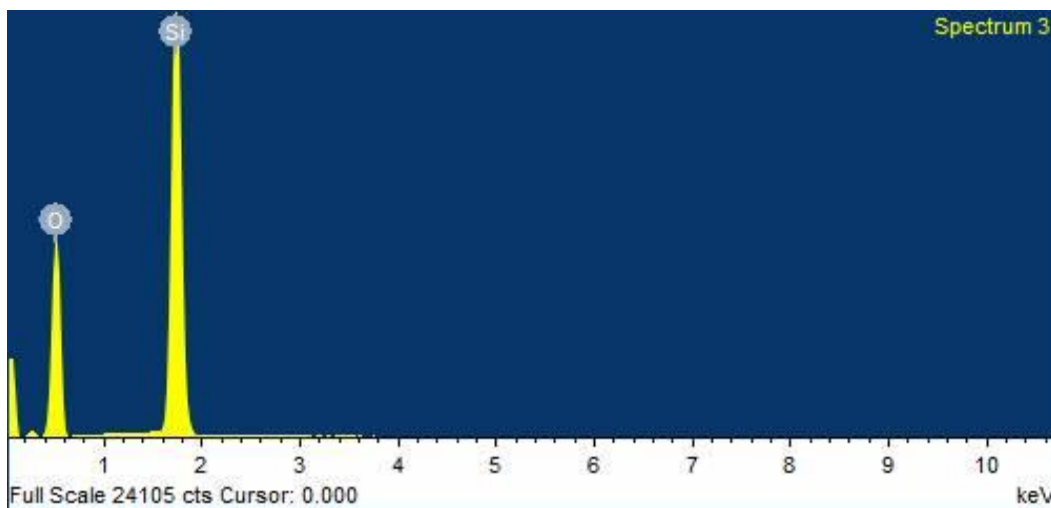


Figure 14: EDS elemental analysis of the clean surface of fine-grained sandstone rock sample

Figure 17 shows the EDS data of the dominant phase on the fine-grained sandstone. It shows the presence of Si and O and this is in line with the data from the XRF analysis in Table 4 which shows that SiO_2 is the major constituent of the fine-grained sandstone.

Table 6: Chemical composition of the clean surface of the fine-grained sandstone rock sample

Element	Weight%	Atomic%
O K	55.48	68.63
Si K	44.52	31.37
Totals	100.00	

Table 7 is the chemical composition of the dominant phase in the fine-grained sandstone. It shows the presence of Si and O and this correlates to the XRF data that shows SiO₂ as the major phase.

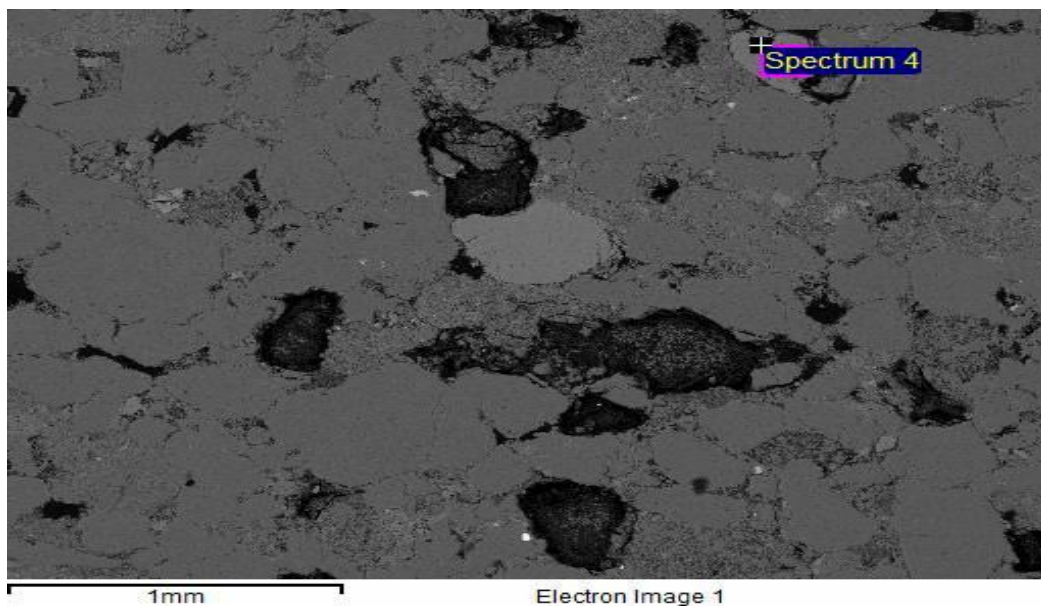


Figure 15: SEM image showing the contaminated surface of the fine-grained sandstone

Figure 18 is the image showing spectrum 4 which is the one of the trace elements found in the fine-grained sandstone. It is seen to have a lighter shade of gray as compared to the dominant phase in the fine-grained sandstone.

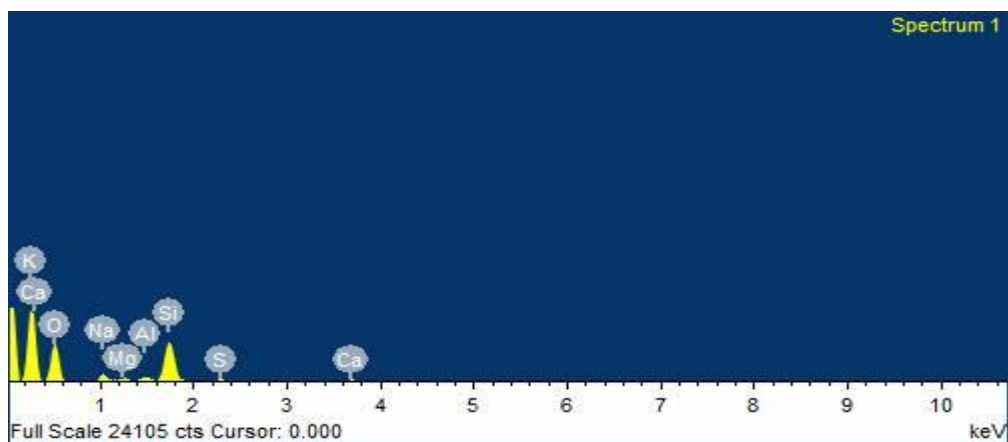


Figure 16: EDS elemental analysis of the contaminated surface of the fine-grained sandstone rock sample

Figure 19 which is the EDS data for the contaminated phase on the fine-grained sandstone, shows a variety of minerals found in this rock sample. The presence of Si, O, Na, Al, Ca, Na, Mg and K are observed on this figure. The availability of this large number of minerals means the fine-grained sandstone has more contaminants reducing the amount of SiO₂ as evident in the XRF data.

Table 7: Chemical composition of the contaminated surface of the fine-grained sandstone rock sample

Element	Weight%	Atomic%
O K	57.79	70.99
Na K	5.18	4.43
Mg K	1.36	1.10
Al K	2.00	1.46
Si K	27.46	19.21
S K	1.06	0.65
K K	0.67	0.34
Ca K	1.78	0.87
Fe K	2.69	0.95
Totals	100.00	

Table 8 shows the chemical composition of the contaminated surface in the fine-grained sandstone. It portrays the presence of a huge variety of minerals present in significant amounts (Na, O, Al, Si, Ca, and Fe) and others available as trace elements (Mg, S, and Fe). This data is also in line with the XRF data, proving the accuracy of the data.

4.2.3 Analysis of Coarse-grained Sandstone

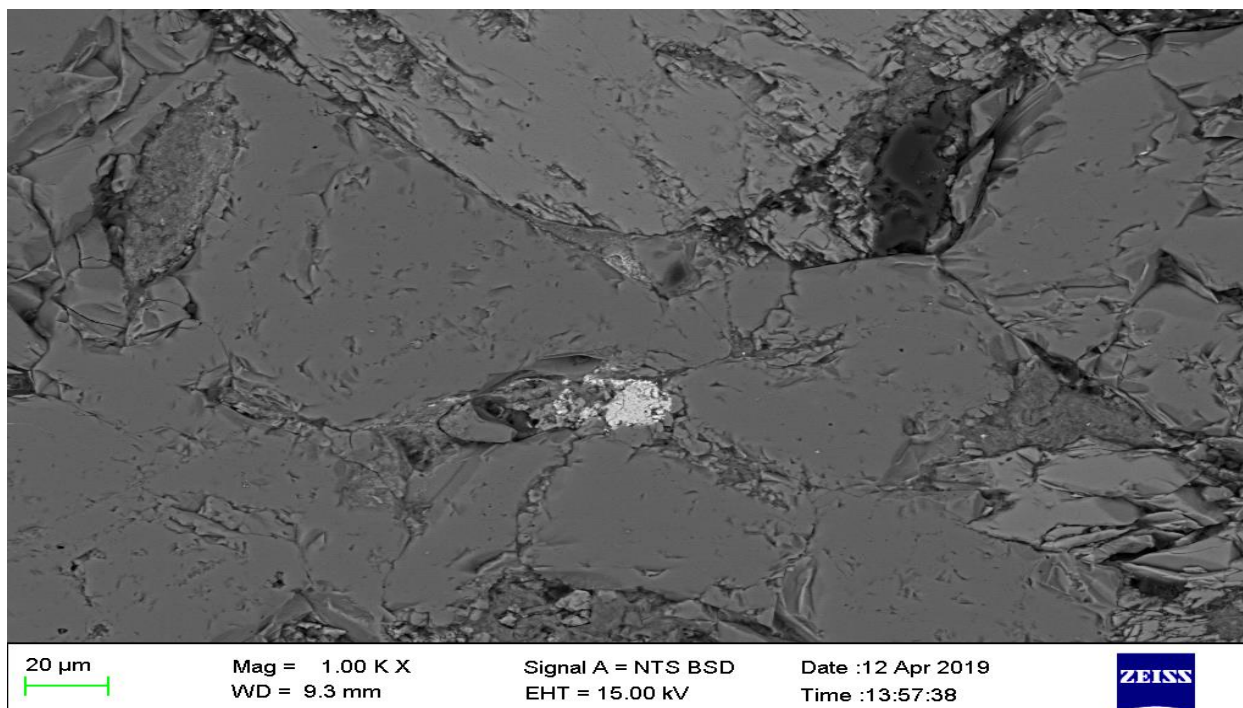


Figure 17: A section of the Coarse-grained Sandstone showing different phases of the rock sample

Figure 20 is a section on the coarse-grained sandstone that shows the different phases available. It is seen to have more of the grey phase and very few white phases. This means that it has less contaminants than the fine-grained sandstone shown in Figure 15. This is also in line with the XRF data that shows presence of more minerals in fine-grained sandstone than in the coarse-grained sandstone.

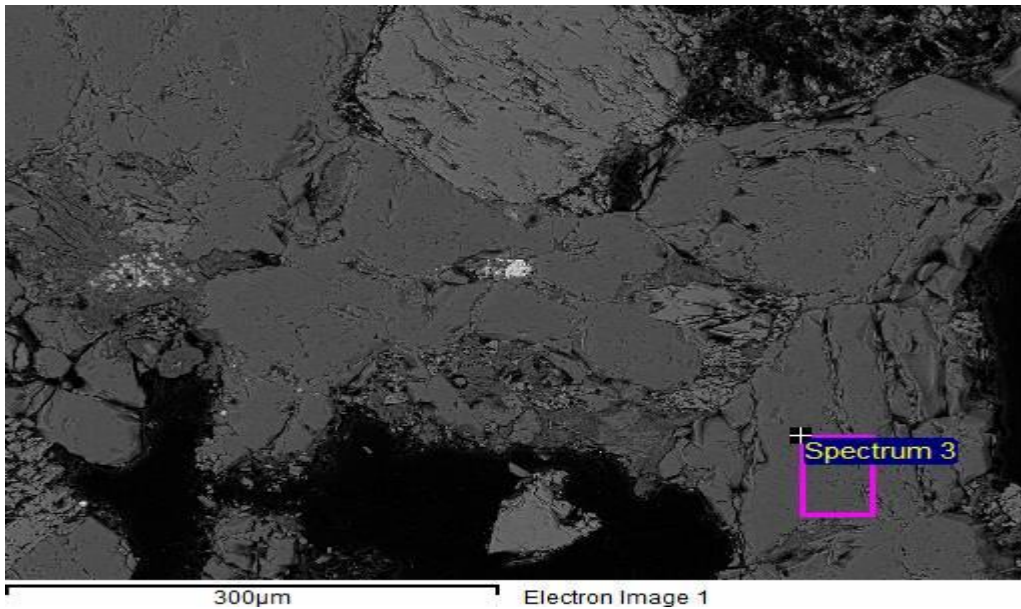


Figure 18: SEM image showing the clean surface of the coarse-grained Sandstone Spectrum 3 in Figure 21 is the clean surface without any contaminating minerals. It represents the availability of SiO₂ as the major constituent present.

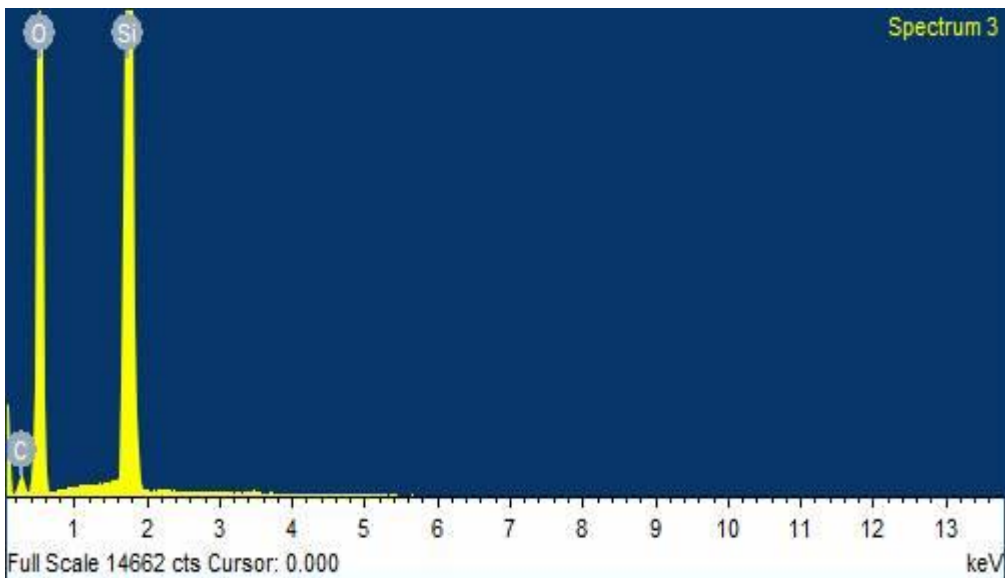


Figure 19: EDS elemental analysis of the clean surface of the coarse-grained sandstone

The EDS data in Figure 22 shows the presence of Si and O and this is in line with the XRF data that shows the SiO₂ as the major mineral found in the coarse-grained sandstone.

Table 8: Chemical composition of the clean surface of the fine-grained sandstone rock sample

Element	Weight%	Atomic%
C K	8.48	12.96
O K	55.29	63.39
Si K	36.22	23.65
Totals	100.00	

Table 9 shows the elemental composition of the dominant phase of the coarse-grained sandstone. It shows the presence of the Si and O in the 1:2 ratio. This is also in correlation with the mineral data from the XRF analysis.

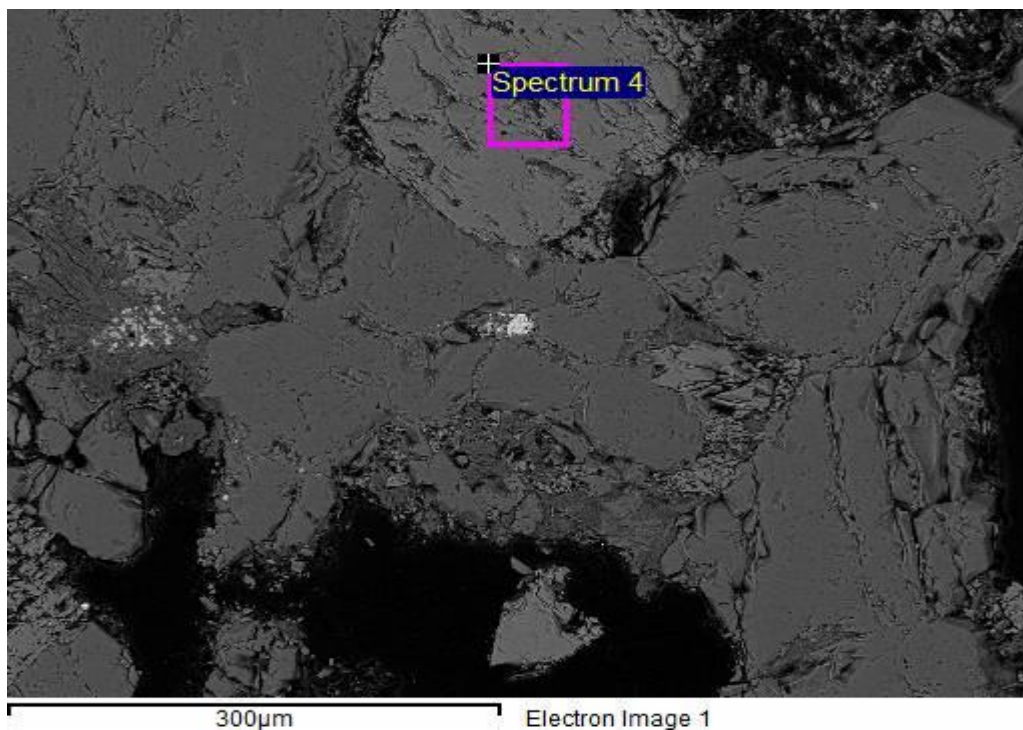


Figure 20: SEM image showing the contaminated surface of the coarse-grained sandstone rock sample

Figure 23 shows the contaminated area on the coarse-grained sandstone. Only a few patches of this phase are observed across the surface.

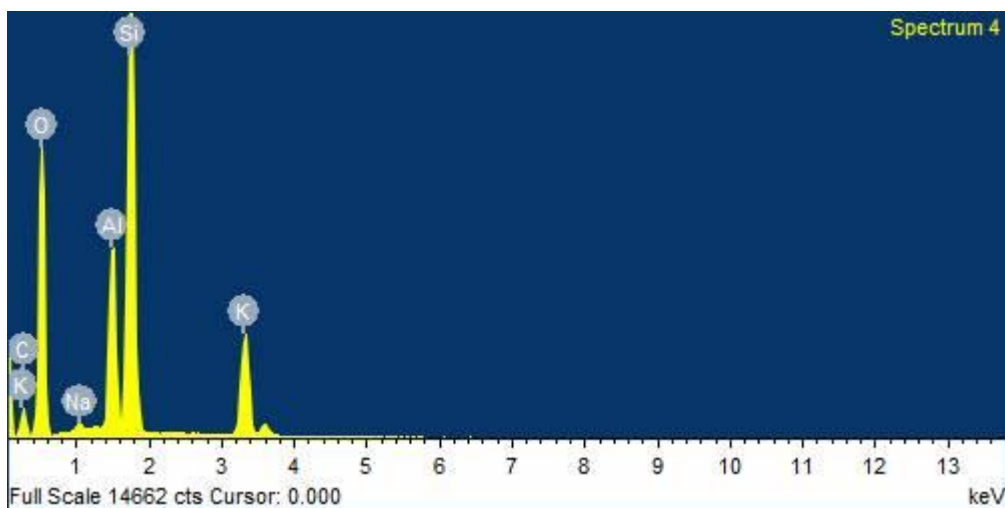


Figure 21: EDS elemental analysis of the contaminated surface of the coarse-grained sandstone rock sample

Figure 24 shows the elemental composition of the contaminated surface of the coarse-grained sandstone. The number of minerals is lower compared to that found in the fine-grained sandstone as observed in figure 19. This means that the coarse-grained sandstone is less contaminated compared to the fine-grained sandstone.

Table 9: Chemical composition of the contaminated surface of the coarse-grained sandstone rock sample

Element	Weight%	Atomic%
C K	11.13	17.47
O K	48.01	56.60
Na K	0.31	0.26
Al K	7.56	5.28
Si K	23.66	15.89
K K	9.33	4.50
Totals	100.00	

Table 10 shows the chemical composition of the contaminated surface in the coarse-grained sandstone. It shows the presence of major minerals present in significant amounts (Si, O, Al, and Si) and others available as trace elements (Na). This data is also in line with the XRF data, proving the accuracy of the data.

In all the characterization analyses conducted on the three rock samples, the XRF, XRD, and SEM/ EDS data have proven that the rock samples have the highest content of silica as compared to the other minerals, and quartzite has the highest silica content followed by coarse-grained sandstone then fine-grained sandstone. These results correlate with those from the uniaxial compressive stress (UCS) tests in Table 3 which show that quartzite is the hardest of all the rocks and this is due to the presence of the silica which is the major determining factor of the rock hardness.

4.3 XRD ANALYSIS

The data in Figures 7, 8 and 9, represent results from the XRD analysis of Coarse-grained Sandstone, Fine-grained Sandstone, and Quartzite. The results show that the samples contain a majority of Quartz (SiO_2) and other trace minerals. This is also in line with data given by the XRF Analysis as shown by Table 4, especially with regards to the presence of SiO_2 as the dominating mineral followed by Al, Fe and K. The data correlates with that from Scott (2010) where the author was analysing a Waterberg Sandstone sample during his investigation. Scott (2010) discovered that his sample mostly contained quartz and smaller amounts of orthoclase (KAlSi_3O_8) and kyanite (Al_2SiO_5), and his diffractogram portrayed similar peaks as these below.

The XRD data shows that quartzite contains Silicon dioxide (SiO_2) and Aluminium Oxide Silicate (Al_2SiO_5) also known as Kyanite, while Coarse-grained sandstone contained Silicon dioxide (SiO_2) and Potassium Aluminium Silicate (KAlSi_3O_8) a form of feldspar known as Orthoclase and fine-grained sandstone contained Silicon dioxide (SiO_2), Magnesium Manganese Oxide ($\text{MgO} \cdot \text{MnO} \cdot \text{O}$), Sodium sulfate ($\text{Na}_2\text{S}_2\text{O}_3$), Calcium (Ca) and Potassium (K).

In the quartzite rock, the main peaks representing SiO_2 are shown at 2Theta position of 21, 27 and 50° , while Al_2O_3 appears at 41, 46, and 50° . For coarse-grained sandstone, the major peaks for SiO_2 appear at 21, 27, and 50° , and Al_2O_3 appears at 36, 43, and 50° . The fine-grained

sandstone was seen to have a variety of components as evident by the XRF data and SEM data. The SiO_2 peaks were found at, 21 and 27°, then the MgO peaks at 37 and 43°, Ca peak at 27° then the K peaks at 50 and 60°. This shows that the fine-grained sandstone was highly impure. For all the rock samples, the SiO_2 peak found around 27° was the highest, proving further that the rocks are silica based and contain traces of other elements as well as silica in other forms, as shown by its distribution through the spectra.

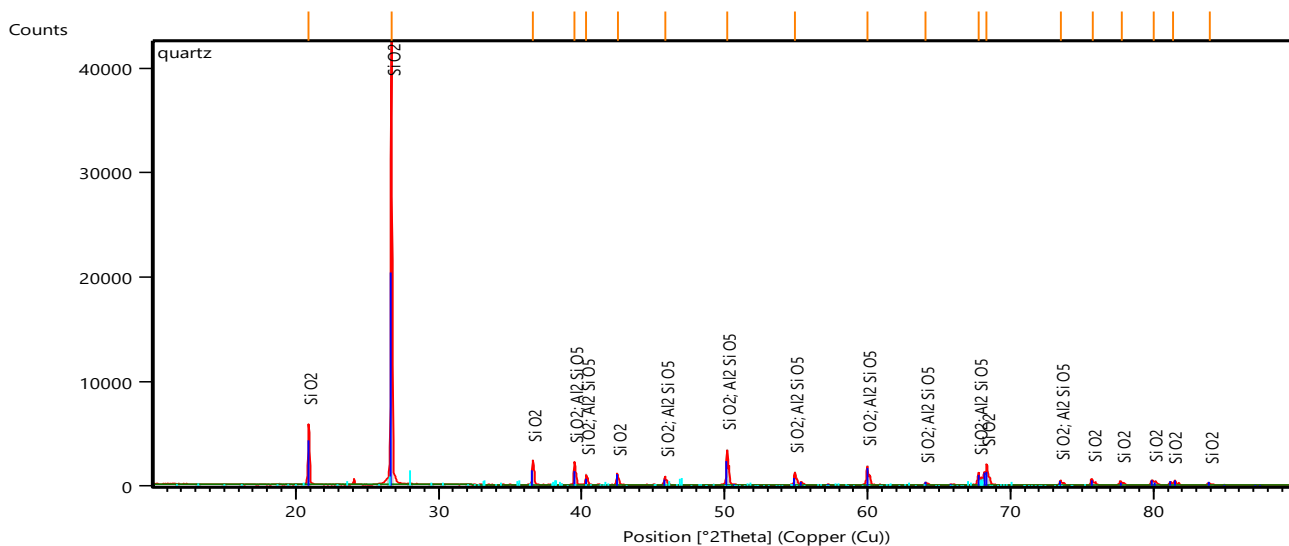


Figure 22: X-ray Diffractogram of Quartzite

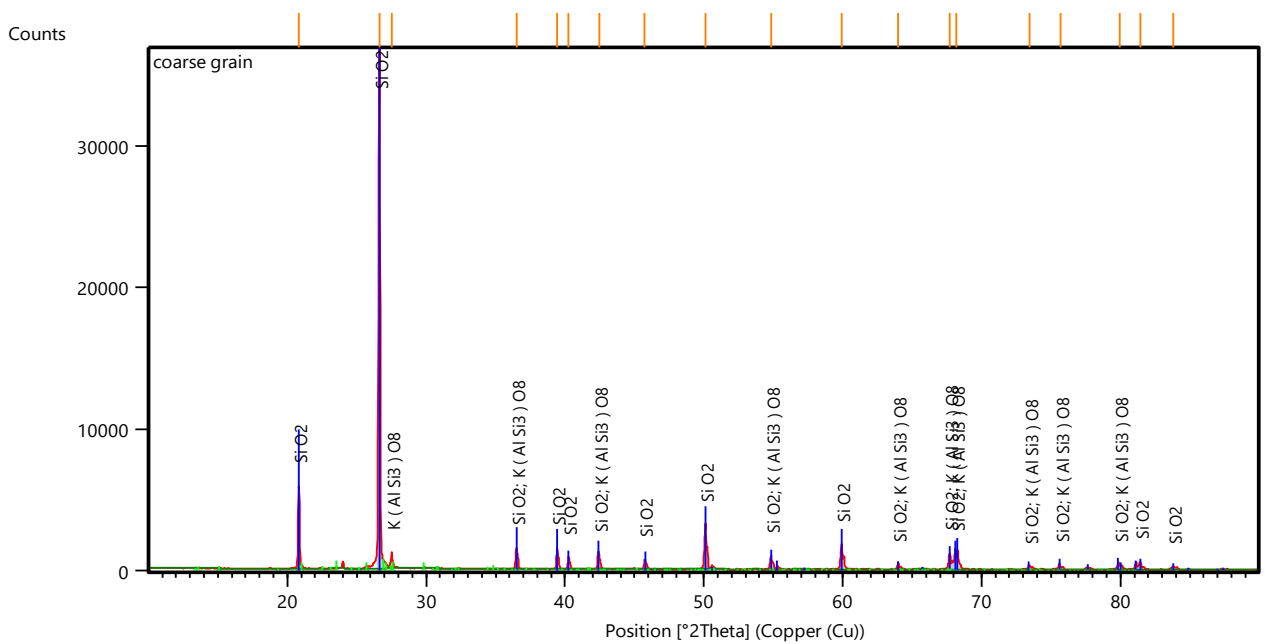


Figure 23: X-ray Diffractogram of Coarse-grained Sandstone

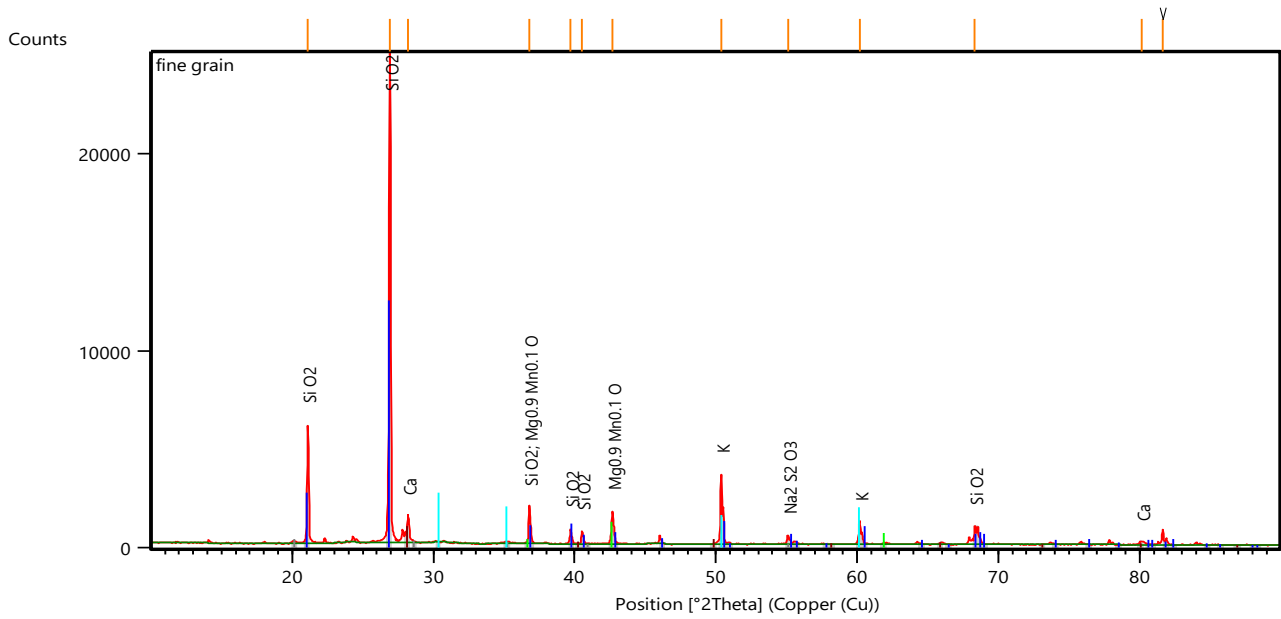


Figure 24: X-ray Diffractogram of Fine-grained Sandstone

4.4 HARDNESS TESTING

Table 10: Load at failure for rock samples during Uniaxial Compressive Strength testing

Rock type	Length (mm)	Diameter (mm)	Mass (g)	Load (kN)	Uniaxial Compressive Strength (UCS) (MPa)
Quartzite	105.3	41.9	428.8	273.21	172.38
Coarse-Grained Sandstone	62.8	24.0	66.7	59.32	131.13
Fine-Grained Sandstone	76.9	30.5	128.8	51.95	71.10

The equipment specification (length 105 mm and a diameter of 42 mm) could not be met due to the small size of the investigated rock samples. Therefore, to use the equipment, the ratio of the diameter to the length of 2:5 was maintained. Table 3 shows that quartzite as expected, has the greatest UCS value, which allowed it to carry the largest load before it failed. These results showed that quartzite is harder than the coarse-grained sandstone and the fine-grained sandstone. The coarse-grained sandstone has a higher hardness than the fine-grained sandstone, and this may be attributed to the mineral compositions as depicted in Table 4, where coarse-grained sandstone has a greater quantity of quartz, which is the major determining factor of rock hardness. Since the presence of silica in rocks is the major determining factor of the rock's hardness, quartzite will have the highest hardness as compared to the other two rock samples.

To support the mineralogical analysis results, this investigation used Mohs (1825) hardness scale. The hardness in this scale was determined using scratch tests where one material should scratch the other, but the latter should not be able to scratch the former. The scale was as follows:

1. Talc ($\text{Mg}_3\text{Si}_4\text{O}_{10}(\text{OH})_2$)
2. Gypsum ($\text{CaSO}_4 \cdot 2\text{H}_2\text{O}$)
3. Calcite (CaCO_3)
4. Fluorite (CaF_2)
5. Apatite ($\text{Ca}_5(\text{PO}_4)_3(\text{F}, \text{Cl}, \text{OH})$)
6. Feldspar (KAlSi_3O_8)
7. Quartz (SiO_2)
8. Topaz ($\text{Al}_2\text{SiO}_4(\text{F}, \text{OH})_2$)

- 9. Corundum (Al_2O_3)
- 10. Diamond (C)

The rock sample containing more of Quartz was the hardest. Fine-grained sandstone contains more of MgO, CaO, and Na_2O than coarse-grained sandstone and quartzite, and this means it was softer and easily scratched by the other two rocks. The LOI is also highest for fine-grained sandstone; which is an indication that it contains more water, carbon, organic matter, and volatile compounds. This affects the quality of the rock hence its hardness.

4.5 DRY TESTING

4.5.1 Stainless Steel ball/Rock disc contact under dry conditions

Figure 25 - 27 show the coefficient of friction in different rock types in dry conditions. The experiments were conducted using 6mm diameter ASI 4340 Stainless Steel balls against three rock samples of Fine-Grained Arkose Sandstone, Coarse-Grained Arkose Sandstone and Quartzite. The bit rotating speed was in the range of 100-300 rpm while the weight-on-bit was in the range of 1-9 N. These experiments aim to give an understanding of how friction coefficient is affected by variations in the rotating speed and load under dry conditions.

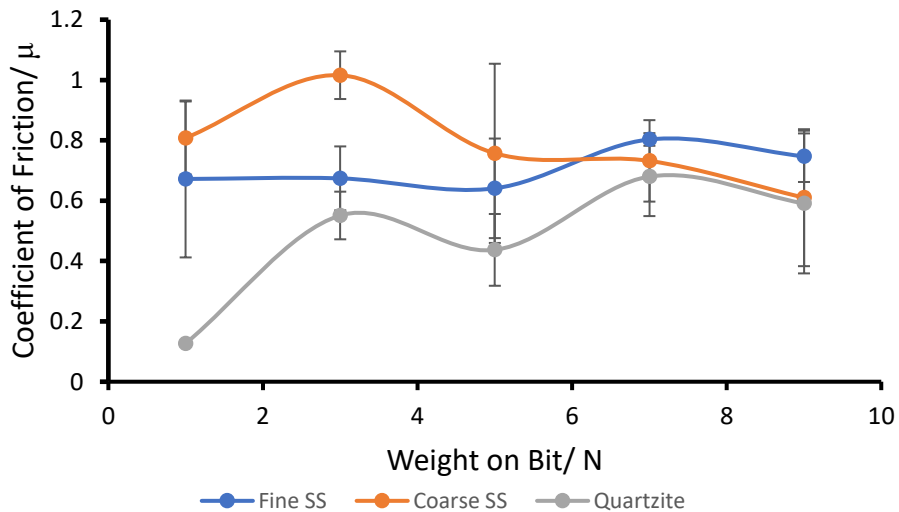


Figure 25: Coefficient of friction for different rock materials at 100 rpm under dry conditions

The COF results were obtained using the Tribometer Software Version 7 that calculates the coefficient of friction at every point and then gives an average value. It also determines the

standard deviation of all the data points. Figure 25 represents the values for the coefficients of friction in three different rock types running at the rotation speed of 100 rpm while varying loads from 1 N to 9 N. It was observed that, the values of the coefficients of friction when using the low speed became very high up to 1, especially when looking at coarse grained sandstone. The COF started off very high and decreased as more load was added when using the coarse-grained sandstone. The fine-grained sandstone did not show much variation in the COF. The COF was initially high, then no change was seen when the load was increased to 3 and 5 N. Increasing the weight further resulted in an increase in the COF for fine-grained sandstone. Quartzite showed a fluctuating increase in the COF. The COF started very low around 0.12 and increased to 0.60.

The reason for the great value of the COF observed may be due to the large asperities found on the surface of the rock samples for fine and coarse-grained sandstone. The low load is not able to create enough cutting stress to overcome the asperities. This results in a lot of friction between the stainless ball and the rocks, which lead to high friction and apparent wear of the ball. For quartzite, the rock surface is quite smoother meaning less friction is generated hence the low COF. An increase in the COF would mean that the rock eventually becomes polished by the motion since the speed is not enough to exert enough pressure to result in any rock penetration. A lot of heat is generated, and wear follows. The standard deviation is very high for the fine-grained sandstone, this means that more studies should be conducted to find out the reason behind the irregularity.

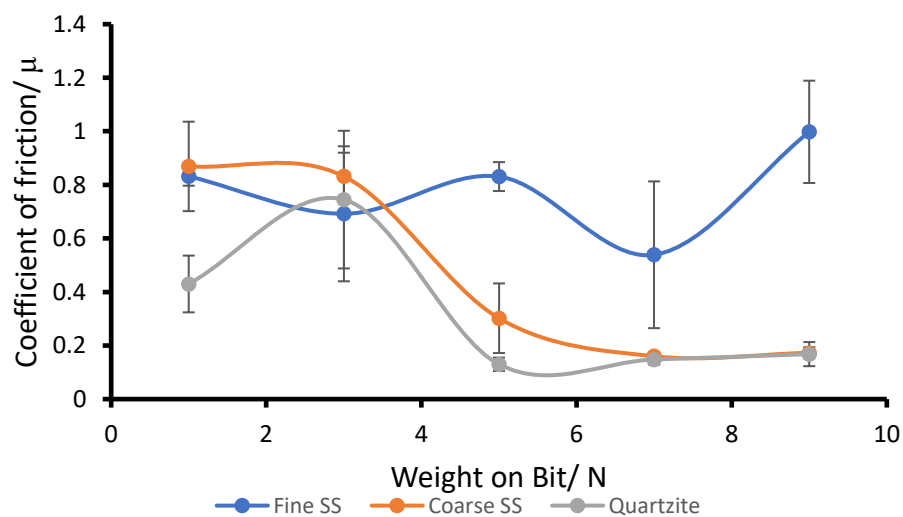


Figure 26: Coefficient of friction on different rock materials at 200rpm under dry conditions

Figure 26 represents the values for the coefficients of friction in three different rock types running at the rotation speed of 200 rpm while varying loads from 1 N to 9 N. The trend observed for coarse-grained sandstone and quartzite, shows that the COF decreases by 402 % and 156 %, respectively, while it increases by 19% for the fine-grained sandstone. This is a clear indication that the bit rotating speed is an influential factor when it comes to the efficiency of a drilling process, and different operating conditions apply for different rock types. Coarse-grained sandstone and quartzite almost show a similar trend. It is seen that their COF are lowest at 5, 7 and 9 N. Since at the end of the day, the aim is to save on operating costs, it would be wiser to work with speed of 200 rpm and load of 5 N, since increasing the load does not have a significant impact on the COF as observed in the figure. For fine-grained sandstone, it would be safe to operate at 200 rpm using load 7 N. Dougherty *et al.* (2015) explains this by asperities found on the surface of the rock materials. When the drilling process begins, the asperities found on the surfaces of both materials are still very rough, so an increase in the rotating speed results in an increase in the contact pressure on the two surfaces, reducing the roughness of the surfaces, hence reducing the COF.

The trend observed here where the fine-grained sandstone has higher COF may be due to the fact that, as the experiments were conducted, the rock was abraded, and in the absence of the drilling fluid, the loose particles piled up and resulted in more friction. This is because the rock is more brittle and can easily be broken unlike the other two. This is in line with what Zorlu *et al.*, (2008) and Vutukuri *et al.*, (1974) that the rocks which contain quartz as a binding material are stronger than those that contain calcites and ferrous minerals. Then those that contain clay binding material are the weakest and are easily broken. This is also proven by the mineral composition of these rocks from XRF, XRD and SEM/SDS data. The hardness of the rock samples is also proven by the USC data in Table 3.

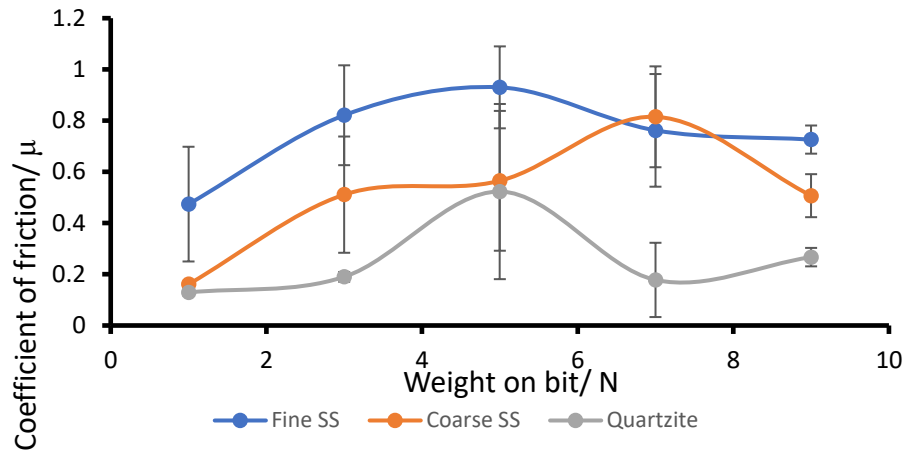


Figure 27: Coefficient of friction on different rock materials at 300 rpm under dry conditions

Figure 27, shows the coefficients of friction in three different rock types running at the rotation speed of 300 rpm while varying loads from 1 N to 9 N. The trend observed is a fluctuation in the coefficient of friction while increasing the weight-on-bit. For the fine-grained sandstone, the COF was low at 1 N, then increased at 3 and 5 N, only to drop at 7 and 9 N. For coarse-grained sandstone, The COF was very low and increased when the load was increased. For the quartzite, at low and high loads, the COF was seen to be very low, but high when the 5 N load was used. At very low loads of 1 N, this where the best results of the lowest COF in the three rock samples is found.

The XRF data on Table 4 shows there is a higher LOI for fine-grained sandstone than the other two rocks, making it more impure since it has more mineral matter. These impurities affect the hardness of the rocks, making fine-grained sandstone least hard. It also has a greater amount of MgO, CaO, Na₂O, and Ti₂O. All these weaken the rocks integrity making it easily abraded. So, in the absence of drilling fluid, the COF becomes very high as the abraded rock particles are not carried away but remain on the wear track increasing abrasivity of the rock, hence high COF. The high standard deviations are a challenge so more experiments must be conducted to find out where the problem lies.

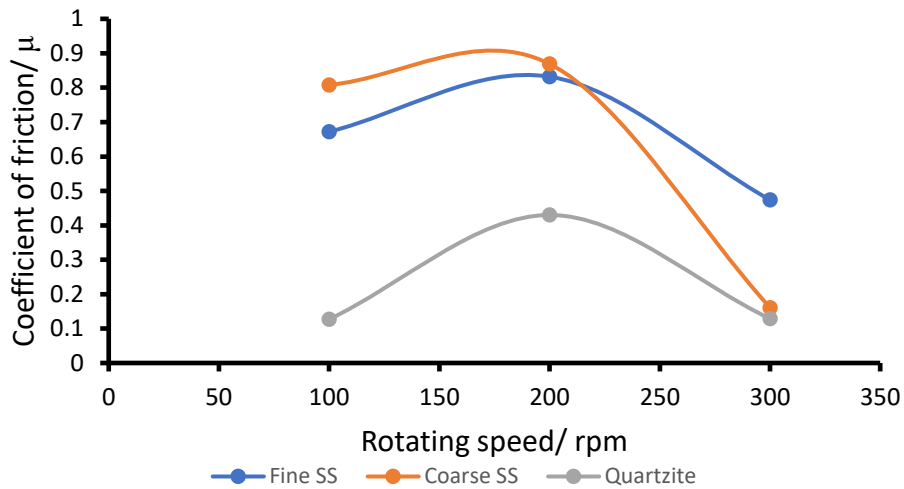


Figure 28: The coefficients of friction at 1 N using speeds of 100 rpm, 200 rpm, and 300 rpm

Figure 28 shows the coefficients of friction of the three types of rocks were investigated when using the 1 N weight-on-bit at the three rotating speeds of 100 rpm, 200 rpm, and 300 rpm. There is a clear decrease in the COF in fine-grained sandstone and coarse-grained sandstone, when the speed is increased and the COF decreased by 41.8 % and 401.9 %, respectively. The use of quartzite showed that at very low speed of 100 rpm and high speed of 300 rpm, the COF significantly drops, but remained high when speed of 200 rpm was used.

Figure 28 also shows that at high speeds, it is best to operate at a low load of 1 N in fine-grained and coarse-grained sandstone, but in quartzite, the low load of 100 rpm can be used to save costs as it yielded the similar results as when high load was used.

The high COF observed for 100 and 200 rpm in fine and coarse-grained sandstone, may be explained by the asperities found on the contacting surfaces as in Figure 26. These rotating speeds at the low load of 1 N, are not enough to overcome the asperities, hence the high COF is observed. Increased speeds then results in a decrease in the COF due to a reduction in the surface roughness at the very speed. Dougherty et al., (2015), also had the same observation when dealing with Carthage marble in dry conditions.

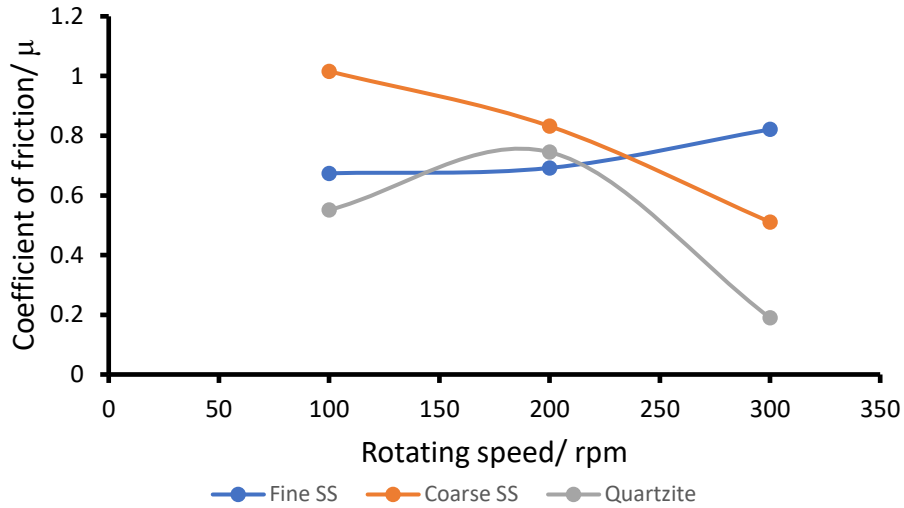


Figure 29: The coefficients of friction at 3N using speeds of 100 rpm, 200 rpm, and 300 rpm

Figure 29 represents the coefficients of friction of the three types of rocks when using the 3 N weight-on-bit at the three rotating speeds of 100 rpm, 200 rpm, and 300 rpm. The COF is seen to decrease for coarse-grained sandstone by 9808 % while it fluctuates in quartzite. The COF increases from 100 rpm to 200 rpm, then significantly drops at 300 rpm. The COF increased for fine-grained sandstone by 21.8 %. The COF values are higher when the 3 N load is used, compared to the use of 1 N load.

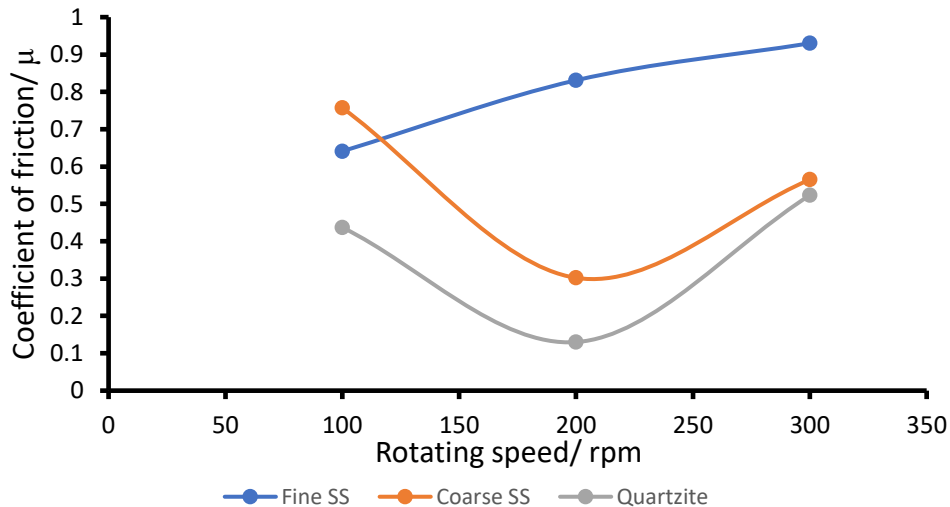


Figure 30: The coefficients of friction at 5 N using speeds of 100 rpm, 200 rpm, and 300 rpm

Figure 30 represents the coefficients of friction of the three types of rocks when using the 5 N weight-on-bit at the three rotating speeds of 100 rpm, 200 rpm, and 300 rpm. The COF in coarse-grained sandstone and quartzite was seen to fluctuate. High COF values were seen when low speed of 100 rpm and high speed of 300 rpm were used. Significant decrease was observed when using the medium speed of 200 rpm in both rocks. The COF was seen to increase in fine-grained sandstone and this may be due the resistance of the rock against the ploughing motion of the ball.

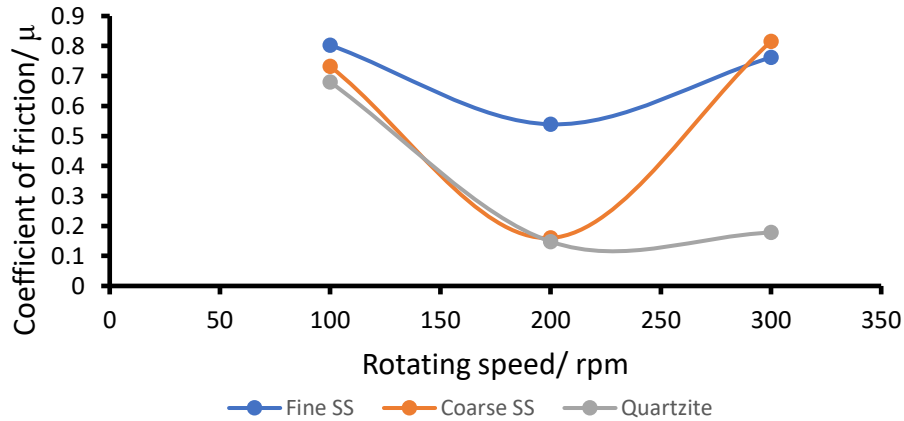


Figure 31: The coefficients of friction at 7 N using speeds of 100 rpm, 200 rpm, and 300 rpm

Figure 31 represents the coefficients of friction of the three types of rocks when using the 7 N weight-on-bit at the three rotating speeds of 100 rpm, 200 rpm, and 300 rpm. A fluctuating trend is observed in all three rock types, where the COF is high at low speed of 100 rpm, decreases at 200 rpm, then increase again when a higher speed of 300 rpm is used. At this load, the COF is lowest in all rocks at 200 rpm, confirming that at this rotating speed, a load of 7 N is needed to overcome resistance from the rocks hence improve the efficiency of drilling, resulting in reduced COF. These results are also in line with those found by Dougherty et al., (2015), at higher loads, the COF decreases as the high load exerts a very high pressure to smooth asperities polishing the surface hence low COF.

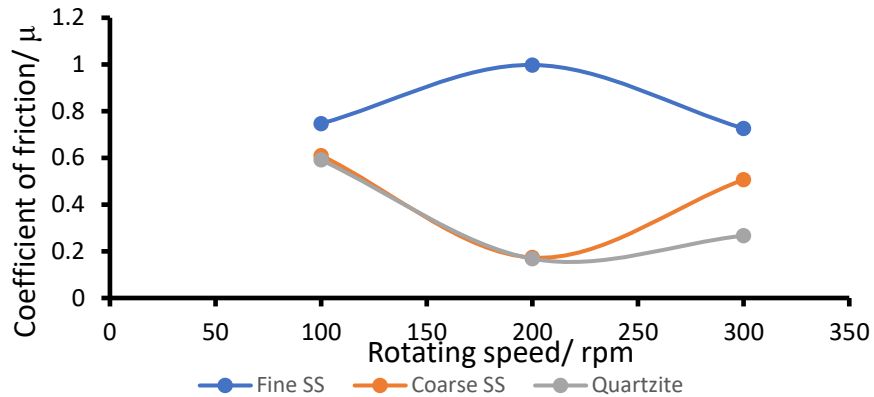


Figure 32: The coefficients of friction at 9 N using speeds of 100 rpm, 200 rpm, and 300 rpm

Figure 32 represents the coefficients of friction of the three types of rocks when using the 9 N weight-on-bit at the three rotating speeds of 100 rpm, 200 rpm, and 300 rpm. The COF was seen to fluctuate in all rocks when using highest load of 9 N. In the fine-grained sandstone, low and high speed yielded similar COF, which were lower than using 200 rpm. This means optimum results can be found when using low rotating speeds for high loads. Coarse-grained sandstone and quartzite almost show a similar trend of high COF when using speeds of 100 rpm and 300 rpm. They show a decrease when 200 rpm is used. This means that for these two rock types, at this high load, the best speed to yield optimum results is the 200 rpm. These results have not deviated much from when the 7 N weight-on-bit was used. This means that it would not be economically feasible to use higher load when we can get more or less similar results when using lower load especially for coarse-grained sandstone and quartzite.

4.5.2 Wet Testing

For wet testing, different sets of lubricants were used to determine how they each affect the COF at different operating conditions. Solutions of 25 wt% of additives of bentonite and sodium chloride in the ratio 4:1, respectively, were prepared using water and castor oil. Another set was prepared using 50 wt% of additives of bentonite and sodium chloride still in the ratio of 4:1, respectively, using water and castor oil as the base fluid.

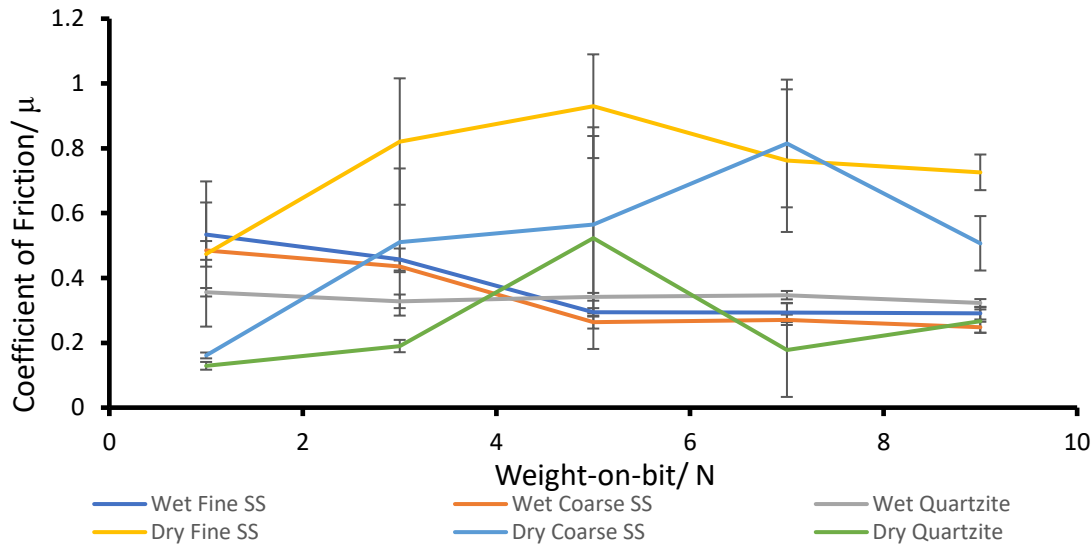


Figure 33: Coefficient of friction on different rock materials at 300 rpm using 25 wt% of additives in the water

Figure 33 shows how the addition of a lubricant affects the coefficient of friction. In this case, the drilling fluid was used at the rotating speed of 300rpm and varying weights from 1 N to 9 N. It was observed that the addition of the lubricant, with comparison to the dry testing results from Figure 27, an increase in the load reduced the coefficient of friction by 83.51 %, 95.56 % and 10.21 % for fine-grained sandstone, coarse-grained sandstone, and quartzite, respectively. Figure 33 showed a very clear trend for all the three rock types with the highest decrease seen in coarse-grained sandstone. When compared with the dry testing, it is clearly seen that the use of a lubricant greatly influences the value of the COF. Despite the use of the lubricant, quartzite still showed a decreased COF than when the lubricant was used. This may be due to the chemical reactions between the rock and the contents of the fluid, which make the rock even harder to drill, but more research should be conducted to better understand this behavior.

Though there were visible reductions in the COF when using lubricants than without lubricants, an increase in the WOB did not affect the COF much. At lower loads, the COF was higher than at high loads but with very little difference. When Dougherty et al., (2015) used Carthage marble under lubricated conditions, they found that the COF was not really affected by the load. This was because the lubricant effectively separated the two surfaces through hydrodynamic lift, and this remained constant throughout drilling.

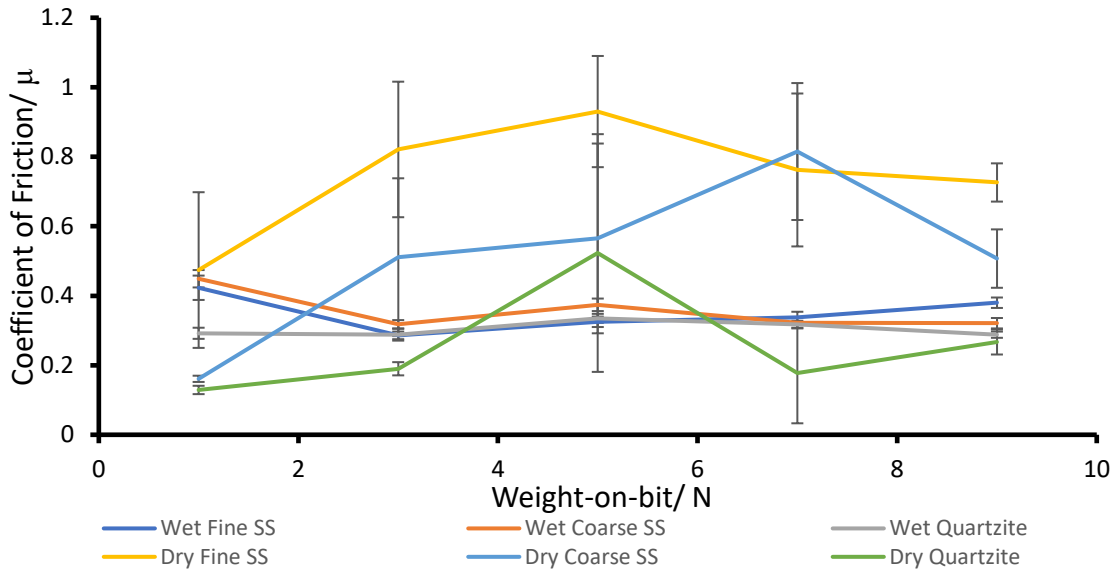


Figure 34: Coefficient of friction on different rock materials at 300 rpm using 50 wt% additives in the water

Figure 34 shows how the addition of a lubricant affected the coefficient of friction. The drilling solution was used with the rotating speed of 300 rpm and varying weights from 1 N to 9 N. It was observed that the addition of this lubricant, while increasing the load reduced the coefficient of friction by 11.32 %, 39.88 %, and 1.39 % for fine-grained sandstone, coarse-grained sandstone and quartzite, respectively. These values are not so different when using 25 wt% of additives. This means that further addition of bentonite has no significant impact on the coefficient of friction. And more tests should be conducted to find the minimum bentonite concentration that will give the best results. Lower COF was also observed in quartzite in dry testing than when the lubricants were used. Further research must be conducted in order to understand this behavior.

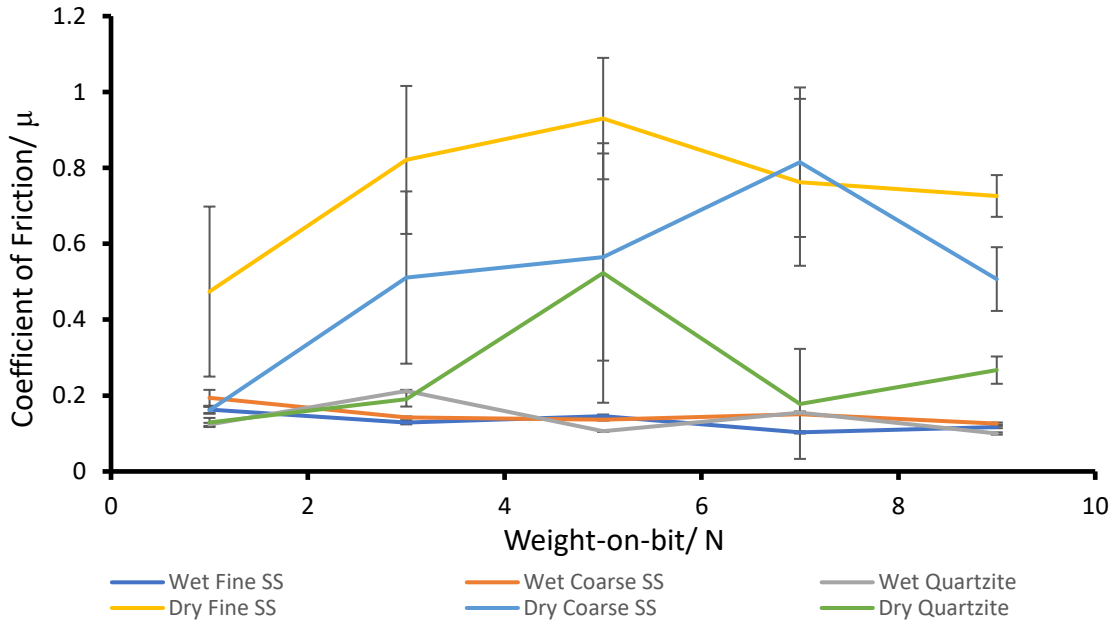


Figure 35: Coefficient of friction on different rock materials at 300 rpm using 25 wt% additives in castor oil

Figure 35 indicates how the addition of a lubricant affect the coefficient of friction. In this case, 25 wt % of additives were added to castor oil and the rotating speed used was 300 rpm with varying weights from 1 N to 9 N. It was observed that the addition of lubricant with an increase in the weight-on-bit reduced the coefficient of friction by 39.32 %, 53.97 % and 24.00 % for fine-grained sandstone, coarse-grained sandstone, and quartzite, respectively. This is an indication that the use of castor oil is more effective in the reduction of COF than water. It is also an advantage since castor oil is readily available in South Africa; and as a plant product, it is a non-edible and biodegradable oil. A clear trend is shown for the decreasing COF and there is no significant change seen in all the three rock types. The comparison of the dry testing from Figure 27 with the addition of the castor oil lubricant, significantly showed a reduction in COF.

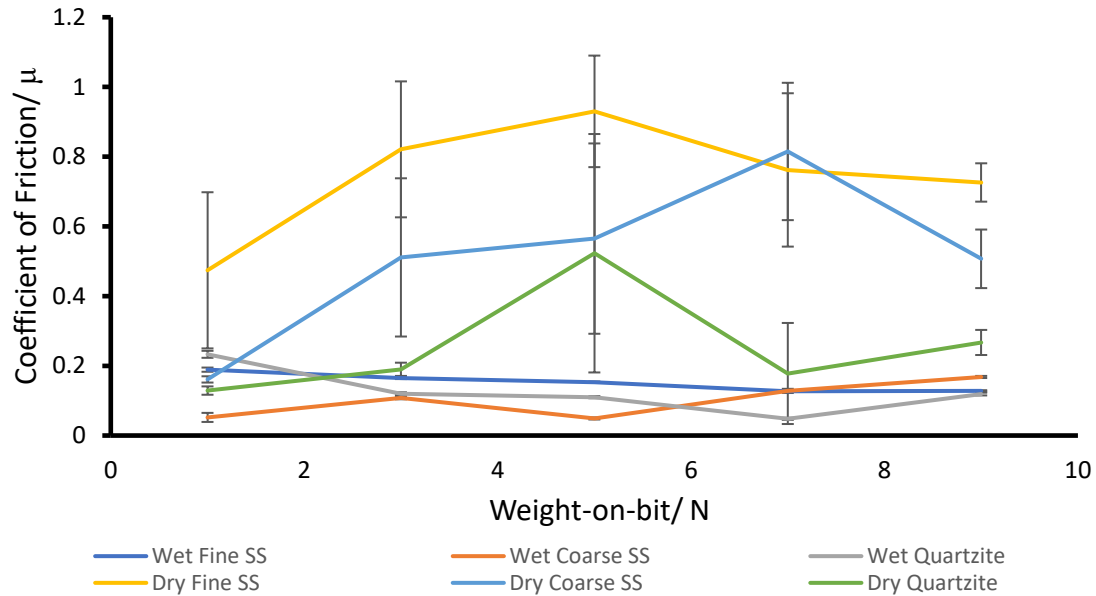


Figure 36: Coefficient of friction on different rock materials at 300 rpm using 50 wt% additives in castor oil

The Figure 36 shows how the addition of lubricant affected the coefficient of friction. In this case, 50 wt % additives in castor oil solution was used with the rotating speed of 300 rpm and varying weights from 1 N to 9 N. It was observed that the addition of this lubricant while increasing the weight-on-bit reduced the coefficient of friction by 47.00 % and 95.80 % for fine-grained sandstone and quartzite, respectively, but showed an increase of 69.05 % in coarse-grained sandstone. The COF was significantly reduced as compared to dry wear tests and also when using water as the base fluid. This means that the usage of castor oil is more effective in the reduction of COF for all rock types when using lowest and highest loads. Castor oil also has more benefits compared to water-base lubricants as already discussed. When comparing the 25 wt% and 50 wt% of the additives when using castor oil, there was no significant difference observed, meaning the use of 25 wt% of additives was more beneficial and cost-effective.

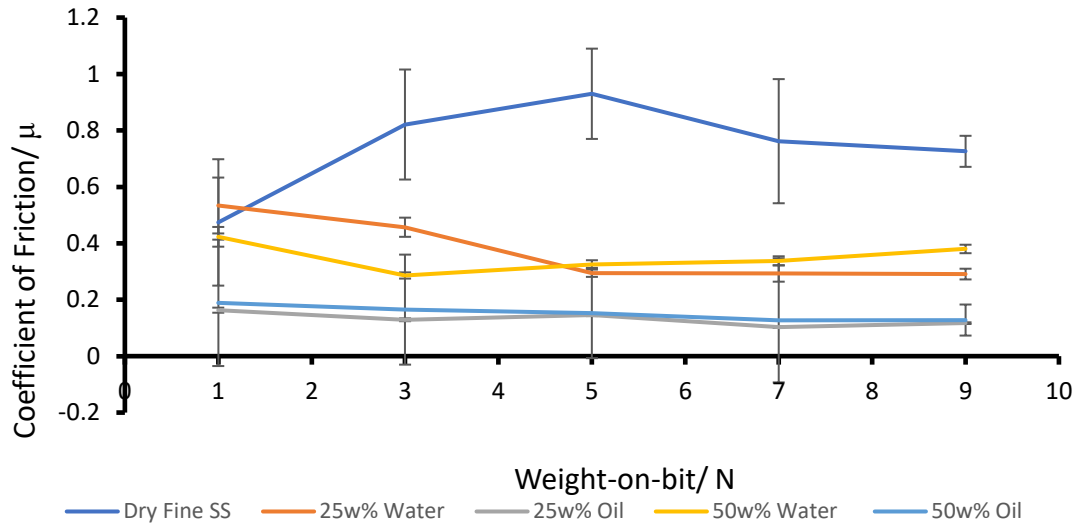


Figure 37: Coefficients of friction for fine-grained sandstone under different lubrication concentrations

Figure 37 represents the coefficients of friction of fine-grained sandstone under 25 wt% and 50 wt% of additives when water and castor oil were used. These results are also compared to the results obtained from the dry testing. It was clearly observed that usage of castor oil effectively decreases the coefficient of friction as compared to the usage of water as the base fluid. For fine-grained sandstone, the best performance is seen with the usage of 25 wt% oil solution. This is beneficial as fewer additives are used, resulting in reduced costs.

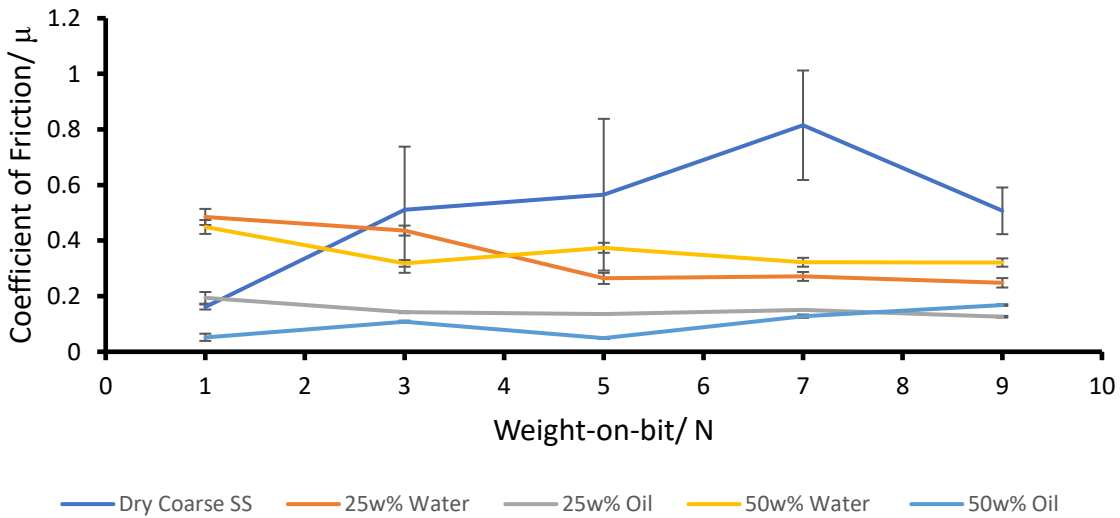


Figure 38: Coefficients of friction for coarse-grained sandstone under different lubrication concentrations

Figure 38 represents the coefficients of friction of coarse-grained sandstone under 25 wt% and 50 wt% of additives added to water and castor oil. It clearly observed that usage of castor oil effectively decreases the coefficient of friction as compared to the usage of water as the base fluid. For the coarse-grained sandstone, the best performance is seen with the usage of the 50wt% additives and castor oil solution which significantly reduces the COF. But since there is not much difference observed when 25 wt% and 50 wt% additives are used, it was wise to use the 25 wt% to use fewer additives hence reduce operating costs.

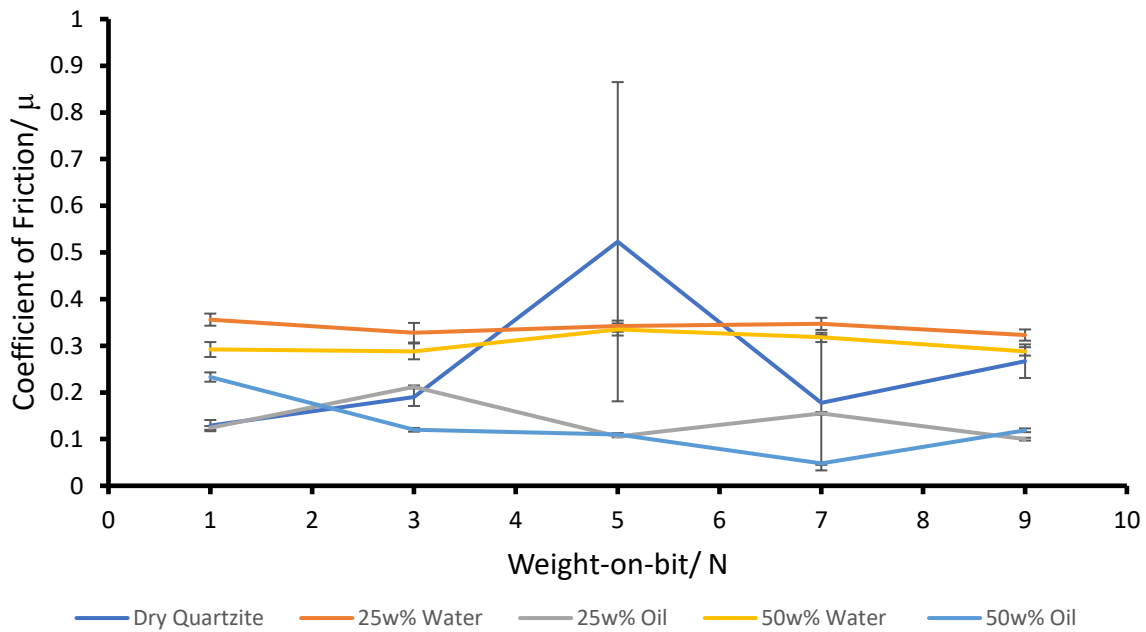


Figure 39: Coefficients of friction for quartzite under different lubrication concentrations

Figure 39 represents the coefficients of friction of quartzite under 25 wt% and 50 wt% additives in water and castor oil solutions. It was shown that the usage of oil is effective in decreasing the coefficient of friction as compared to the usage of water as the base fluid. For this rock sample, the best performance is also observed with the usage of 50 wt% additives and castor oil solution which significantly reduces the COF. More studies should be performed to find the minimum additive concentration that gives the lowest COF.

4.6 USE OF NANOPARTICLES IN DIFFERENT CLAYS USING FRESH WATER AND SEA WATER

Attapulгите, sepiolite, and bentonite were used as clays in the synthesis of different drilling fluids using freshwater and seawater. Cellulose nanocrystals (CNC) were added to improve their rheological behavior, hence lubricity of the drilling muds. Figures 40 to 46 show how the coefficient of friction was affected using each different type of clay.

4.6.1 Freshwater as the Base Fluid

Freshwater is naturally occurring with very small amounts of dissolved salts. Because of its abundant availability, it is a base of choice for the oil and gas drilling fluids. The use of bentonite in Figure 40 and attapulгите in Figure 41, show a steady decrease in the coefficient of friction in all three rocks, with an almost similar decrease in coarse-grained sandstone and quartzite when using bentonite and a similar decrease in fine-grained sandstone and coarse-grained sandstone when using attapulгите. A slight deviation is observed for coarse-grained sandstone at a weight of 7 N when using bentonite, this means that more studies should be conducted to properly explain this behavior. Figure 43 and Figure 44 portray a significant decrease in the COF from dry testing when no fluid was used. This is quite different from Figure 45 where sepiolite was used. It shows a steady increase for coarse-grained sandstone and quartzite and a steady decrease in fine-grained sandstone. When compared with the dry tests, there is not much difference observed in the COF when sepiolite was used.

The significant decrease observed in bentonite and attapulгите may be due to the very fine particles (10-25 nm diameter) content, which have very good colloidal properties making them stable throughout the drilling process. The high surface area of the particles means they can absorb water and hence improve the performance of the drilling fluid.

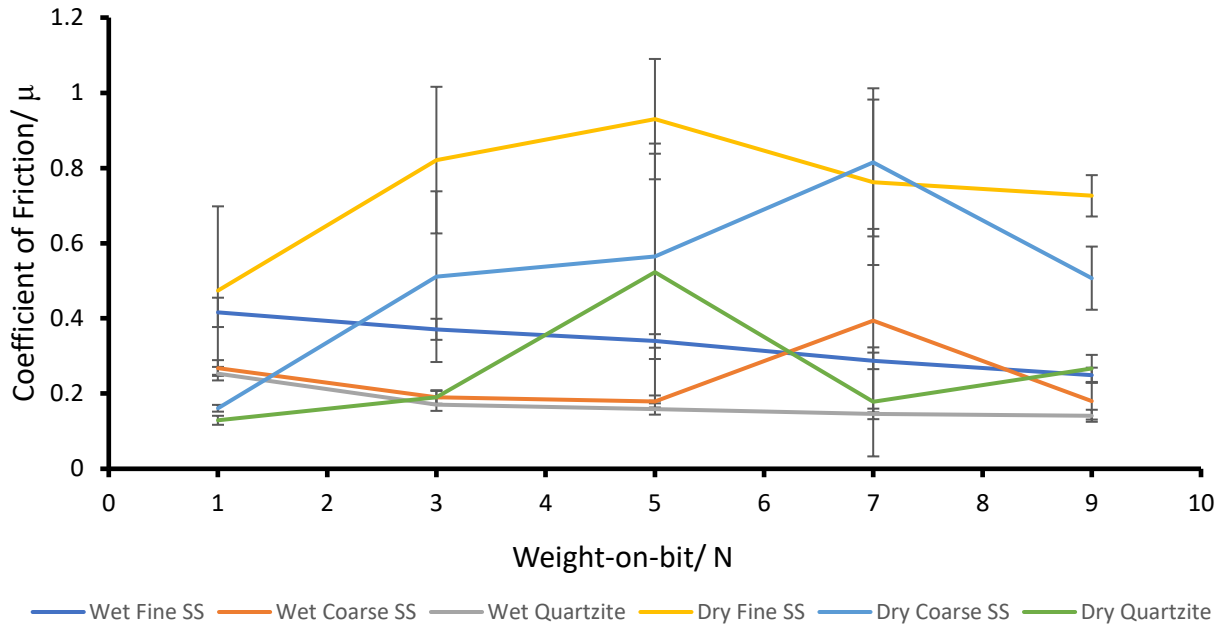


Figure 40: Coefficients of friction for different rock types when using CNC-Bentonite-Freshwater solution at 300 rpm

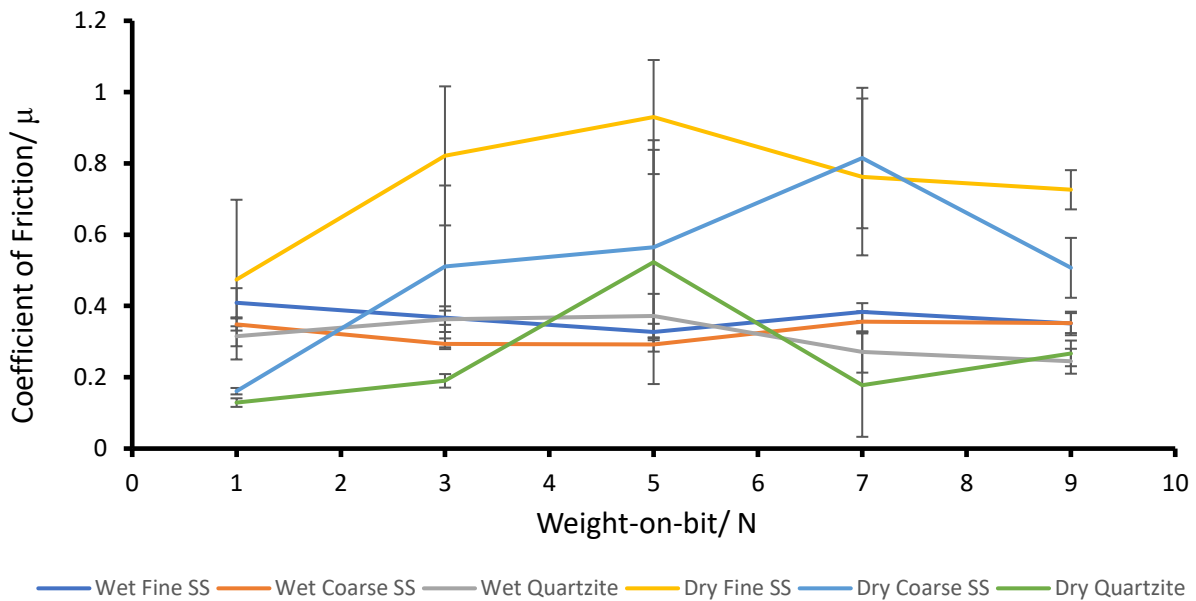


Figure 41: Coefficients of friction for different rock types when using CNC-Attapulgate-Freshwater solution at 300 rpm

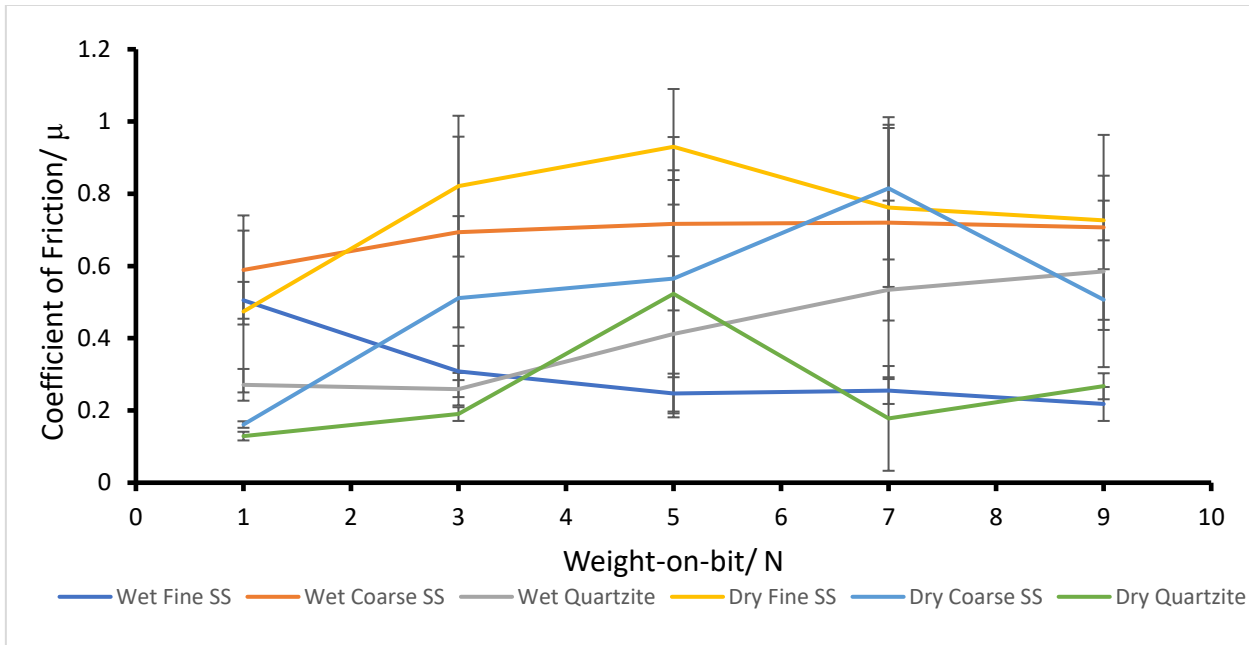


Figure 42: Coefficients of friction for different rock types when using CNC-Sepiolite-Freshwater solution at 300 rpm

4.6.2 Seawater as the Base Fluid

Seawater also known as saltwater, is water from the ocean that has at least 3.5% of dissolved salts with the majority as sodium chloride (NaCl). For offshore and coastal area drilling operations, this is usually the best base fluid of choice due to availability. A steady decrease was observed in all the three drilling fluids, and it shows better COF reduction as compared to when the freshwater was used. This is further agreed upon by O'Brien (1955) where two types of seawater drilling muds were used and it was found that the seawater was more desirable due to satisfying performance than the freshwater drilling muds and that the costs were almost as equal to that of the freshwater drilling muds in offshore operations. Hayatdavoudi, (2001), found that despite the low gel strength of the seawater drilling water, it was still able to effectively remove cuttings in the borehole, hence enables easy movement of the drill string and reducing the COF.

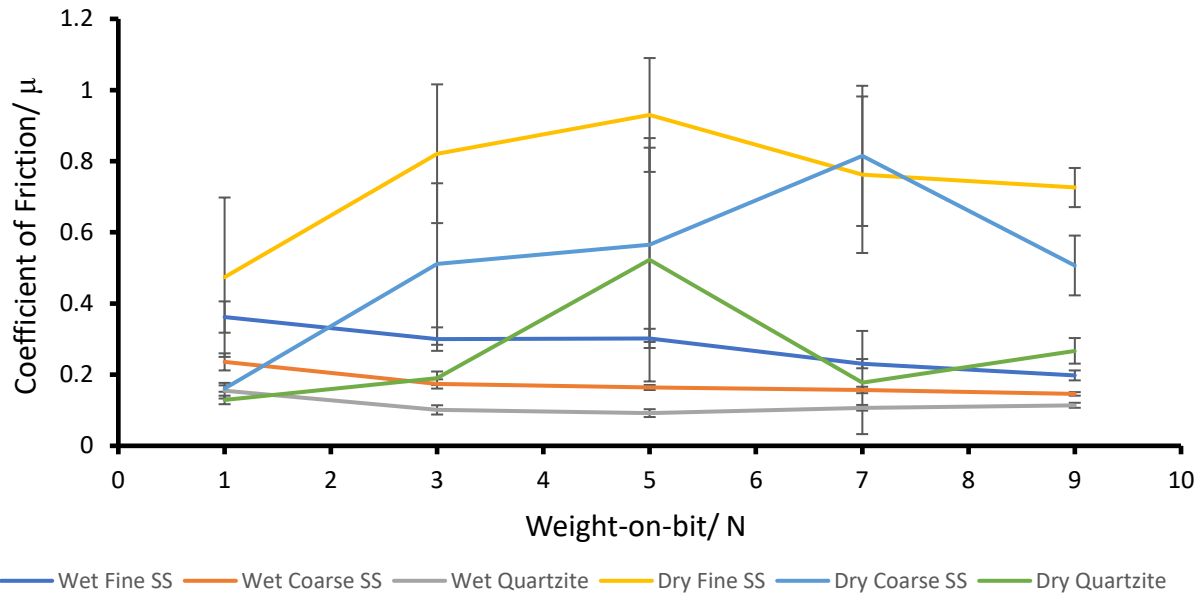


Figure 43: Coefficients of friction for different rock types when using CNC-Bentonite-Seawater solution at 300 rpm

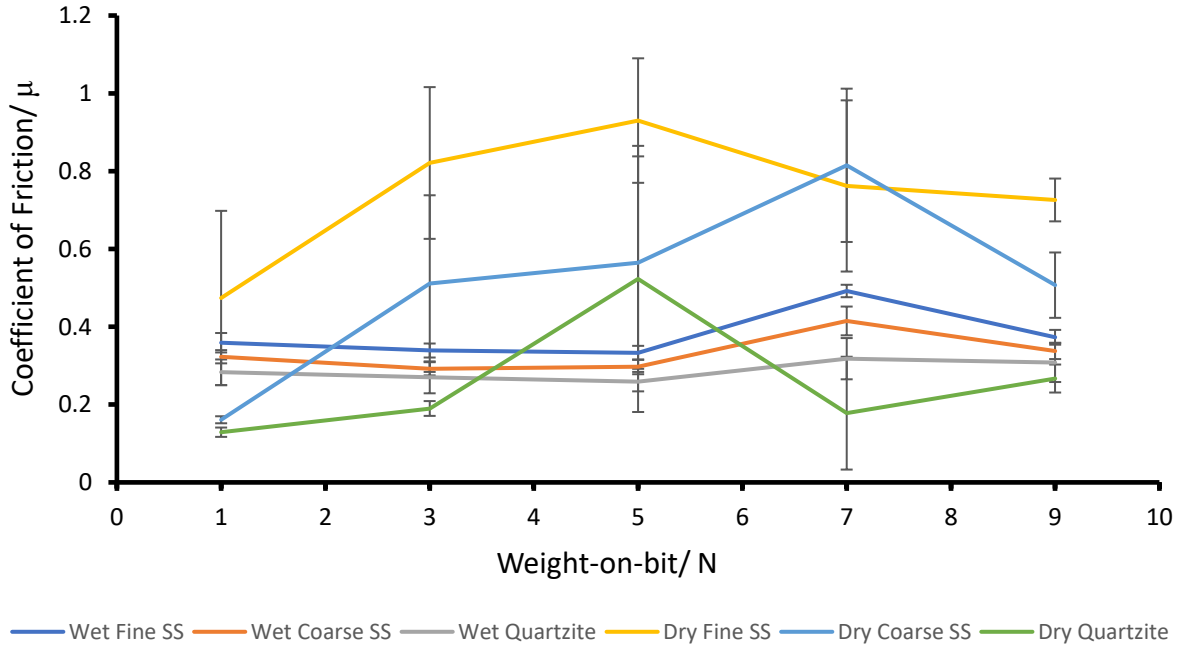


Figure 44: Coefficients of friction for different rock types when using CNC-Attapulgate-Seawater solution at 300 rpm

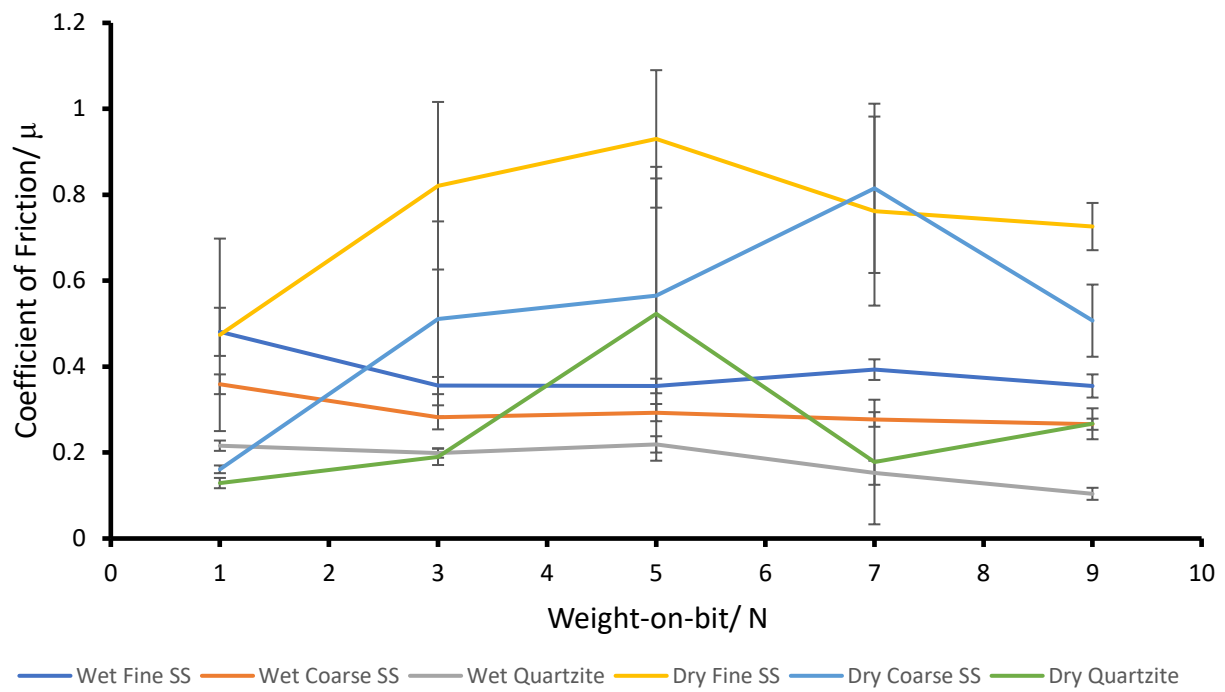


Figure 45: Coefficients of friction for different rock types when using CNC-Sepiolite-Seawater solution at 300 rpm

CHAPTER FIVE

5.0 CONCLUSIONS AND RECOMMENDATIONS

This study was helpful in designing drilling processes that effectively increase production and reduce possible mechanical failures in deep drilling processes, by proper selection of drilling equipment, drilling muds and drilling parameters specific for different rock formations.

The mineralogical (XRD, XRF, SEM/ EDS) and physical (UCS) characterizations were successfully done on the fine-grained sandstone, coarse-grained sandstone and quartzite rock samples. The XRD confirmed that the rock samples contained quartz as the major component, with trace minerals of kyanite and orthoclase. The XRF and EDS data correlated with the XRD data showing that the rock samples have higher concentrations of silica and then lower for the trace elements.

The UCS data showed that the rock with the highest silica was able to carry the highest load, making it harder than the other two samples. And this rock was the quartzite. These results were able to give a clear picture of the characteristics of the rock samples making it easier to understand their behavior during the drilling process.

In dry drilling conditions, the COF are seen to be lowest when the coarse-grained sandstone and quartzite, when using high speeds on 200 and 300 rpm. There is so significant difference observed when the two speeds are used, where the COF goes below 0.16 for coarse grained sandstone and below 0.13 for quartzite. Therefore, for the purpose of saving costs, the rotating speed of 200 rpm can be used in both rocks to yield efficient results. In fine-grained sandstone, the variation in the bit rotating speed does not have a significant impact on the COF. The COF ranges between 0.46 and 0.54 when the three rotating speeds are used. This means that any bit rotating speed can be used to give the favorable results, but the lowest would be preferred as it would more cost-effective.

When using the water-based and oil-based lubricants, the oil-based were seen to give the lowest COF in all the three rock samples. The COF were reduced to 0.127, 0.049, and 0.048 for fine-

grained sandstone, coarse-grained sandstone, and quartzite, respectively. These low COF were observed when the 7 N WOB and the 50 wt% of weighted material were used in all the three rock samples. The use of the 25 wt% of the weighted material in oil, produced slightly higher COF in all the rock samples, which were 0.103, 0.126 and 0.1 for fine-grained sandstone, coarse-grained sandstone, and quartzite, respectively. These COF were obtained when the higher load of 9 N was used. A clear feasibility study would have to be made to determine which process would be cheaper when using more concentrated drilling fluid at lower load or using less concentrated fluid but at a much higher load.

The use of attapulgite, bentonite, and sepiolite also showed improvements in the reduction of the COF. Seawater compared to freshwater, showed greater improvements in the COF of friction, where bentonite performed better than attapulgite and sepiolite. The lowest COF observed was when bentonite was used in seawater at a high load of 9 N for coarse and fine-grained sandstone and then at the load of 5 N for quartzite. The COF values were 0.198, 0.146 and 0.092 for fine-grained sandstone, coarse-grained sandstone, and quartzite, respectively. These are a bit higher than when the oil-based mud is used.

This concludes that the oil-based muds are the future of the oil and gas industry and more research much be conducted to improve them and make them easily available, especially due to their nature of being biodegradable, hence environmentally friendly.

From the outcome of this research, the following recommendations can add values to this investigation

- When using bentonite as an additive, more tests should be conducted to find the minimum bentonite concentration that will give the lowest COF, hence improve drilling efficiency while minimizing costs.
- The standard deviations were very high in dry testing, this means that more tests should be conducted, especially for fine-grained sandstone, to find out the reason behind the irregularity.

- Porosity tests and TEM analysis should be conducted on the rock samples, to determine how the porosity and crystal structure of the rock samples affects their performance during drilling.

REFERENCES

- Abdo, J., and Haneef, M.D. (2011). Nano-Enhanced Drilling Fluids: Pioneering Approach to Overcome Uncompromising Drilling Problems. *J. Energy Resour. Technol.* *134*, 014501-014501–014506.
- Abdo, J., and Haneef, M.D. (2013). Clay nanoparticles modified drilling fluids for drilling of deep hydrocarbon wells. *Appl. Clay Sci.* *86*, 76–82.
- Addy, J.M., Hartley, J.P., and Tibbetts, P.J.C. (1984). Ecological effects of low toxicity oil-based mud drilling in the Beatrice oilfield. *Mar. Pollut. Bull.* *15*, 429–436.
- Adhvaryu, A., Liu, Z., and Erhan, S.Z. (2005). Synthesis of novel alkoxyated triacylglycerols and their lubricant base oil properties. *Ind. Crops Prod.* *21*, 113–119.
- Ahmadi, M.A., Galedarzadeh, M., and Shadizadeh, S.G. (2015). Colloidal gas aphron drilling fluid properties generated by natural surfactants: Experimental investigation. *J. Nat. Gas Sci. Eng.* *27*, 1109–1117.
- Akpan, U.G., Jimoh, A., and Mohammed, A.D. (2006). Extraction, Characterization and Modification of Castor Seed Oil. *Leonardo J. Sci.* *8*, 43–52.
- Albdiry, M.T., and Almensory, M.F. (2016). Failure analysis of drillstring in petroleum industry: A review. *Eng. Fail. Anal.* *65*, 74–85.
- Allen, C., and Ball, A. (1996a). A review of the performance of engineering materials under prevalent tribological and wear situations in South African industries. *Tribol. Int.* *29*, 105–116.
- Allen, C., and Ball, A. (1996b). A review of the performance of engineering materials under prevalent tribological and wear situations in South African industries. *Tribol. Int.* *29*, 105–116.
- Al-malki, N., Pourafshary, P., Al-hadrami, H., and Abdo, J. (2016). Controlling bentonite-based drilling mud properties using sepiolite nanoparticles. *Pet. Explor. Dev.* *43*, 717–723.
- Amani, M., Al-Jubouri, M., and Shadravan, A. (2012). Comparative study of using oil-based mud versus water-based mud in HPHT fields. *Adv. Pet. Explor. Dev.* *4*, 18–27.
- Amanullah, M., and Al-Tahini, A.M. (2009). Nano-Technology - Its Significance in Smart Fluid Development for Oil and Gas Field Application. (Society of Petroleum Engineers), p.
- Amanullah, M., AlArfaj, M.K., and Al-abdullatif, Z.A. (2011). Preliminary Test Results of Nano-based Drilling Fluids for Oil and Gas Field Application. (Society of Petroleum Engineers), p.
- Amorim, L.V., Nascimento, R.C.A.M., Lira, D.S., and Magalhães, J. (2011). Evaluation of the behavior of biodegradable lubricants in the differential sticking coefficient of water-based drilling fluids. *Braz. J. Pet. Gas* *5*, 197–207.

- Appl, F.C., Wilson, C.C., and Lakshman, I. (1993). Measurement of forces, temperatures and wear of PDC cutters in rock cutting. *Wear* 169, 9–24.
- Argillier, J.-F., Audibert, A., Janssen, M., and Demoulin, A. (1996). Development of a New Non-Polluting Ester Based Lubricant for Water Based Muds: Laboratory and Field Tests Results. (Society of Petroleum Engineers), p.
- Asadauskas, S., Perez, J.M., and Duda, J.L. (1996). Oxidative stability and antiwear properties of high oleic vegetable oils©.
- Atabani, A.E., Silitonga, A.S., Ong, H.C., Mahlia, T.M.I., Masjuki, H.H., Badruddin, I.A., and Fayaz, H. (2013). Non-edible vegetable oils: A critical evaluation of oil extraction, fatty acid compositions, biodiesel production, characteristics, engine performance and emissions production. *Renew. Sustain. Energy Rev.* 18, 211–245.
- Ataei, M., KaKaie, R., Ghavidel, M., and Saeidi, O. (2015). Drilling rate prediction of an open pit mine using the rock mass drillability index. *Int. J. Rock Mech. Min. Sci.* 73, 130–138.
- Baba Hamed, S., and Belhadri, M. (2009). Rheological properties of biopolymers drilling fluids. *J. Pet. Sci. Eng.* 67, 84–90.
- Barry, M.M., Jung, Y., Lee, J.K., Phuoc, T.X., and Chyu, M.K. (2015). Fluid filtration and rheological properties of nanoparticle additive and intercalated clay hybrid bentonite drilling fluids. *J. Pet. Sci. Eng.* 127, 338–346.
- Bart, J.C.J., Gucciardi, E., and Cavallaro, S. (2012). *Biolubricants: Science and Technology* (Elsevier).
- Beste, U. (2002). Tribological aspects on rock and drill in rock drilling. *Mater. Eng.* 254–260.
- Beste, U. (2004). On the Nature of Cemented Carbide Wear in Rock Drilling. 964.
- Beste, U., and Jacobson, S. (2002). Friction between a cemented carbide rock drill button and different rock types. *Wear* 253, 1219–1221.
- Beste, U., and Jacobson, S. (2003). Micro scale hardness distribution of rock types related to rock drill wear. *Wear* 254, 1147–1154.
- Beste, U., and Jacobson, S. (2008). A new view of the deterioration and wear of WC/Co cemented carbide rock drill buttons. *Wear* 264, 1129–1141.
- Beste, U., Hartzell, T., Engqvist, H., and Axén, N. (2001). Surface damage on cemented carbide rock-drill buttons. *Wear* 249, 324–329.
- Beste, U., Lundvall, A., and Jacobson, S. (2004). Micro-scratch evaluation of rock types - A means to comprehend rock drill wear. *Tribol. Int.* 37, 203–210.

- Beste, U., Coronel, E., and Jacobson, S. (2006). Wear induced material modifications of cemented carbide rock drill buttons. *Int. J. Refract. Met. Hard Mater.* *24*, 168–176.
- Beste, U., Jacobson, S., and Hogmark, S. (2008). Rock penetration into cemented carbide drill buttons during rock drilling. *Wear* *264*, 1142–1151.
- Boneh, Y., and Reches, Z. (2018). Geotribology - Friction, wear, and lubrication of faults. *Tectonophysics* *733*, 171–181.
- Borugadda, V.B., and Goud, V.V. (2016). Improved thermo-oxidative stability of structurally modified waste cooking oil methyl esters for bio-lubricant application. *J. Clean. Prod.* *112*, 4515–4524.
- Bourgoyne, A.T.J., Millheim, K.K., Chenevert, M.E., and Young, F.S.J. (1986a). *Applied Drilling Engineering Chapter 8 Solutions*.
- Bourgoyne, A.T.J., Millheim, K.K., Chenevert, M.E., and Young, F.S.J. (1986b). *Applied drilling engineering. Volume 2*.
- Brandon, N.P., Panesar, S.S., Bonanos, N., Fogarty, P.O., and Mahmood, M.N. (1993). The effect of cathodic currents on friction and stuck pipe release in aqueous drilling muds. *J. Pet. Sci. Eng.* *10*, 75–82.
- Brazzel, R.L. (2009). Multi-component drilling fluid additive, and drilling fluid system incorporating the additive.
- Brett, J.F., Warren, T.M., and Behr, S.M. (1989). *Bit Whirl: A New Theory of PDC Bit Failure*. (Society of Petroleum Engineers), p.
- Brookfield Engineering Labs Inc. (2010). More solutions to sticky problems: A Guide to getting motr from your viscometer. 1–53.
- Bruton, G., Crockett, R., Taylor, M., DenBoer, D., Lund, J., Fleming, C., Ford, R., Garcia, G., and White, A. (2014). PDC bit technology for the 21st century. *Oilfield Rev.* *26*, 48–57.
- Caenn, R., Darley, H.C.H., and Gray, G.R. (2011). *Composition and Properties of Drilling and Completion Fluids* (Gulf Professional Publishing).
- Campanella, A., Rustoy, E., Baldessari, A., and Baltanás, M.A. (2010). Lubricants from chemically modified vegetable oils. *Bioresour. Technol.* *101*, 245–254.
- Chen, X., Gao, D., Guo, Y., and Feng, Y. (2016). Real-time optimization of drilling parameters based on mechanical specific energy for rotating drilling with positive displacement motor in the hard formation. *J. Nat. Gas Sci. Eng.* *35*, 686–694.
- Chhabra, R.P., and Richardson, J.F. (2011). *Non-Newtonian Flow and Applied Rheology: Engineering Applications* (Butterworth-Heinemann).

Cvengroš, J., Paligová, J., and Cvengrošová, Z. (2006). Properties of alkyl esters base on castor oil. *Eur. J. Lipid Sci. Technol.* *108*, 629–635.

Cyr, P. (2008). Number 1 and Pale Pressed Castor Oil Products.

Darley, H.C.H., and Gray, G.R. (1988). *Composition and Properties of Drilling and Completion Fluids* (Gulf Professional Publishing).

DeGeare, J.P. (2014). *The Guide to Oilwell Fishing Operations: Tools, Techniques, and Rules of Thumb* (Gulf Professional Publishing).

Deng, Y., Chen, M., Jin, Y., Zhang, Y., Zou, D., and Lu, Y. (2016). Theoretical and experimental study on the penetration rate for roller cone bits based on the rock dynamic strength and drilling parameters. *J. Nat. Gas Sci. Eng.* *36*, 117–123.

Dodd, A.A. (1978). Method of reducing drag and rotating torque in the rotary drilling of oil and gas wells.

Dougherty, P.S.M., Pudjoprawoto, R., and Fred Higgs, C. (2014). Bit cutter-on-rock tribometry: Analyzing friction and rate-of-penetration for deep well drilling substrates. *Tribol. Int.* *77*, 178–185.

Dougherty, P.S.M., Mpagazehe, J., Shelton, J., and Higgs III, C.F. (2015). Elucidating PDC rock cutting behavior in dry and aqueous conditions using tribometry. *J. Pet. Sci. Eng.* *133*, 529–542.

Drown, D.C., Harper, K., and Frame, E. (2001). Screening vegetable oil alcohol esters as fuel lubricity enhancers. *JAOCS J. Am. Oil Chem. Soc.* *78*, 579–584.

Ersoy, A., and Waller, M.D. (1995a). Prediction of drill-bit performance using multi-variable linear regression analysis. *Int. J. Rock Mech. Min. Sci. Geomech. Abstr.* *6*, 279A.

Ersoy, A., and Waller, M.D. (1995b). Textural characterisation of rocks. *Eng. Geol.* *39*, 123–136.

Ersoy, A., and Waller, M.D. (1995c). Wear characteristics of PDC pin and hybrid core bits in rock drilling. *Wear* *188*, 150–165.

Ersoy, A., and Waller, M.D. (1997). Drilling detritus and the operating parameters of thermally stable PDC core bits. *Int. J. Rock Mech. Min. Sci.* *34*, 1109–1123.

Espagne, B.J., Lamrani-Kern, S., and Rodeschini, H. (2014). Biodegradable lubricating composition and use thereof in a drilling fluid, in particular for very deep reservoirs.

Evdokimov, I.N., Eliseev, N.P., Losev, A.P., and Novikov, M.A. (2006). *Emerging Petroleum-Oriented Nanotechnologies for Reservoir Engineering*. (Society of Petroleum Engineers), p.

- Fereydouni, M., Sabbaghi, S., Saboori, R., and Zeinali, S. (2012). Effect of Polyanionic Cellulose Polymer Nanoparticles on Rheological Properties of Drilling Mud. *Int. J. Nanosci. Nanotechnol.* *8*, 171–174.
- Fetting, A. (2016). Deep-hole drilling continues to evolve. *Manuf. Eng.* *91*, 10.
- Fink, J. (2015). *Petroleum Engineer's Guide to Oil Field Chemicals and Fluids* (Gulf Professional Publishing).
- Foroulis, Z.A., and Tsao, Y.H. (1987). Method for reducing friction in drilling operations.
- Foxenberg, W.E., Ali, S.A., Long, T.P., and Vian, J. (2008). Field Experience Shows That New Lubricant Reduces Friction and Improves Formation Compatibility and Environmental Impact. (Society of Petroleum Engineers), p.
- Gan, C., Cao, W., Wu, M., Chen, X., Lu, C., Hu, Y., and Wen, G. (2016). Intelligent Nadaboost-ELM modeling method for formation Drillability Using well logging data. *J. Adv. Comput. Intell. Intell. Inform.* *20*, 1103–1111.
- Gan, C., Cao, W., Wu, M., Chen, X., Hu, Y., Wen, G., Gao, H., Ning, F., and Ding, H. (2017). An Online Modeling Method for Formation Drillability Based on OS-Nadaboost-ELM Algorithm in Deep Drilling Process. *IFAC-Pap.* *50*, 12886–12891.
- Gan, C., Cao, W., and Liu, K. (2018a). To Improve Drilling Efficiency by Multi-objective Optimization of Operational Drilling Parameters in the Complex Geological Drilling Process. In *2018 37th Chinese Control Conference (CCC)*, pp. 10238–10243.
- Gan, C., Cao, W., Wu, M., and Chen, X. (2018b). A new bat algorithm based on iterative local search and stochastic inertia weight. *Expert Syst. Appl.* *104*, 202–212.
- Gan, C., Cao, W., and Liu, K. (2018c). To Improve Drilling Efficiency by Multi-objective Optimization of Operational Drilling Parameters in the Complex Geological Drilling Process. In *2018 37th Chinese Control Conference (CCC)*, pp. 10238–10243.
- Gan, C., Cao, W., Wu, M., Liu, K.-Z., Chen, X., Hu, Y., and Ning, F. (2019a). Two-level intelligent modeling method for the rate of penetration in complex geological drilling process. *Appl. Soft Comput.* *80*, 592–602.
- Gan, C., Cao, W., Wu, M., Liu, K., Chen, X., Hu, Y., and Ning, F. (2019b). Two-level intelligent modeling method for the rate of penetration in complex geological drilling process. *Appl. Soft Comput.* *80*, 592–602.
- Gao, Y., Chen, Y., Wang, Z., Chen, L., Zhao, X., and Sun, B. (2019). Experimental study on heat transfer in hydrate-bearing reservoirs during drilling processes. *Ocean Eng.* *183*, 262–269.
- Getliff, J.M., and James, S.G. (1996). The Replacement of Alkyl-Phenol Ethoxylates to Improve the Environmental Acceptability of Drilling Fluid Additives. (Society of Petroleum Engineers), p.

Goodrum, J.W., and Geller, D.P. (2005). Influence of fatty acid methyl esters from hydroxylated vegetable oils on diesel fuel lubricity. *Bioresour. Technol.* *96*, 851–855.

Gradishar, J., Ugueto, G., and van Oort, E. (2014). Setting Free the Bear: The Challenges and Lessons of the Ursa A-10 Deepwater Extended-Reach Well. *SPE Drill. Complet.* *29*, 182–193.

Green, D.A., Lewis, R., and Cripps, J. (2007). Friction and wear testing for a down-hole oil well centraliser. *Wear* *263*, 57–64.

Greene, D.L., Hopson, J.L., and Li, J. (2006). Have we run out of oil yet? Oil peaking analysis from an optimist's perspective. *Energy Policy* *34*, 515–531.

Guan, Z.C., and Chen, M. (2006). Theory and Technogy of drilling Engineering. *Pet. Press* 130–138.

Guo, J., Guo, X., Wang, S., and Yin, Y. (2016). Effects of ultrasonic treatment during acid hydrolysis on the yield, particle size and structure of cellulose nanocrystals. *Carbohydr. Polym.* *135*, 248–255.

Haber, R.E., Haber-Haber, R., Jiménez, A., and Galán, R. (2009). An optimal fuzzy control system in a network environment based on simulated annealing. An application to a drilling process. *Appl. Soft Comput.* *9*, 889–895.

Hahn, D., and Makohl, F. (2002). Apparatus and method for simultaneous drilling and casing wellbores.

Haldenwang, R. (2003). Flow of Non-Newtonian fluids in open channels. PhD Thesis. Cape Technikon.

Hincapié, G., Mondragón, F., and López, D. (2011). Conventional and in situ transesterification of castor seed oil for biodiesel production. *Fuel* *90*, 1618–1623.

Hossain, M.E., and Wajheeuddin, M. (2016). The use of grass as an environmentally friendly additive in water-based drilling fluids. *Pet. Sci.* *13*, 292–303.

Ibarz, A., Castell-Perez, E., and Barbosa-Canovas, G.V. (2015). Newtonian and Non-Newtonian flow. *Food Eng.* *11*.

Jacobson, S., and Hogmark, S. (2009). Surface modifications in tribological contacts. *Wear* *266*, 370–378.

J. Moon, R., Martini, A., Nairn, J., Simonsen, J., and Youngblood, J. (2011). Cellulose nanomaterials review: structure, properties and nanocomposites. *Chem. Soc. Rev.* *40*, 3941–3994.

Jones, J.R. (1971). *Lubrication, Friction and Wear* (Hampton, Virginia: NASAISP).

- Kania, D., Yunus, R., Omar, R., Abdul Rashid, S., and Mohamad Jan, B. (2015). A review of biolubricants in drilling fluids: Recent research, performance, and applications. *J. Pet. Sci. Eng.* *135*, 177–184.
- Karol, R.H. (2003). *Chemical Grouting And Soil Stabilization, Revised And Expanded* (CRC Press).
- Knothe, G. (2005). *The History of vegetable oil-based diesel fuels* (Champaign: AOCS Press).
- Koltermann, T.J., and Dick, A.J. (2009). *Lubricated Diamond Bearing Drill Bit*.
- Krizek, R.R., and Pepper, S.F. (2004). *Slurries in geotechnical engineering* (Texas< USA: Texas A & M Univerity).
- Lagerquist, M. (1975). A STUDY OF THE THERMAL FATIGUE CRACK PROPAGATION IN WC-Co CEMENTED CARBIDE. *Powder Metall.* *18*, 71–88.
- Larsen-Basse, J. (1973). Wear of hard-metals in rock drilling: A survey of the literature. *Powder Metall.* *16*, 1–32.
- Larsen-Basse, J. (1983). Effect of composition, microstructure, and service conditions on the wear of cemented carbides. *J. Met.* *35*, 35–42.
- Larsen-Basse, J. (1985). Binder exclusion in sliding wear od WC-Co alloys. *Wear* *105*, 247–256.
- Larsen-Basse, J. (1992). Wear Particles from Abrasion of WC-Co Cemented Carbides. *Tribol. Ser.* *21*, 131–138.
- Li, M.C., Wu, Q., Song, K., Qing, Y., and Wu, Y. (2015a). Cellulose Nanoparticles as Modifiers for Rheology and Fluid Loss in Bentonite Water-based Fluids. *ACS Appl. Mater. Interfaces* *7*, 5006–5016.
- Li, M.C., Wu, Q., K., K., De Hoop, C.F., Lee, S., Qing, Y., and Wu, Y. (2016). Cellulose Nanocrystals and Polyanionic Cellulose as Additives in Bentonite Water-Based Drilling Fluids: Rheological Modeling and Filtration Mechanisms. *Ind. Eng. Chem. Res.* *55*, 133–143.
- Li, W., Zhao, X., Li, Y., Ji, Y., Peng, H., Liu, L., and Yang, Q. (2015b). Laboratory investigations on the effects of surfactants on rate of penetration in rotary diamond drilling. *J. Pet. Sci. Eng.* *134*, 114–122.
- Ling, T.D., Liu, P., Xiong, S., Grzina, D., Cao, J., Wang, Q.J., Xia, Z.C., and Talwar, R. (2013). Surface Texturing of Drill Bits for Adhesion Reduction and Tool Life Enhancement. *Tribol. Lett.* *52*, 113–122.
- Livescu, S., and Craig, S. (2015). Increasing Lubricity of Downhole Fluids for Coiled-Tubing Operations. *SPE J.* *20*, 396–404.

- Luckham, P.F., and Rossi, S. (1999). The colloidal and rheological properties of bentonite suspensions. *Adv. Colloid Interface Sci.* 82, 43–92.
- Lyons, K.D., Honeygan, S., and Mroz, T. (2008). NETL Extreme Drilling Laboratory Studies High Pressure High Temperature Drilling Phenomena. *J. Energy Resour. Technol.* 130, 043102.
- Ma, H. (2011). Formation drillability prediction based on multi-source information fusion. *J. Pet. Sci. Eng.* 78, 438–446.
- Macdonald, K.A., and Bjune, J.V. (2007). Failure analysis of drillstrings. *Eng. Fail. Anal.* 14, 1641–1666.
- MacDonald, R.P., Krueger, V., Nasr, H.N., Harrell, J.W., and Fincher, R.W. (2001). Drilling system with integrated bottom hole assembly.
- Maidla, E.E., and Wojtanowicz, A.K. (1990). Laboratory Study of Borehole Friction Factor With a Dynamic-Filtration Apparatus. *SPE Drill. Eng.* 5, 247–255.
- Mohamad, S.A., Ahmed, N.S., Hassanein, S.M., and Rashad, A.M. (2012). Investigation of polyacrylates copolymers as lube oil viscosity index improvers. *J. Pet. Sci. Eng.* 100, 173–177.
- Mohs, F. (1825). *Treatise on Mineralogy: Or, The Natural History of the Mineral Kingdom* (A. Constable and Company, Edinburgh, and Hurst, Robinson, and Company, London).
- Montgomery, R.S. (1968). The mechanism of percussive wear of tungsten carbide composites. *Wear* 12, 309–329.
- Mueller, H., Herold, C.P., Bongardt, F., Herzog, N., and Tapavicza, S.V. (2004). Lubricants for drilling fluids.
- Nan, F., Xu, Y., Xu, B., Gao, F., Wu, Y., and Tang, X. (2014). Effect of natural attapulgite powders as lubrication additive on the friction and wear performance of a steel tribo-pair. *Appl. Surf. Sci.* 307, 86–91.
- Neff, J.M., McKelvie, S., and Ayers, R.C. (2000). *Environmental Impacts of Synthetic Based Drilling Fluids*.
- Obadele, B.A., Andrews, A., Shongwe, M.B., and Olubambi, P.A. (2016). Tribocorrosion behaviours of AISI 310 and AISI 316 austenitic stainless steels in 3.5% NaCl solution. *Mater. Chem. Phys.* 171, 239–246.
- Ogugbue, C.E., Rathan, M.P., and Shah, S.N. (2010). *Experimental Investigation of Biopolymer and Surfactant Based Fluid Blends as Reservoir Drill-In Fluids*. (Society of Petroleum Engineers), p.
- Olsson, M., Yvell, K., Heinrichs, J., Bengtsson, M., and Jacobson, S. (2017). Surface degradation mechanisms of cemented carbide drill buttons in iron ore rock drilling. *Wear* 388–389, 81–92.

- Patel, A., Zhang, H.J., Ke, M., and Panamarathupalayam, B. (2013). *Lubricants and Drag Reducers for Oilfield Applications - Chemistry, Performance, and Environmental Impact*. (Society of Petroleum Engineers), p.
- Pavković, D., Deur, J., and Lisac, A. (2011). A torque estimator-based control strategy for oil-well drill-string torsional vibrations active damping including an auto-tuning algorithm. *Control Eng. Pract.* *19*, 836–850.
- Peña, R., Romero, R., Martínez, S.L., Ramos, M.J., Martínez, A., and Natividad, R. (2009). Transesterification of Castor Oil: Effect of Catalyst and Co-Solvent. *Ind. Eng. Chem. Res.* *48*, 1186–1189.
- Pessier, R., and Damschen, M. (2011). Hybrid Bits Offer Distinct Advantages in Selected Roller-Cone and PDC-Bit Applications. *SPE Drill. Complet.* *26*, 96–103.
- Pradhan, S., Madankar, C.S., Mohanty, P., and Naik, S.N. (2012). Optimization of reactive extraction of castor seed to produce biodiesel using response surface methodology. *Fuel* *97*, 848–855.
- Rafati, R., Smith, S.R., Sharifi Haddad, A., Novara, R., and Hamidi, H. (2018). Effect of nanoparticles on the modifications of drilling fluids properties: A review of recent advances. *J. Pet. Sci. Eng.* *161*, 61–76.
- Randles, S.J. (1992). Environmentally considerate ester lubricants for the automotive and engineering industries. *J. Synth. Lubr.* *9*, 145–161.
- Rudnick, L. (2005). *Synthetics, Mineral Oils and Bio-Based Lubricants* (CRC Press).
- Schorode, J., Richards, A., and Yorty, J. (2016). Bearing innovations extended roller cone bit life. *Oil Na Gas J.* *114*, 50–55.
- Shah, S.N., Shanker, N.H., and Ogugbue, C.C. (2010). *Future Challenges of Drilling Fluids and Their Rheological Measurements*. (Houston, Texas), p.
- Shaughnessy, J.M., Daugherty, W.T., Graff, R.L., and Durkee, T. (2007). *More Ultra-Deepwater Drilling Problems*. (Society of Petroleum Engineers), p.
- Singer, A., and Galan, E. (2000). *Palygorskite-Sepiolite: Occurrences, Genesis and Uses* (Elsevier).
- Skalle, P. (2011). *Drilling Fluid Engineering*.
- Song, K., Yin, Y., Salmén, L., Xiao, F., and Jiang, X. (2014). Changes in the properties of wood cell walls during the transformation from sapwood to heartwood. *J. Mater. Sci.* *49*, 1734–1742.
- Song, K., Wu, Q., Li, M.C., Wojtanowicz, A.K., Dong, L., Zhang, X., Ren, S., and Lei, T. (2016a). Performance of low solid bentonite drilling fluids modified by cellulose nanoparticles. *J. Nat. Gas Sci. Eng.* *34*, 1403–1411.

Song, K., Wu, Q., Li, M., Ren, S., Dong, L., Zhang, X., Lei, T., and Kojima, Y. (2016b). Water-based bentonite drilling fluids modified by novel biopolymer for minimizing fluid loss and formation damage. *Colloids Surf. Physicochem. Eng. Asp.* *507*, 58–66.

Sudo, T., and Shimoda, S. (1978). *Clays and Clay Minerals of Japan* (Elsevier).

Talke, F.E. (1997). A review of 'contact recording' technologies. *Wear* *207*, 118–121.

Taylor, H.F.W. (1997). *Cement Chemistry* (Thomas Telford).

Temraz, M.G., and Hassanien, I. (2016). Mineralogy and rheological properties of some Egyptian bentonite for drilling fluids. *J. Nat. Gas Sci. Eng.* *31*, 791–799.

Torbacke, M., Rudolphi, A.K., and Kassfeldt, E. (2014). *Lubricants: Introduction to Properties and Performance* (John Wiley & Sons).

Vingsbo, O., and Hogmark, S. (1981). Wear of steels. *Am. Soc. Met.* *373–408*.

Vutukuri, V.S., Lama, R.D., and Saluja, S.S. (1974). Handbook of mechanical properties of rocks. *Trans Tech Publ.* *1*, 280.

Wang, H., Ge, Y., and Shi, L. (2017). Technologies in deep and ultra-deep well drilling: Present status, challenges and future trend in the 13th Five-Year Plan period (2016–2020). *Nat. Gas Ind. B* *4*, 319–326.

Wang, X., Yu, J., Sun, Y., Yang, C., Jiang, L., and Liu, C. (2018). A solids-free brine drilling fluid system for coiled tubing drilling. *Pet. Explor. Dev.* *45*, 529–535.

Wang, Z., Abdo, J., Zhang, J., Liu, S., Gao, Y., Xiang, H., and Sun, B. (2019). Improved thermal model considering hydrate formation and deposition in gas-dominated systems with free water. *Fuel* *236*, 870–879.

Wei, L., and McDonald, A.G. (2016). A Review on Grafting of Biofibers for Biocomposites. *Materials* *9*, 303.

Wise, J.L., Raymond, D.W., and Cooley, C.H. (2002). Effects of design and processing parameters on performance of PDC drag cutters for hard-rock drilling.

Yang, X., Shang, Z., Liu, H., Cai, J., and Jiang, G. (2017). Environmental-friendly salt water mud with nano-SiO₂ in horizontal drilling for shale gas. *J. Pet. Sci. Eng.* *156*, 408–418.

Yang, Y., Zhang, C., Lin, M., and Chen, L. (2018). Research on rock-breaking mechanism of cross-cutting PDC bit. *J. Pet. Sci. Eng.* *161*, 657–666.

Yu, H.L., Xu, Y., Shi, P.J., Xu, B.S., Wang, X.L., Liu, Q., and Wang, H.M. (2008). Characterization and nano-mechanical properties of tribofilms using Cu nanoparticles as additives. *Surf. Coat. Technol.* *203*, 28–34.

Zamora, M., Broussard, P.N., and Stephens, M.P. (2000). The Top 10 Mud-Related Concerns in Deepwater Drilling Operations. (Society of Petroleum Engineers), p.

Zha, C., Liu, G., Li, J., Li, Y., Xi, Y., and Guo, B. (2017). Combined Percussive-Rotary Drilling to Increase Rate of Penetration and Life of Drill Bit in Drilling Hard Rock Formation. *Chem. Technol. Fuels Oils* 53, 254–262.

Zhang, Q., Lian, Z., Lin, T., Deng, Z., Xu, D., and Gan, Q. (2016). Casing wear analysis helps verify the feasibility of gas drilling in directional wells. *J. Nat. Gas Sci. Eng.* 35, 291–298.

Zhang, X., Zhai, Y.H., Xue, C.J., and Jiang, T.X. (2011). A Study of the Distribution of Formation Drillability. *Pet. Sci. Technol.* 29, 149–159.

Zhang, Z., Wu, Q., Song, K., Lei, T., and Wu, Y. (2015a). Poly(vinylidene fluoride)/cellulose nanocrystals composites: rheological, hydrophilicity, thermal and mechanical properties. *Cellulose* 22, 2431–2441.

Zhang, Z., Wu, Q., Song, K., Ren, S., Lei, T., and Zhang, Q. (2015b). Using Cellulose Nanocrystals as a Sustainable Additive to Enhance Hydrophilicity, Mechanical and Thermal Properties of Poly(vinylidene fluoride)/Poly(methyl methacrylate) Blend. *ACS Sustain. Chem. Eng.* 3, 574–582.

Zhao, X., Qiu, Z., Huang, W., and Wang, M. (2017). Mechanism and method for controlling low-temperature rheology of water-based drilling fluids in deepwater drilling. *J. Pet. Sci. Eng.* 154, 405–416.

Zhao, X., Qiu, Z., Wang, M., Xu, J., and Huang, W. (2019). Experimental investigation of the effect of drilling fluid on wellbore stability in shallow unconsolidated formations in deep water. *J. Pet. Sci. Eng.* 175, 595–603.

Zhou, F.S., Xiong, Z.Q., Cui, B.L., Liu, F.B., Li, G.H., Wei, J.R., and Cui, H. (2013). Effect of Nitric Acid on the Low Fluorescing Performance of Drilling Fluid Lubricant Based Animal and Vegetable Oils.

Zorlu, K., Gokceoglu, C., Ocakoglu, F., Nefeslioglu, H.A., and Acikalin, S. (2008). Prediction of uniaxial compressive strength of sandstones using petrography-based models. *Eng. Geol.* 96, 141–158.